DOT/FAA/RD-92/16,II

Research and
Development Service
Washington, D.C. 20591

Runway Exit Designs for Capacity Improvement Demonstrations

Phase II—Computer Model Development

A.A. Trani
A.G. Hobeika
B.J. Kim
V. Nunna
C. Zhong

Virginia Polytechnic Institute and State University
Center for Transportation Research
Blacksburg, Virginia 24061

January 1992

Final Report

U.S. Department of Transportation
Federal Aviation Administration

NOTICE

Technical Report Documentation Page

1. Report No.	2. Government Accession No.	3. Recipient's Catalog No.
DOT/FAA/RD-92/6, II		

4. Title and Subtitle	5. Report Date
Runway Exit Designs For Capacity Improvement Demonstrations (Phase II: Computer Model Development)	January 15, 1992
	6. Performing Organization Code
7. Author(s) A. A. Trani, A. G. Hobeika, B. J. Kim, V. Nunna, C. Zhong	8. Performing Organization Report No. CTR-R-1-92
9. Performing Organization Name and Address Center for Transportation Research 106 Faculty Street Virginia Tech University Blacksburg, VA 24061	10. Work Unit No. (TRAIS) 11. Contract or Grant No. NAS1-18471 TASK NO 15
12. Sponsoring Agency Name and Address Federal Aviation Administration (ARD-200) 800 Independence Avenue Washington, DC 20591	13. Type of Report and Period Covered Technical Report 14. Sponsoring Agency Code FAA ARD-200

15. Supplementary Notes

Hisao Tomita (ARD-200) Technical Monitor at FAA
David Middleton Technical Monitor at NASA LARC

16. Abstract

This report describes the work accomplished in the development of a computer simulation/optimization model to: 1) estimate the optimal locations of existing and proposed runway turnoffs and 2) to estimate the geometric design requirements associated with newly developed high-speed turnoffs. The model described in this report named REDIM 2.0 represents a stand alone application to be used by airport planners, designers and researchers alike to estimate optimal turnoff locations. The report describes in detail the main procedures implemented in the software package and illustrates possible applications using 6 major runway scenarios. The main output of the computer program is the estimation of the weighted average runway occupancy time for a user defined aircraft population. Also, the location and geometric characteristics of each turnoff are provided to the user.

17. Key Words	18. Distribution Statement
Runway exits, high-speed turnoffs, runway occupancy times	This document is available to the public through the National Technical Information Service, Springfield, Virginia 22161

19. Security Classif. (of this report)	20. Security Classif. (of this page)	21. No. of Pages	22. Price
Unclassified	Unclassified	150	

Foreword

This report describes the work accomplished in the development of a computer simulation/optimization model to 1) estimate the optimal locations of existing and proposed high-speed runway turnoffs and 2) estimate the geometric design requirements of high-speed turnoffs. This work is an extension of the activities performed for the National Aeronautics and Space Administration (NASA) and the Federal Aviation Administration (FAA) in conjunction with the research project entitled "Runway Exit Designs for Capacity Improvement Demonstrations: Phase II" funded under NASA contract NAS1-18471 Task 15 with the Center for Transportation Research at Virginia Polytechnic Institute and State University. Phase I was reported in document DOT/FAA/RD-90-32,I.

The model described here and named REDIM 2.0 (runway exit design interactive model) is a stand alone application to be used by airport planners, designers and research individuals to estimate the optimal locations of existing and newly proposed runway turnoffs. The model has been coded in Microsoft Basic 7.0 Professional Development System (PDS) and requires a standard DOS compatible computer with one megabyte or more RAM memory and Enhanced Graphics Adapter (EGA) capabilities. A math coprocessor is not required although strongly recommended to speed up the computer intensive tasks involved in the optimization procedure used in REDIM 2.0.

The work presented here would not have been possible without the contribution of many individuals. Mr. Hisao Tomita (Federal Aviation Administration) and Mr. David Middleton (NASA Langley Research Center) acted as project monitors for this research and provided invaluable insights to the development of the software package. Mr. Jiefing Qin revised the output module of the new software package and his effort should also be recognized. Finally, we would like to thank the FAA and NASA for their strong support and confidence in the Virginia Tech research team.

A.A. Trani, A.G. Hobeika, B.J. Kim, V. Nunna, C. Zhong

Blacksburg, Virginia

Executive Summary

This report presents the results of a study performed by the Center for Transportation Research (UCTR) at Virginia Polytechnic Institute and State University concerning the development of a computer program to estimate the optimal locations and geometric design requirements of high-speed runway turnoffs. This study was conducted for the Federal Aviation Administration System Technology Division (ARD-200) to assess the impact of optimal turnoff locations in runway occupancy time and ultimately in the assessment of possible runway capacity gains. The report covers the second phase of this research effort and emphasizes in the development of a micro-computer program to ascertain the impact of turnoff placement in the expected weighted average runway occupancy time for a given runway/aircraft mix configuration.

The resulting simulation/optimization model called REDIM 2.0 (runway exit design interactive model) is a stand alone application requiring minimal computer hardware (i.e., an IBM or compatible personal computer and EGA capabilities) that can be used in the planning and design of new runway turnoff upgrades or in the location of turnoffs for future runway facilities. REDIM 2.0 is capable of handling all existing turnoff geometries (including "wide throat" geometries) for added flexibility as well as newly proposed high-speed geometries with user-defined turnoff angles.

The main conclusions found during the development of the REDIM 2.0 computer model can be summarized as follows:

- The computer program developed uses a combination of a Monte Carlo simulation and a Polynomial Dynamic Programming algorithm to estimate turnoff candidates and optimize locations that minimize the aircraft weighted average runway occupancy time (WAROT).
- The model results computed for various runway/turnoff configurations seem to be in good agreement with empirical observations made by previous researchers

[Koenig, 1978; Weiss and Barrer, 1984, Weiss, 1985 and Ruhl, 1990]. It must be pointed out that most of the previous data reported aircraft per TERP group [except for Ruhl, 1990] while the model described in this report considers the differences in landing aircraft dynamics between individual vehicles even if they belong to the same TERP group classification.

- Significant reductions in runway occupancy time are possible with the optimal location and geometric tailoring of turnoff geometries for a known aircraft population. For a single runway reductions in WAROT of up to 15% are possible with the use of proposed super-acute angle exits (i.e., 20 degree turnoff angle) compared with standard 30 degree angle geometries. Further reductions are possible while converting right angle turnoffs to super-acute angle exits. This reduction in WAROT could translate in moderate gains in runway capacity under mixed operations due to the stretching effect on the departure slots.
- Reductions in WAROT down to 36-40 seconds seem feasible with the use of optimally located super-acute turnoffs. This WAROT could support a 2.0 nautical mile interarrival separation (assuming some advances in terminal ATC automation take place and solutions to the wake vortex problem are found).
- Three and four degree of freedom aircraft simulations seem to indicate that super-acute turnoff geometries could allow consistent exit speeds of up to 35 m./s. (78 m.p.h.) for transport type aircraft operations. While the land use requirements of these turnoffs are high it might well payoff in runways operated almost exclusively by transport-type aircraft over a 20 year life cycle.
- Proposed lateral separation distance nomographs between a runway and parallel taxiways were derived for all types of high-speed geometries using fairly conservative aircraft deceleration assumptions on the tangent portion of a turnoff. These nomographs could be used in preliminary airport planning to estimate land use requirements.
- Current testing is being done at the FAA Boeing 727-200 six-degree of freedom simulator to validate the results of the aircraft turnoff model used in REDIM 2.0. At the same time several airfield observations are being conducted to validate the results of REDIM 2.0 for various airport/aircraft mix configurations.

Several recommendations derived from this report are:

- Investigate the use of turnoff superelevation to reduce the land use requirements of the proposed super-acute angle turnoff.
- Investigate in detail the aircraft landing gear dynamics associated with the proposed high-speed turnoffs as this might eventually be a deterrent for their operational implementations from the airline point of view.
- An extension to the existing model is possible where further consideration is given to the complex interactions between existing taxiway/runway subsystems and the placement of new runway turnoff locations. Also some consideration could be

given in this analysis to airline/ATC motivational practices in locating runway turnoffs.

- Implement the microscopic results of this research into more macroscopic airport capacity and delay models such as the FAA ACM (airport capacity model) and SIMMOD in order to provide airport planners and designers with more comprehensive tools to ascertain capacity gains and delay reductions at a more macroscopic scale for specific airport network topologies.
- Implement lateral distance guidelines between runway and taxiway centerlines in FAA AC/150-5300-13 to provide minimum requirements for the implementation of high-speed runway turnoffs.

Table of Contents

List of Figures

List of Tables

CHAPTER 1

Introduction

1.1 Background and Problem Statement

Air transportation infrastructure in recent times has been burdened by high demand compared to the limited capacity available causing numerous delays. The gap between air transportation supply and demand seems to be closing even as the number of annual aircraft operations increases at modest pace. These delays have economic impact on the users and the suppliers of air transportation. Recent statistics indicate that nearly $3 billion are paid by the air travellers due to the delays in the U.S. with another $2.1 billion paid by airlines according to the Federal Aviation Administration [FAA, 1988]. U.S., scheduled air carriers recorded a total of 429.1 billion revenue passenger miles in fiscal year 1989 and over the 12-year forecast period the revenue passenger miles are projected to increase at an average annual rate of 4.9 percent, reaching 765.6 billion in fiscal year 2001 [FAA, 1990]. Airlines have changed their routing system from predominantly linear operations to a hub-and-spoke system. The development of connecting hub airports has led to high frequencies in peak hours at major airports and as a result approximately 21 airports are experiencing serious congestion problems. Another side effect of hub and spoke system is the chain effect of delays experienced by the interconnected airports. According to FAA the number of congested airports will increase to fifty by the end of the century [FAA,1988] and one-fifth of them will experience more than 50,000 hours of system imposed delays. The construction of new airports to alleviate this problem is a slow and iterative process due to the scarcity of land, limited financial resources and, local opposition due to possible environmental pollution. The FAA currently engaged in the development of system wide strategies to increase the National Airspace System (NAS) capacity in several fronts ranging from upgrades to the existing Air Traffic Control System to methods to reduce the runway service time.

In order to study an airport as a system, it has been customary to characterize an airport into two main components:1) Airside and 2) Landside.These are in turn divided into subcom-

ponents. The Airspace and Air Traffic Control (ATC), the runways, taxiways and aprons and gates constitute subcomponents of the airside while terminal buildings, parking and ground access facilities are categorized as landside subcomponents.

Every subcomponent has influence towards the capacity of the airport and each one should complement each other. Capacity is defined as the processing capability of a service facility over some period of time. Traditionally the capacity of individual airport subcomponents have been evaluated and the most critical one would dictate the airport capacity. Of the two main components the airside has in general been the critical component which dictated the capacity of the airport. To increase the capacity of the existing air transportation system several topics of interest have been identified by FAA one of them being the possible reduction of runway occupancy time and its variance.

Runway occupancy time (ROT) of aircraft is one of the important factors affecting the capacity of a runway which in turn translates in an airport capacity. ROT is the time that an aircraft occupies the runway until a new operation (arrival or departure) can be processed. Some of the most important factors that influence runway capacity are:

- Intrail separations
- Aircraft population mix
- Exit locations and their type

Several studies have suggested that by improving some of these factors there would be an increase in capacity of a single runway by 20% [Barrer and Diehl, 1988].

1.2 Previous Research

Research on the subject started with the pioneering work of Robert Horonjeff in the late fifties [Horonjeff, et al., 1959, 1960 and 1961]. Horonjeff proposed standards for 45 and 30 Degree angle geometries that later were adopted by the FAA and ICAO with subtle differences [FAA, 1989; ICAO, 1986]. This work was the first one to recognize the critical relationship between turnoff location and turnoff geometry and the research culminated with the developed a mathematical model to locate exit taxiways for a limited number of scenarios (i.e., two exit taxiway speeds and a reduced aircraft population). The results of this model concluded that the optimum location of runway turnoffs is quite sensitive to aircraft population, number of exits, and exit speeds. The same model used external atmospheric corrections to modify the baseline results due to meteorological and geographical conditions. However, only two exit speeds (i.e., 40 and 60 m.p.h.) and a limited number of aircraft populations were investigated thus making the model of limited use. Furthermore, since the aircraft populations used comprised "old" aircraft by current standards the results need revision. The pioneering effort of the Horonjeff team, however, generated a good amount of information regarding the cornering capabilities of aircraft and also obtained data on several lighting schemes to help pilots negotiate these turnoffs under adverse weather conditions. The Horonjeff team performed extensive experiments to find the acceptable turning radius at a given exit speed. The results suggested two centered curves for the turnoff geometry approximating the tracks derived from empirical observations for a Boeing KC-135 aircraft.

In 1970, FAA proposed standards for high speed exits using Horonjeff's results for 30 and 45 Degree geometries. A 1800 ft. radius of curvature was adopted for the centerline track of the turnoff for the 30 Degree exit geometry with a baseline design speed of 26.7 m./sec. (60 MPH). According to Horonjeff's findings the 45 Degree turnoff was rated at 17 m./sec. (40 MPH). The high speed turnoff incorporated a straight 61 m. entrance track emulating a large radius of curvature suggested by Horonjeff. ICAO adopted the Horonjeff standard using two radii of curvature (ICAO, 1977).

Schoen et. al. [Schoen et. al., 1985] investigated the turnoff trajectory of high speed taxiing aircraft in an isolated basis. The resulting shape of the aircraft turnoff was a variable curvature geometry with a continuously decreasing radius of curvature. The end result of this research was a computer program to calculate the (x, y) coordinates of the geometry, considering exit speed and aircraft turning ability. The findings of this research suggested that aircraft moment of inertia played an important factor in dictating the initial trajectory of the turnoff maneuver. This research also showed that ROT values of 30 seconds are possible at the expense of large turning radius and extremely high exit speeds (e.g., 110 MPH for a Boeing 747). Very high-speed turnoff results should, however, be treated cautiously since at such high speeds the controllability of aircraft on the ground could become a serious operational deterrent.

A recent study on turnoff geometries was conducted by Aviation Department staff of Dade County, Florida (Carr et. al., 1980; Witteveen, 1987; and Haury, 1987).After testing various types of geometries, lighting, and marking scenarios in an L1011 flight simulator a "wide throat" geometry was derived having an entrance spiral length of 244 m. (800 ft.) and tapering off with a 122 m. (400 ft.). radius of curvature.Figure A.3 in Appendix A depicts graphically the peculiarities of this turnoff geometry. This type of turnoff geometry has been implemented at Miami International, Baltimore-Washington International, Indianapolis and Orlando International Airports. The wide entrance throat of this geometry is appealing in situations where lateral spacing restrictions between the runway and the nearest parallel taxiway are severe (i.e., less than 183 m.). However, the ending radius of curvature of only 244 m. might be a limiting factor in the operational capabilities of this exit to handle large aircraft above 17 m./s. (37 knots) in a routine basis. The FAA is currently engaged in evaluating this geometry in the Boeing 727-200 simulator and in a real aircraft.

The publication of Advisory Circular 150/5300-12 [FAA, 1983] incorporated several significant changes to the well established 30 degree angle exit geometry adopted in the early seventies.The most notable change has been the incorporation of a 427 m. (1400 ft.) spiral transition curve to smooth the initial aircraft path while transitioning from a straight line path (i.e., an infinite radius centerline track) to a finite centerline turnoff trajectory.

Regarding the optimal location of runway turnoffs the problem has been researched in at least four well documented instances. Horonjeff et al. [Horonjeff et al., 1961] proposed an optimization model based upon the maximization of the aircraft arrival acceptance rate under saturated operational conditions. The main problem with this model however, was the uncertainty of input parameters in terms of bivariate random variables represented by the mean distance and time for an aircraft to decelerate to a predetermined exit speed. This model could not address airfield specific environmental factors nor aircraft operational variables (e.g., aircraft landing weight variations) dictating the landing distance and time

distributions.

In 1974, Daellenbach [1974] developed a dynamic programming model which in many respects is equivalent to the Horonjeff's approach with added extensions. Daellenbach removed the assumption of a specific arrival pattern thus adding more realism to the model. Daellenbach's model. however, also requires the knowledge of joint landing distributions which are in fact difficult to assess unless extensive data is available under many scenarios.

In a parallel effort Joline [Joline, 1974] developed another dynamic programming model to find the optimal number of exits and their locations with respect to the combined objective function of ROT and exit construction cost. While Horonjeff's model and Daellenbach's model required the joint distributions of landing distance and time for each aircraft type, Joline's model used a univariate distribution of 'ideal exit location' for a mixed aircraft population. Joline classified aircraft into three categories based on the aircraft size, and found the distributions of ideal exit locations for these three aircraft classes based on the observations of aircraft landing operations in Chicago O'Hare Airport. The ideal exit location distribution for entire aircraft population was found by combining the three distributions according to the proportions of the three aircraft classes. As mentioned earlier, there are several factors influencing the aircraft landing distance such as the design exit speed, landing weight, etc. Joline's model, like the previous models, did not address these variables.

The last effort in the optimal location of runway exits was performed at the Center for Transportation Research at Virginia Tech. The effort in the previous research phase was to develop algorithms suitable to be used in a realistic airport environment with the inclusion of several aircraft specific variables in the model developed. This work suggested the use of a a combination of a dynamic programming algorithm with continuous simulation producing an first generation REDIM model [Sherali et al., 1991; Trani and Hobeika et al., 1990]. This new phase tries to expand on the notions previously reported and incorporates more flexibility and realism to the existing REDIM model.

1.3 Research Objectives

The purpose of this research is to investigate the viability of optimizing the location and geometric design of rapid runway turnoffs and develop a computer simulation model to execute these tasks in a routine and interactive basis. This report represents a second phase in a task to fully develop and implement rapid runway turnoffs under realistic airport scenarios as part of the research program sponsored by the Federal Aviation Administration and NASA to reduce the service time of current and future runway facilities. This report builds upon algorithms to developed in Phase I using an integrated dynamic simulation and dynamic programming approach to estimate optimal runway turnoff locations minimizing the weighted average runway occupancy time, WAROT. This phase enhances the features of the Runway Exit Design Interactive Model (REDIM) whose preliminary development was reported in FAA/DOT research report RD-90/32,I [Trani and Hobeika et al., 1990].The model was revised to provide variable angle turnoffs consistent with FAA safety standards and ultimately to design guidelines and operational issues associated with newly developed turnoff geometries.

The Runway Exit Design Interactive Model version 2.0 (REDIM 2.0) developed in this research effort, incorporates several upgrades from its predecessor in order to provide added flexibility in the estimation of optimal turnoff locations and geometries. The model, like its predecessor, addresses specific airfield variables that affect the landing performance of the aircraft as well as important operational constraints (e.g., aircraft mix) that have a direct impact on the selection of the turnoff location and their geometry. The model is comprised of three modules: 1) an interactive input module, 2) a dynamic simulation and optimization module to estimate the ROT times for individual aircraft and their optimal exit locations and 3) an output module to show graphically and in tabular form the suggested runway turnoff configuration and display some measures of effectiveness of aircraft landing operations. The program contains a library of geometric and operational aircraft characteristics to allow the analyst to choose from a wide selection of aircraft operating under realistic airport conditions. Enhancements to the input module allow quick prototyping of various runway scenarios through very simple data input screens.Also enhancements to the output capabilities of the program have been made to facilitate the output of hard copies in a variety of printers.

The program considers four broad types of analyses: 1) evaluation of an existing runway, 2) improvement of an existing runway 3) design of a new runway facility and 4) individual aircraft landing roll behavior. In the evaluation mode REDIM estimates several measures of effectiveness indicative of the operational capabilities of an existing runway facility. In this mode the user inputs the number, type and location of existing turnoffs as well as the relevant aircraft population data and the model predicts the average runway occupancy time (WAROT), the particular exit(s) that an aircraft can take, and the probability of each aircraft taking the assigned exit(s). Another potential use of this mode is to serve as a benchmark to perform valid comparisons between different runway alternatives.

The second mode of operation deals with the redesign of a runway facility. In this scenario it is expected that the user might want to explore the possibility of adding new high-speed turnoffs to an existing facility and examine their impact in the operational efficiency of the facility. Inputs in this mode are the number and type of existing turnoffs, their locations, the number of new turnoffs to be constructed and a reliability parameter. The outputs are the location and geometry of each new turnoff, the weighted average runway occupancy time, and an aircraft assignment table containing individual runway occupancy times and the individual aircraft probabilities of taking every existing and new exits.

In the third mode of operation REDIM estimates the optimal location of runway turnoffs and their corresponding geometries. An assignment table is given to the user indicating the turnoff(s) associated with each aircraft and their individual runway occupancy times. The weighted average runway occupancy time is also estimated as a global runway operational parameter and sensitivity studies can easily be conducted by changing the number of turnoffs allocated to a specific runway. Inputs by the user in this mode are the number of exits to be constructed and the desired exit reliability parameter.

The fourth mode addresses an individual aircraft landing roll scenario where the user wants to know specific results about the expected runway occupancy time and landing roll dynamics of a particular aircraft. This mode is primarily envisioned to serve as an individual calibration tool for critical aircraft analyses.

More detailed descriptions of these four modes of operation will be given in the remaining chapters of this report. REDIM blends the principles of continuous simulation with those of mathematical optimization to find the best turnoff locations and corresponding turnoff geometries for a myriad of possibilities. The program was designed to be interactive and a great effort was made to reduce the number of inputs expected from the user. A large aircraft data base is included to simplify the analyst input task but flexibility is also built-in to allow future aircraft additions. The overall effort was to make the program interactive and easy to use. Many suggestions from previous users have been incorporated in this new version and extra features have been added to extend the flexibility of the program.

1.4 Methodology

1.4.1 Monte Carlo Simulation Technique

In the development of REDIM 2.0 a great deal of effort has been made to realistically simulate aircraft operations as they would occur in actual practice. Due to the stochastic nature of aircraft landing roll deviations observed in practice [HNTB, 1975; Koenig, 1978; Ruhl, 1989] its was decided to use a Monte Carlo simulation procedure in the dynamic simulation algorithms embedded into REDIM 2.0. The Monte Carlo simulation technique used here was primarily to estimate landing roll distance dispersions using aircraft normal distributions for some of the aircraft parameters dictating landing roll performance.

1.4.2 Interactive Software Package

The software package developed as part of this research consists of three important modules: 1) Input, 2) Dynamic Simulation/Optimization and 3) Output routines. The model called REDIM 2.0 incorporates significant improvements over its predecessor, REDIM 1.5, described in detail by Trani and Hobeika et al. [Trani and Hobeika et al., 1990]. Chapter 5 in this report fully documents the software package developed as part of this research. A users manual of the software is also available.

1.5 Differences with Previous REDIM Model

REDIM 2.0 incorporates several enhancements from its predecessor that add flexibility to every analysis. Differences in the new program encompass all three modules but specifically the dynamic and optimization routines have been improved to allow Monte Carlo simulations of landing aircraft operations. Additions to the new program have been primarily to account more realistically for variations in the aircraft landing dynamics. Weight factors have been added to the program to represent more accurately aircraft landing conditions at the airport facility of interest.

1.5.1 Aircraft Landing Weight Factors

The aircraft weight factor is a nondimensional parameter varying from 0 to 1 representing the proportion of the useful load carrying capacity of an aircraft at any point in time. The landing load factor is a major determinant of the aircraft nominal approach speed of a vehicle. The load carrying capacities of certain aircraft make their approach speed range large enough to justify the inclusion of this parameter in REDIM 2.0. A Boeing 727-200 for example has a 30 knot differential between the approach speeds at the operating empty and maximum landing weights and ISA, wet airfield conditions [Boeing, 1986].The reference landing runs at these two extreme landing weights are 1190 and 1615 m., respectively, thus providing an idea of the large variations in landing roll performance for transport-type aircraft.

1.5.2 Aircraft Landing Data Generation Methods

In the optimization procedure used in REDIM it is necessary to emulate a large number of aircraft operations through a Monte Carlo simulation procedure in order to assess accurately the landing distance dispersions of a large aircraft population.This procedure although more accurate necessitates considerably longer running times. Chapter 3 in this report describes in detail the basic assumptions regarding the aircraft kinematic behavior and the probability density functions used in estimating landing roll parameters.

1.5.3 Addition of Runway Reference Analysis

Another addition to the current computer simulation/optimization model has been the provision of a runway reference analysis run that estimates the lower boundaries of runway occupancy time gains for a specific scenario.The main purpose of this reference run is to provide the analyst with a "benchmark" result of the minimum WAROT value attainable for a runway under "extremely favorable" conditions with no consideration of the physical, lateral runway constraints. The reference run is an option provided to the user and it is recommended in order to give some insight of potential WAROT reductions. This reference run is executed using the highest exit speeds available for each one of the aircraft TERP categories and no lateral constraint limitations (i.e., no closely spaced taxiways). Also the number of exits is iterated to yield the lowest WAROT. The end result represents a fictitious runway with the minimum WAROT parameter that the user should anticipate under extremely ideal conditions. The provision of this reference run is aimed at those individuals not readily familiar with the concept of runway occupancy time and with typical aircraft/airport operational parameters.

1.5.4 Range Solution for Exit Locations

Due to the stochastic nature of the problem the solutions provided by REDIM 2.0 represent ranges of solutions to locate turnoff exit locations rather than a deterministic location as in REDIM 1.0. The motivation behind this approach is to provide optimal location ranges where the construction of a new turnoff yields near similar WAROT values for a given aircraft population and airport environmental conditions.This approach should point out the analyst sensitivity of the model to input parameters.The range solutions for turnoff

locations are derived from five internal iterations performed for all the aircraft data selected by the user. All five runs use different pseudorandom numbers and therefore have the same weightage in the solutions presented. More details of this method are presented in Chapter 3 of this report.

CHAPTER 2

Dynamic Formulation of Aircraft Landing Processes and Simulation

2.1 Model Formulation

The aircraft dynamic model used in this new version of REDIM has been enhanced with better deceleration heuristics providing more fidelity in the simulation process. Just like in REDIM 1.0 the aircraft landing maneuver starts at the runway threshold crossing point and ends at a point where the aircraft wingtip clears the imaginary, vertical plane defined by the runway edge. The aircraft landing phases modeled in all REDIM versions are: 1) an air phase, 2) a free roll segment between touchdown and the initiation of braking, 3) a braking phase, 4) a second free roll phase between the end of the braking phase and the start of the turnoff maneuver and 5) the turnoff maneuver phase. These landing phases are depicted graphically in Fig. 2.1. It can be seen from this figure that the major contributors to runway occupancy time are the braking and turnoff phases as these usually take about 60% and 25%, respectively of the total ROT.

2.1.1 Air Phase

The air distance can be estimated assuming the longitudinal flight path of landing aircraft is a compound of a linear descending maneuver and a circular arc flare maneuver. Lan and Roskam [Lan and Roskam, 1981] suggested an analytical expression for estimating air distance, which is:

$$S_{air}=\frac{h_{th}}{\gamma} + \frac{v_{fl}^2 \gamma}{2g(n_{fl}-1)} \qquad (2.1)$$

FIGURE 2.1 **Aircraft Landing Roll Phases Modeled.**

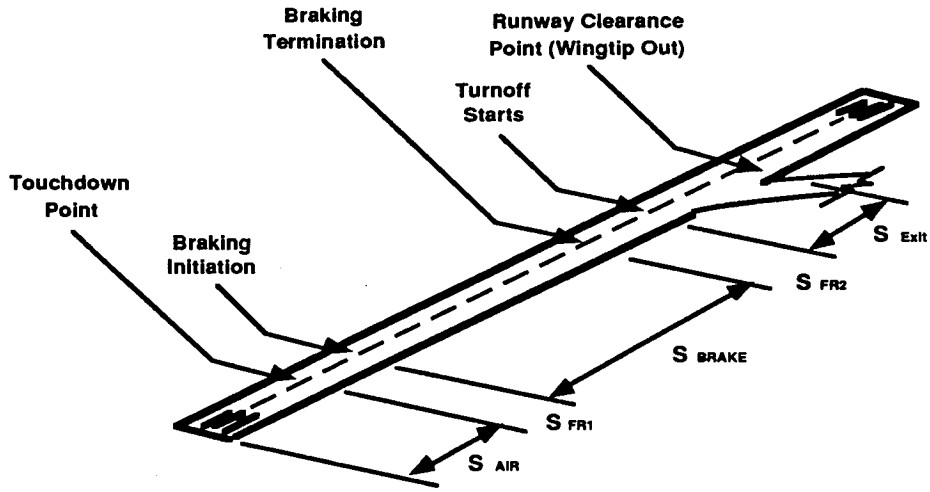

S_{AIR}	Air Distance to Touchdown
S_{FR1}	Free Roll Distance Between Touchdown and Application of Brakes
S_{BRAKE}	Braking Distance
S_{FR2}	Free Roll Distance Between Brake Termination and Start of Turn
S_{Exit}	Longitudinal Exit Distance to Clear the Runway

where

S_{air} = air distance (m)

h_{th} = threshold crossing altitude (m)

γ = tangent value of descending angle

v_{fl} = flare speed (m/s)

g = acceleration of gravity (m/sec^2)

The first and the second terms of Eqn. 2.1 represent two distinct segments used to model the air distance as shown graphically in Fig. 2.2.

FIGURE 2.2 **Final Flight Path Diagram.**

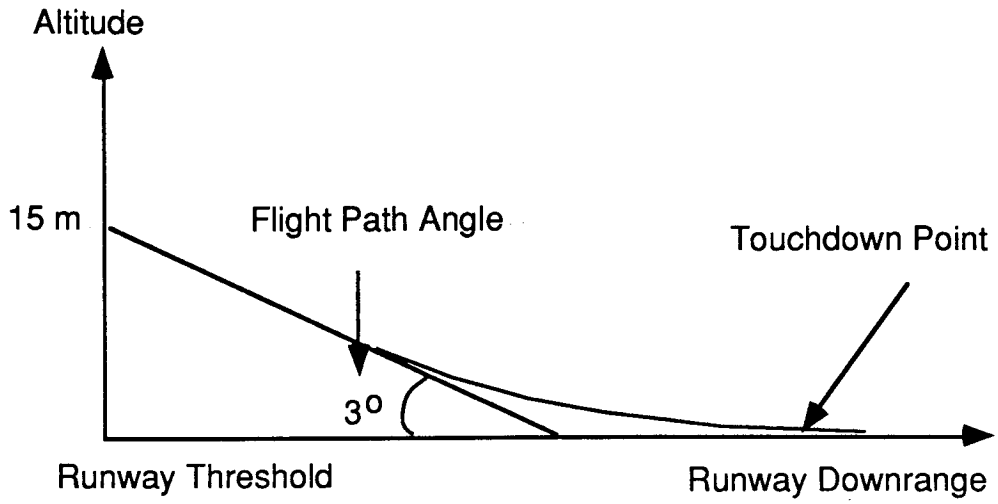

The flare speed is less than the approach speed (v_{app}) due to the in-air deceleration and is assumed to be 95% of v_{app}. The approach speed is assumed to be 1.3 times the stalling speed (v_{stall}) at which the aircraft gets the lifting force just enough to fly. The stalling speed is determined by aircraft geometric and performance characteristics using the following formula:

$$V_{stall}=\sqrt{\frac{2\,M\,g}{\rho c_{atm} cl_{max} A_w}} \tag{2.2}$$

where

v_{stall}: stalling speed (m/sec)

M: aircraft mass (kg)

g: gravity acceleration (m/sec^2)

ρ : standard air density (kg/m^3)

c_{atm}: correction factor for atmosphere condition (unitless)

cl_{max}: maximum landing lift coefficient (unitless)

A_w: wing area (m^2).

The air density (ρ) in the standard atmosphere condition, sea level altitude and 15° C temperature, is 1.225 kg/m^3. The air density varies according to the atmospheric condition, and c_{atm} reflects the changes in the air density. An important factor determining the v_{stall} is cl_{max} which belongs to aircraft characteristics. This factor varies from aircraft to aircraft, and its magnitude ranges from 1.4 to 3.0. The landing weight also influences the stalling speed. The landing weight is determined by the landing weight factor whose distribution information is provided by the analyst. The computation of landing weight based on the landing weight factor is explained in Section 2.3.3.

The duration of the flying phase is simply estimated by dividing the air distance by the average flare speed. That is,

$$t_{air}=\frac{s_{air}}{v_{fl}} \tag{2.3}$$

2.1.2 Free Roll Phases

Two free roll run phases arise during a typical aircraft landing operation: 1) prior to the braking operation after touchdown and 2) prior to the turnoff maneuver after finishing the braking operation phase. The first free roll phase is to simulate an inherent human delay before initiating the braking mechanisms such as thrust reverses, spoilers, and/or normal wheel brake. The second free roll phase is to mimic a delay time arising from the proper suppression of braking action and a recognition of the turnoff geometry prior to exiting the runway. The duration of each phase is specified by user. Nominal values of 3 and 2 seconds are assigned to the first and second free roll phases, respectively. However, the analyst may increase the values if there are proper reasons such as poor visibility.

In this analysis both free roll phases are assumed deterministic because they constitute a relatively small portion of the entire landing process. Moreover, note that free roll deceleration is neglected for the sake of simplicity. With the assumptions above, the free roll distances (s_{fr1},s_{fr2}) are calculated as follows:

$$s_{fr1}=v_{td}\, t_{fr1} \tag{2.4}$$

where

s_{fr1}: the first free roll distance

v_{td}: touchdown speed

t_{fr1}: the first free roll time

$$s_{fr2}=v_{ex}\ t_{fr2} \tag{2.5}$$

where

s_{fr2}: the second free roll distance

v_{ex} : exiting speed

t_{fr2}: the second free roll time

Notice here that v_{td} is assumed to be 90% of v_{app}. The exiting speed v_{ex} is a constant specified by the analyst.

2.1.3 Braking Phase

Under normal conditions, the braking phase constitutes the largest component of the landing process. Hence, it becomes necessary to estimate with some accuracy the distance and duration of the braking phase if one is to have some confidence in the total distance and duration estimation of the whole landing process. The braking distance and duration is determined by the braking capability of an aircraft at given touchdown speed and exiting speed. The braking capability (or deceleration rate) varies from aircraft to aircraft and is also affected by the runway surface wetness and longitudinal runway gradient. It is desirable to estimate the deceleration rate for each aircraft and then to modify that rate according to the runway condition of the airport.

A nominal deceleration rate is estimated by using the landing run distance requirement provided by the aircraft manufacturer. The braking distance for the complete stop is found by subtracting the air distance and free roll distance from the landing run distance. Knowing the braking distance, the initial speed (v_{td}), and a zero final speed, the nominal deceleration rate is estimated using the following equation:

$$a_{nom}=\frac{-v_{td}^2}{2(l_r-s_{air}-s_{fr1})} \tag{2.6}$$

where

a_{nom} : nominal acceleration (m/sec^2)

v_{td} : touchdown speed (m/sec)

l_r : landing run distance (m)

s_{air} : air distance (m)

s_{fr1} : free roll distance before braking (m).

Note that l_r is provided by the aircraft manufacturer as an aircraft characteristic datum and that s_{air} and s_{fr1} are determined by Eqs. 2.1 and 2.3. The touchdown speed (v_{td}) is assumed to be 90% of the approach speed. In Eq.2.5, a_{nom} always takes a negative value.

The aircraft deceleration is modified by runway surface condition (e.g., wet or dry) and longitudinal gradient. Mathematically the actual aircraft deceleration, a_{act}, is:

$$a_{act}=a_{nom}\, c_{wet}\, c_{slope} \tag{2.7}$$

where

$$c_{wet}=\begin{cases} 1., & \text{if runway is dry} \\ .87, & \text{if runway is wet} \end{cases}$$

$$c_{slope}=\{1.0+0.015(\text{average gradient})\}$$

With the actual deceleration of an aircraft, the distance and duration of the braking phase are found by,

$$s_{br}=\frac{(v_{ex}^2-v_{td}^2)}{2a_{act}} \tag{2.8}$$

$$t_{br}=\frac{2s_{br}}{(v_{ex}+v_{td})} \tag{2.9}$$

2.1.4 Turnoff Phase

The purpose of the turnoff phase is to trace the aircraft path throughout the exit maneuver and to estimate the time consumed in the turnoff up to the clearance point. A model is adopted with some modifications to perform this purpose. The exiting maneuver begins when the aircraft decelerates to the user-defined exiting speed and ends with a complete clearance of the runway as depicted in Fig. 2.3. It is assumed that the wingtip dictates the

clearance of runway, which is generally true for all aircraft at high speed exiting. The only exceptions occur at low exit speeds or when an aircraft has an abnormally large tailplane span (STOL aircraft). Since the objective of this research is to investigate the effectiveness of high speed exits, these exceptions would seldomly occur.

FIGURE 2.3 Generalized Aircraft and Turnoff Coordinates.

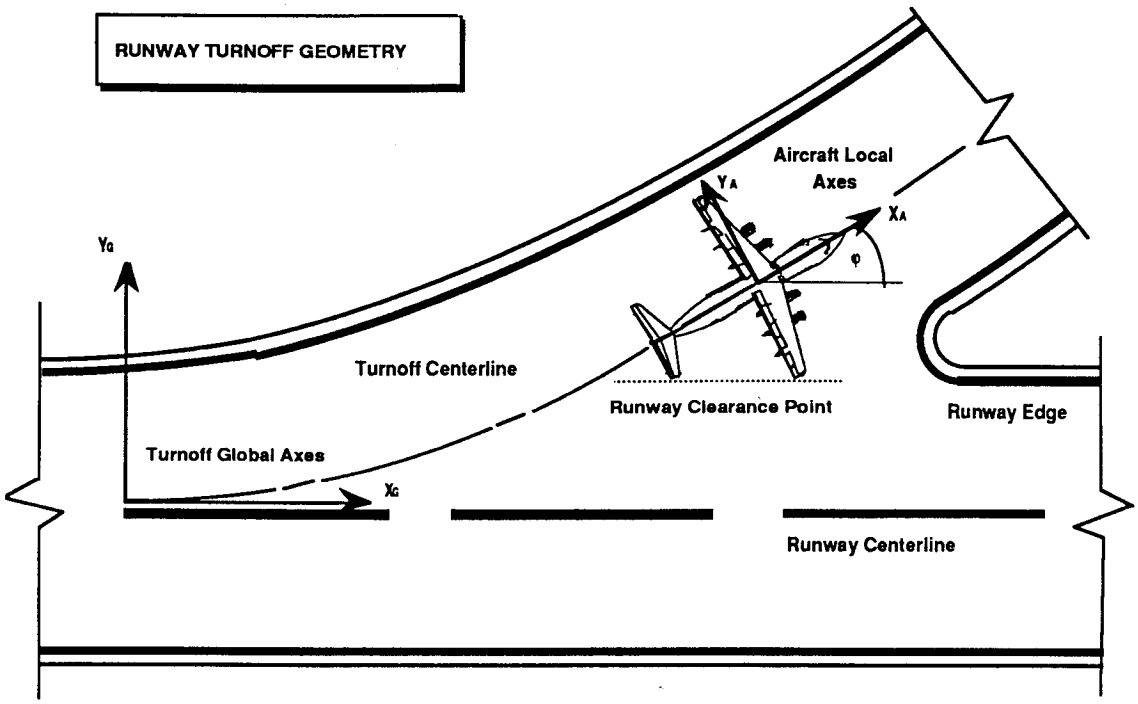

The turning motion of an aircraft at a speed, at which aerodynamic forces are insignificant, can be simply characterized by forces acting on the nose gear. An algorithm developed by Schoen et al. and used in a previous NASA research effort on this topic considers three side force contributions acting on the aircraft nose gear: 1) the centripetal force, 2) the aircraft inertia, and 3) the tire scrubbing resistance to the turn [Schoen et al., 1985]. That is, the total side force acting on the aircraft nose gear is compound of the centripetal force, the aircraft inertia and the tire scrubbing force. The side friction coefficient at skidding condition (f_{skid}) is the sum of the coefficients of above three contributions. Mathematically,

$$f_{skid}=f_c+f_{sc}+f_{Izz} \tag{2.10}$$

where

f_{skid}: nose gear tire skid friction coefficient

f_c : the centripetal acceleration contribution

f_{sc} : the tire scrubbing resistance.

f_{Izz}: the aircraft inertia contribution to the nose gear side load

Originally, Schoen et al. fixed the skid friction coefficient as a conservative value (0.2). It, however, is well documented in the literature that the skid friction coefficient is a function of aircraft tire pressure and speed, among other variables [Harrin, 1958: Wong, 1978]. A summary of this functional relationship is depicted graphically in Fig. 2.4, where four aircraft type categories are represented (i.e., four tire pressures characteristic of each TERP category). The upper curve corresponds to a tire pressure of 50 PSI which is a representative value of TERP A category aircraft. Similarly, the fourth lowest curve corresponds to a tire pressure of 200 PSI, a typical tire pressure of current transport aircraft. Instead of using a single value as the skid friction coefficient, the coefficient is selected from Fig. 2.4 considering the exit speed and aircraft type.

FIGURE 2.4 **Side Skid Friction Coefficient Variations with Speed.**

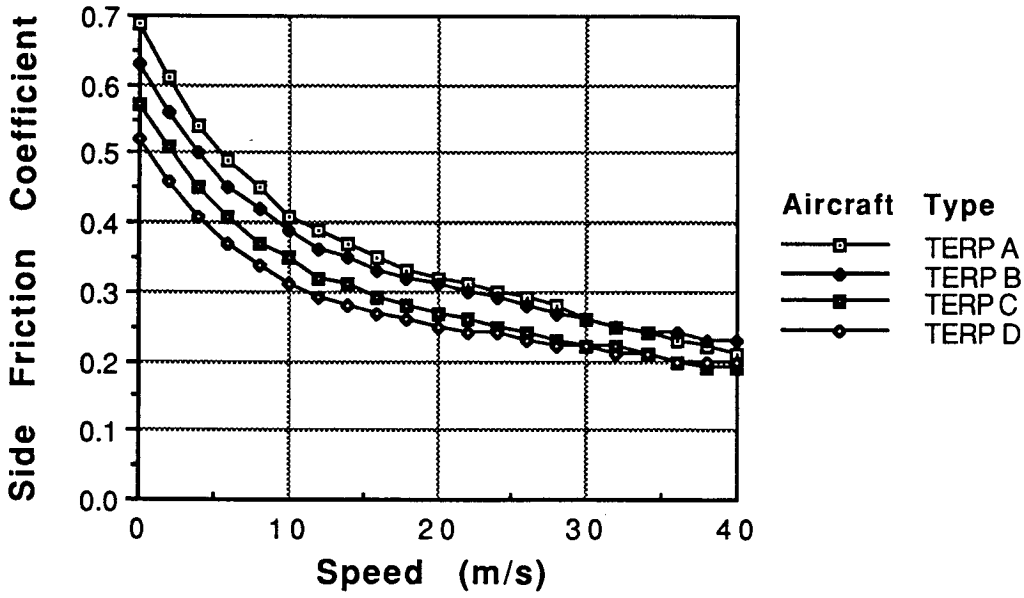

As shown in Eq. 2.10, the skid friction coefficient is modeled as the sum of three terms. These terms are calculated as follows:

The contribution of the centripetal acceleration is:

$$f_c=\frac{v^2}{g\,R} \tag{2.11}$$

where

v: instantaneous speed of the aircraft (m/sec)

R: instantaneous radius of the curve (m)

g: acceleration of gravity (m/sec^2)

The tire scrubbing resistance (f_{sc}) is determined by aircraft mass and the instantaneous radius. The relationship of these variables is depicted in Fig. 2.5.

FIGURE 2.5 Variations of Tire Scrubbing Coefficient with Radius of Curvature.

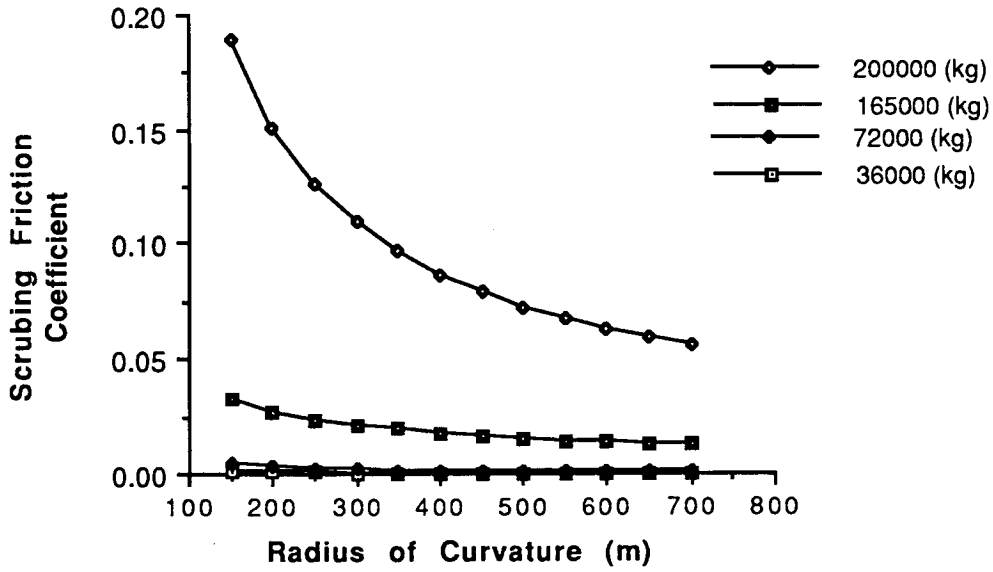

At last, the contribution of aircraft inertia to side load on nose gear is:

$$f_{Izz}=\frac{Izz\left(\frac{-v\dot{R}}{R^2}\right)}{M\,g\left(1-\frac{lm}{100}\right)w_b\frac{lm}{100}} \tag{2.12}$$

where

Izz: moment of inertia about the vertical axis (kgm^2)

v: instantaneous speed (m/sec)

R: instantaneous radius of curvature (m)

R-dot: instantaneous rate of change of radius

M: aircraft mass (kg)

g: acceleration of gravity (m/sec^2)

lm: percentage of aircraft mass loaded on main gear (%)

w_b: aircraft wheelbase (m)

Solving Eq.2.12for R-dot gives:

$$\dot{R}=\frac{f_{Izz}R^2}{Izz\,v}\left\{M\,g\,w_b\frac{lm}{100}\left(1-\frac{lm}{100}\right)\right\} \tag{2.13}$$

With a given aircraft type, for every instantaneous speed and instantaneous radius of curvature, the values of f_{skid}, f_{sc} and f_c can be found via Fig.2.4, Fig.2.5 and Eq.2.11. By substituting these values into the Eq.2.10, the value of F_{Izz} is found. By substituting the F_{Izz} value into Eq.2.13, R-dot can be computed for every instance.With the instantaneous values of R and v, the transient radius of curvature, R_t, can be calculated by integrating R-dot forward in time. That is,

$$R_t=\int_0^t \dot{R}\,dt \tag{2.14}$$

The coordinates of an aircraft's turning path can be calculated by integrating the instantaneous speed multiplied by the sine and cosine value of heading angle. That is,

$$X_t=\int_0^t v\cos(\psi)\,dt \tag{2.15}$$

$$Y_t = \int_0^t v \sin(\psi)\, dt \qquad (2.16)$$

where

X_t: longitudinal coordinate of turning path at time t (m)

Y_t: lateral coordinate of turning path at time t (m)

v: instantaneous speed of aircraft (m/sec)

Ψ: instantaneous heading angle of aircraft (degree)

It should be noted that this simplification may apply only to a speed up to two thirds of the touchdown speed, because this speed is known to be the threshold for significant aerodynamic control for conventional aircraft [Miller and Thomas, 1963]. Even with this restriction, the evaluation of turnoff maneuvers can be accomplished for a large variety of aircraft whose turnoff speed ranges from 10 to 45 m/sec (22.3 - 100.4 MPH). Turnoff design speeds above 45 m./s. are unlikely to ever be used due to possible aircraft ground control problems. The lifting forces acting on the aircraft at high speed can be included in the above equations by modifying the aircraft mass term accordingly.

Another modification on this algorithm is the incorporation of the free roll deceleration during the turnoff phase. Since turnoff phase requires a fairly large amount of time unlike the free roll phase, the free roll deceleration should not be neglected in turnoff phase. The free roll deceleration is assumed to be -0.375 m/s^2 . Hence, the instantaneous speed in the above equations is reduced by this deceleration rate.

The integration of Eqs.2.14 to 2.16 is computed numerically for every 0.01 of a second. Along with the x-y coordinates of the turning path, the position of the wingtip is also computed at every step in the numerical integration until the wingtip leaves the runway boundary. Turnoff time is defined as the duration from the beginning of the turning maneuver to the instance when the wingtip leaves the runway boundary.

2.1.5 Deceleration Distance and ROT

Runway occupancy time as defined in this report represents the time interval between aircraft threshold crossing point and when the aircraft wingtip has cleared the runway edge imaginary line. The estimations of runway occupancy time encompasses the five landing phases explained previously. The corresponding time parameters are: 1) time to touchdown, 2) a free roll time between touchdown and the initiation of braking, 3) braking time, 4) a second free roll time between the end of the braking phase and the start of the turnoff maneuver and 5) the turnoff time. Although at first glance it might seem that the contribu-

tion of the turnoff component is not significant even for moderate speeds (using a typical high-speed turnoff) could amount to 12-13 seconds or about one fourth of the total runway occupancy time.

By definition, the total distance for an aircraft to decelerate to a specified exiting speed is calculated as the sum of distances in the air, free roll, and braking phases, and that ROT is found as the sum of durations of the air, free roll, braking, and turnoff phases. Mathematically,

$$s_{tot}=s_{air}+s_{fr1}+s_{br}+s_{fr2} \tag{2.17}$$

$$t_{tot}=t_{air}+t_{fr1}+t_{br}+t_{fr2}+t_{toff} \tag{2.18}$$

2.2 Data Generation via Monte Carlo Simulation

The landing roll performance of an aircraft is stochastic in nature. For example, the touchdown location and deceleration rate varies for each landing resulting in the different total landing roll distance. In order to incorporate this stochastic nature of landing process into the model, four variables are selected as random variables: the threshold crossing altitude, final flight path angle, landing weight and deceleration. By FAA regulations [FAR 25], the pilots are requested to maintain the threshold crossing altitude and flight path angle as 15m and 3 degree, respectively. To represent the variations in the altitude and the angle, the standard deviation of the altitude and the flight path angle are set to 1.5m and 0.15 degrees, respectively. The mean and standard deviation of landing weight factors for each category is given by the analyst. The mean deceleration rate is estimated by the method explained in section 2.1 and the standard deviation of deceleration rate is set to 7% of the mean value. To improve the model's capability to predict the actual aircraft landing performance, these parameters will be calibrated with field observations and with high fidelity flight simulators such as FAA B-727-200 simulator in Oklahoma City. During the third phase of this research, the calibration of these parameters will be performed as described in Chapter 7.

For an optimization analysis, 200 landing distance data points are generated for each aircraft type via a Monte Carlo simulation. The Monte Carlo simulation is a tool for analyzing a stochastic system by generating random numbers for each random variable involved in the system. For analyzing the landing roll performance, each landing distance value is generated via following steps:

1. Generate four random numbers from the uniform distribution on the interval [0, 1]

2. Generate the values of the threshold crossing altitude, flight path angle, landing weight factor and deceleration rate from truncated normal distribution using the random numbers generated in step 1

3. Calculate the landing distance and deceleration time by substituting the values of four random variables into the dynamic formulation described in section 2.1

4. Repeat the step 1 to 3 two hundred times.

Step 1 is performed by utilizing RND() function of Microsoft BASIC version 7.0. Step 2 is performed by inverse transform method using truncated normal distributions with parameters described previously. Since normal distribution does not have a simple closed form of the inverse cumulative density function, a polynomial approximation of inverse cumulative density function is used for generating the random numbers from normal distributions [Beasley and Springer, 1977]. The method for generating random variables from a truncated distributions is described in Law and Kelton [Law and Kelton, 1982]. Step 3 is a simple calculation, because all the equations and the values of all the variables are known.

2.3 Enhancements of the Model in Phase II

2.3.1 Enhanced Braking Algorithm

The new braking algorithm incorporates a new exit "seeking" deceleration procedure that changes the deceleration of the vehicle as a function of the distance to go to the next available exit. The inclusion of feedback from the current aircraft position on the runway allows shorter runway occupancy times and also seems to represent the pilot's behavior under real airport conditions. To illustrate this new method adopted in REDIM 2.0 refer to Fig. 2.6. Two distinct aircraft deceleration phases are identified: 1) a nominal deceleration phase where the pilot applies an average braking effort and 2) an adjusting braking phase where the pilot modifies continuously the aircraft deceleration schedule to achieve a predefined turnoff speed at the next available runway exit location. A decision point is defined in order to establish the transition between the nominal and the adjusted deceleration phases.

The decision point will generally be a function of variables such as the pilot's eye position with respect to the ground, the airport visibility, the aircraft state variables (i.e., speed, deceleration, etc.), the pilot's situational awareness (i.e., information of various exit locations and their design speeds), and the instantaneous crew workload. Since many of these variables are difficult to validate a simple heuristic rule is used in this approach to determine the decision point in terms of aircraft approach speed solely. This simplification seems valid if one considers that in general the approach speed will dictate to some extent the average workload expected during a typical landing. The faster the aircraft in the approach phase the sooner decisions will have to be made in order to maintain a reasonable safety margin in the landing roll operations. Also, the approach speed is somewhat

correlated with the pilot's eye position in the cockpit for commercial aircraft. This implies that heavy jets will have a definite advantage over general aviation aircraft in reaching their decision point at an earlier stage as pilots have a much better perspective of the location of downrange turnoffs.

In practice pilots flying into an airport facility will probably have knowledge of the approximate exit locations and types of turnoff available for the active runway thus it is likely that they will adjust the aircraft behavior to reach a comfortable exit location at or near a desired exit speed. Figure 2.7 illustrates this heuristic principle using data typical of a Boeing 727-200. The computer simulation results show the adjusted deceleration algorithm and the corresponding individual runway occupancy time for five different turnoff locations and a desired exit speed of 15 m/s. From Figure 2.7 one can see that the braking adjustments start at the decision point for all runs since the same aircraft speed parameters were used in the simulation. The differences in runway occupancy time are solely due to the different adjusting braking rates present once the decision point has been reached.Using the same aircraft and varying the decision point parameter from 100 to 400 m. yields results shown in Figure 2.8. Notice that increases in situational awareness (i.e., increasing the decision point distance) will allow pilots to adjust earlier for a given exit location thus resulting in smaller runway occupancy times. Note that in both cases the adjustments

FIGURE 2.6 Generalized Aircraft Speed Schedule on a Runway.

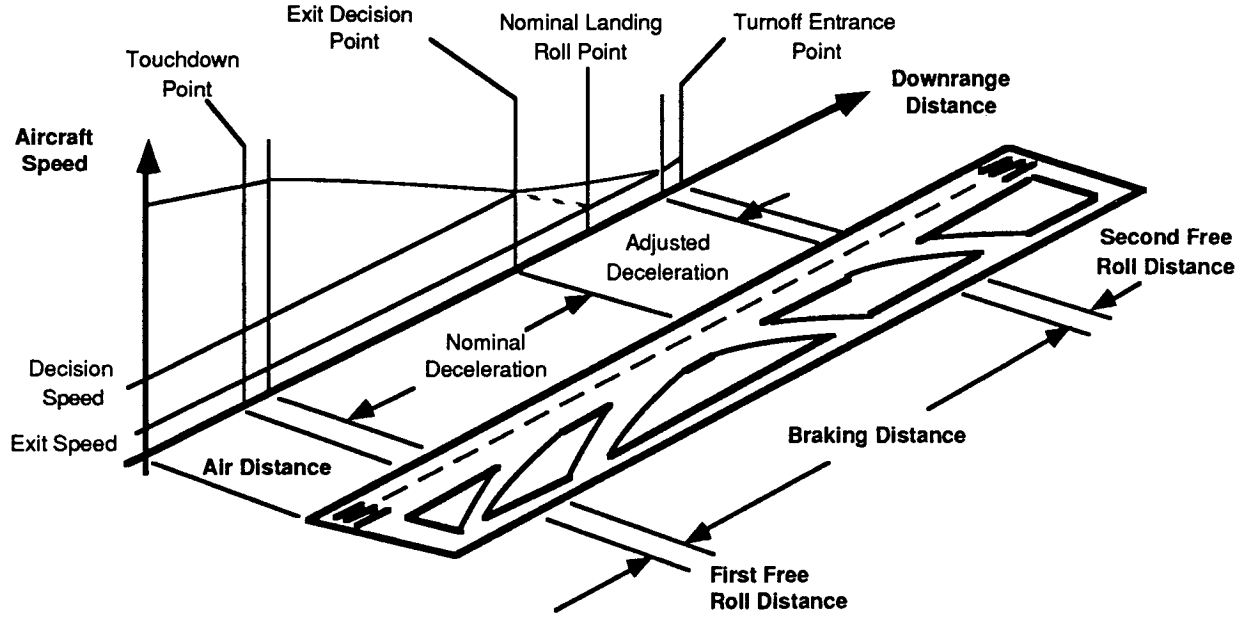

FIGURE 2.7 **Aircraft Nonlinear Deceleration Model Sensitivity for Various Runway Exit Locations.**

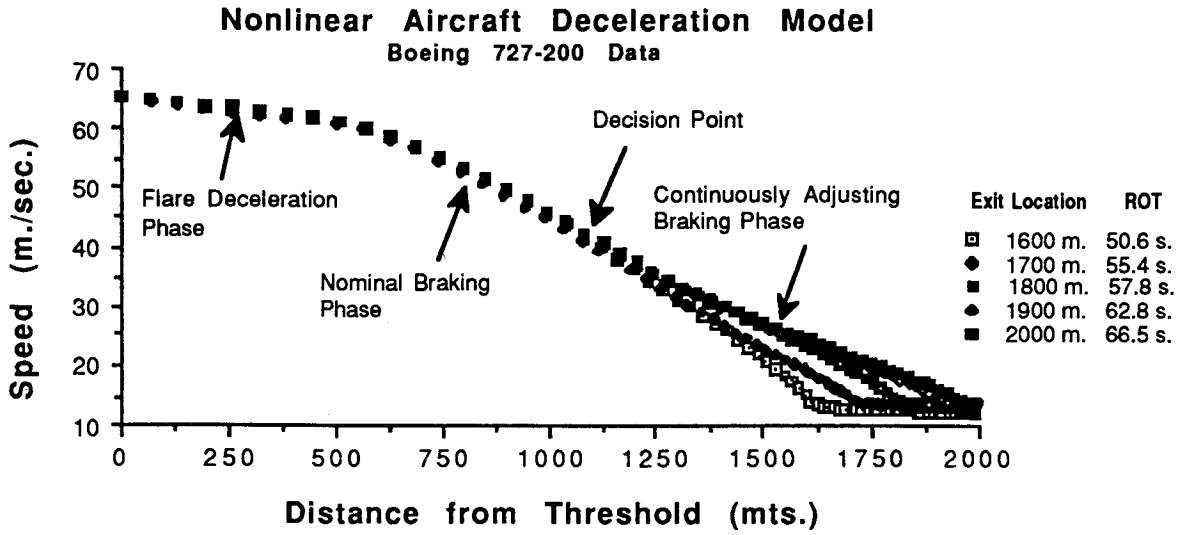

made to the deceleration rate can be easily linearized with little loss in accuracy. This linear approximation of deceleration rate has been embedded into REDIM to simplify the number of internal computations of the model thus reducing CPU time.

2.3.2 Turnoff Algorithm Validation Procedure

The validation of a turning movement procedure has been carried out with the use of a fourth-order aircraft dynamic model considering three degrees of freedom of displacement (lateral, horizontal and vertical motions) and the yawing motion associated with a turning ground vehicle. This model was used to verify the simplified, one degree of freedom aircraft dynamic behavior proposed by Schoen et al. [Schoen et al., 1983] and later adapted by Trani et al. [Trani et al., 1990]. The model estimates the boundaries of a maximum effort turn to verify whether or not a specific turnoff geometry would be feasible under realistic manual control conditions. Results of this model are presented in Figures 2.9 and 2.10 where a turnoff trajectory and tire reaction forces are plotted for a four engine powered business jet [Trani and Zhong,1991].

2.3.3 Aircraft Landing Weight Factors

The aircraft weight factor is a nondimensional parameter varying from 0 to 1 representing the proportion of the useful load carrying capacity of an aircraft at any point in time. The landing load factor is a major determinant of the aircraft nominal approach speed of a vehicle. The load carrying capacities of certain aircraft make their approach speed range large enough to justify the inclusion of this parameter in REDIM 2.0. A Boeing 727-200

FIGURE 2.8 **Aircraft Nonlinear Deceleration Model Sensitivity for Various Decision Point Locations.**

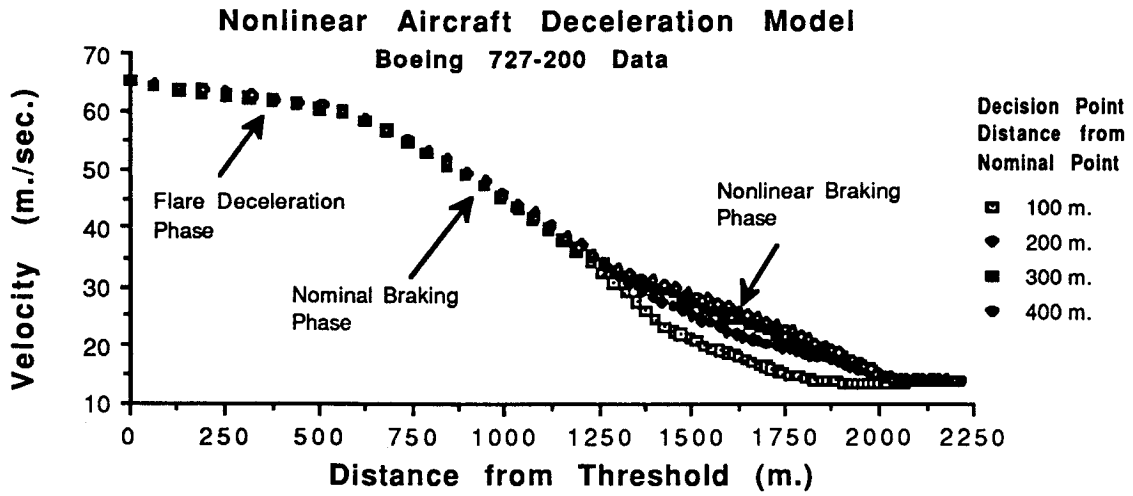

FIGURE 2.9 **Maximum Effort vs. Operational Aircraft Turnoff Trajectory Comparison for a Four Engine Business Jet.**

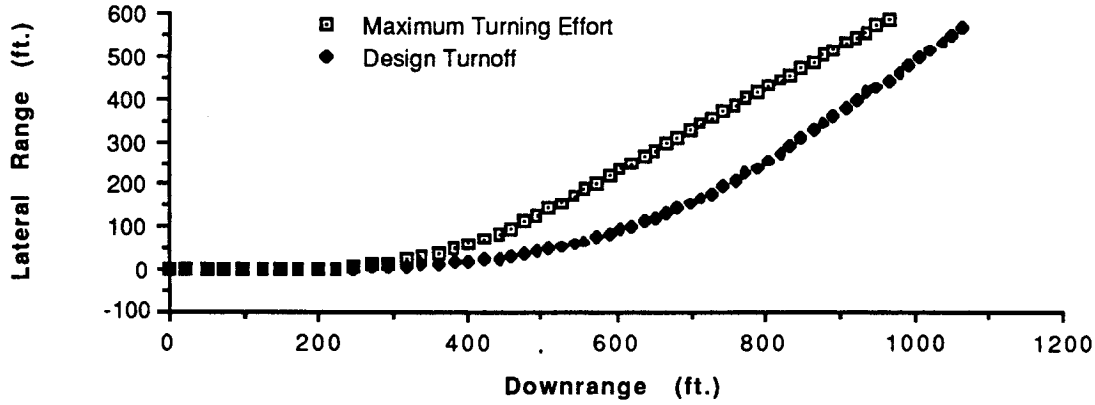

for example has a 30 knot differential between the approach speeds at the operating empty and maximum landing weights, respectively [Boeing, 1986].The reference landing runs at these two extreme landing weights are 1190 and 1615 m., respectively for a wet runway

FIGURE 2.10 **Tire Side Force Histories for Proposed Turnoff Geometries Under a Simple Manual Control Strategy.**

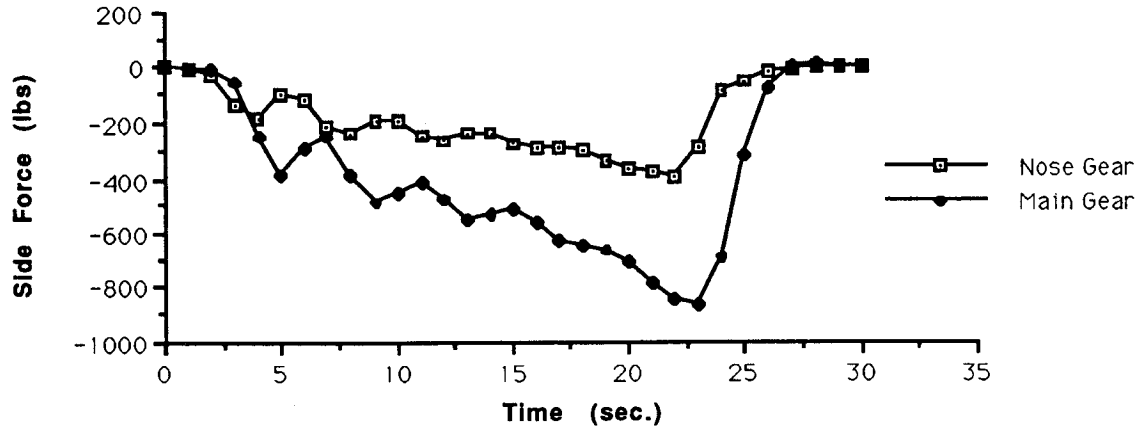

scenario and sea level standard conditions [Boeing, 1985]. Mathematically the weight factor is defined as follows:

$$w_f = \frac{W_{land} - W_{OWE}}{W_{MLW} - W_{OWE}} \tag{2.19}$$

where, w_f is the weight factor for a specific aircraft landing event, W_{land} is the aircraft landing weigh, W_{OWE} is the aircraft operating weight empty and W_{MLW} is the aircraft maximum allowable landing weight. From this definition it is clear that the landing weight of an aircraft can be easily defined in terms of the weight factor as shown below.

$$W_{land} = W_{OWE} + w_f[W_{MLW} - W_{OWE}] \tag{2.20}$$

In practical situations the weight factor is a parameter readily available to the airport engineer and planner since airlines are usually charged landing fees dependent upon the values of landing weights (from which the weight factor can be readily obtained) at all airport facilities.In this fashion it is possible to predict with more accuracy the locations of turnoff geometries for specific airport/airline operational conditions. If data on weight factors is not available the engineer and planner should use high values of w_f in order to provide

some degree of conservatism in the computations. REDIM 2.0 provides default values of w_f in order to ease the task of the analyst as shown in Table 2.1.

TABLE 2.1 Default Landing Weight Factors Parameter Values Used in REDIM 2.0.

Parameter	TERP A	TERP B	TERP C	TERP D
w_f	0.8	0.8	0.6	0.6
σ_{wf}	0.1	0.1	0.1	0.1

Variations of w_f depend heavily upon various airline policies such as fuel reserve factors and stage length segments flown. Data on weight factors can be obtained from airline statistics and should be used in the estimation of runway turnoff locations as this will have a significant payoff in aircraft operations. Airline data suggests that weight factors can in fact be approximated using normal distributions [Credeur and Caprone, 1989]. With this in mind one can approximate the weight factor as a normal distribution with mean w_f and standard deviation σ_{wf} representing operational dispersions of aircraft landing weights. Figure 2.11 depicts a typical weight factor distribution for United Airlines Boeing 737-200A aircraft landing at a major airport facility [Credeur and Capron, 1989].

It is interesting to note that many short haul operations will have weight factors means very close to 0.5 and their standard deviations seem to be below 0.2. In general it is expected that values of landing w_f will increase as the size of the aircraft decreases since the fuel fractions of general aviation aircraft are usually smaller than those of long range transport aircraft [Torenbeek, 1987] thus resulting in proportionately lower landing weights. The airport planner and designer is encourage to investigate specific values of w_f applicable to airlines operating in the facility to be upgraded. If a new facility is to be constructed the planner should also contact airlines in order to have a better assessment of aircraft weight factors.

Figure 2.12 illustrates the expected landing roll distance variations (down to 15 m/s) for a twin engine, heavy aircraft using a high mean weight factor (0.8) and a standard deviation of 0.1. These results were derived from REDIM 2.0 and represent typical values expected in airline practice. In order to have an appreciation of landing roll distance deviations for the same vehicle under different weight factors refer to Figure 2.13 where a low mean weight factor was used maintaining the same standard deviation as that of Figure 2.12.

FIGURE 2.11 **PDF Plot of Boeing 737-200 Weight Factor Variations (Adapted from Credeur and Capron, 1989).**

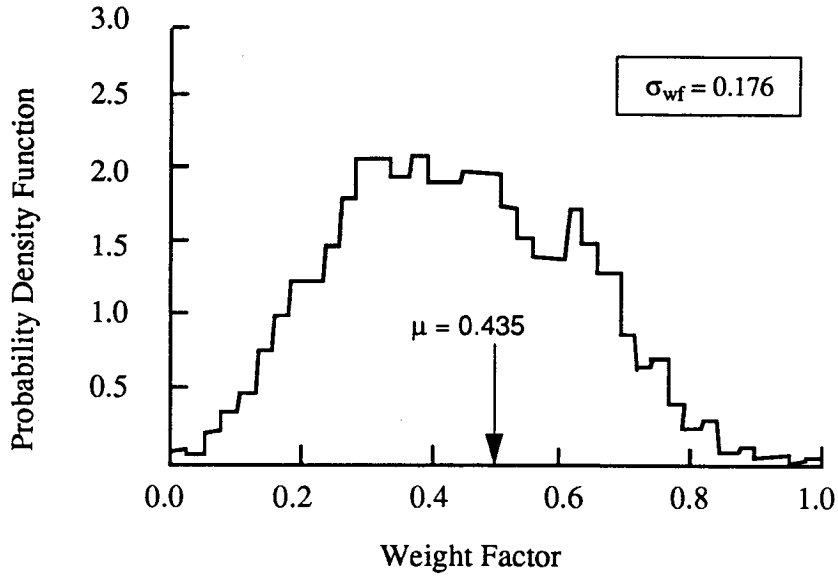

FIGURE 2.12 **Landing Roll Distance Histogram for Airbus A-300-600 (High w_f).**

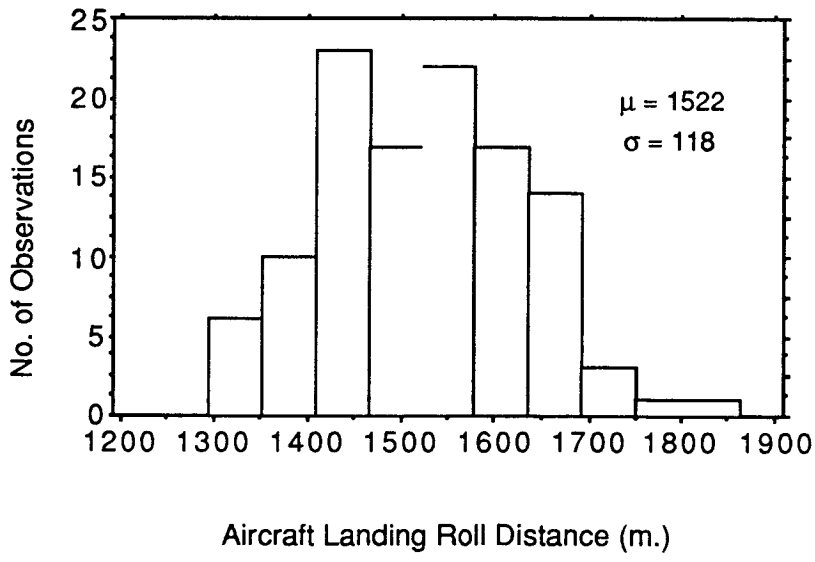

FIGURE 2.13 Landing Roll Distance Histogram for Airbus A-300-600 (Low w_f).

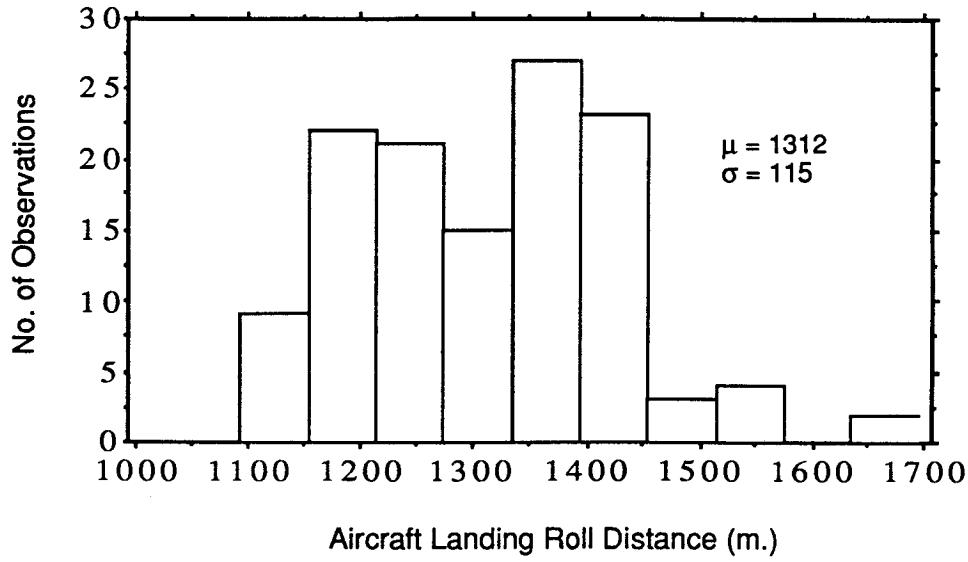

2.4 Turnoff Time Estimation

The computation of turnoff times is explicitly modeled for every aircraft/exit candidate as turnoff times generally account for 15-25% of the total runway occupancy time depending upon the exit type being analyzed. This estimation is executed in REDIM 2.0 using a continuous simulation algorithm predicting the turnoff trajectory of every aircraft from point of curvature to the point where the aircraft wingtip clears the runway edge imaginary plane.The equations of motion for this simulation are shown in detail in Chapter 3.

2.5 Touchdown Variations with Runway Length

It has been observed in practice that pilots have a clear tendency to vary their touchdown point depending upon specific runway characteristics such as location of terminal buildings, runway length, obstacles in the final approach path, etc. Ruhl, for example, observed significant variations in the touchdown point for the same type of transport aircraft for various airport conditions [Ruhl. 1989]. Koenig also observed important motivational behaviors in pilots from various airlines as they landed at two major airport facilities [Koenig, 1974]. With these factors in mind it is possible to establish a correspondence between the touchdown point and the runway length. An even more important consideration from the pilot standpoint is the remaining runway distance available as this is an important parameter the pilot can assess easily from his own experience or looking at runway distance remaining signs. Current FAA regulations for precision runways operated by turbofan/turbojet aircraft mandate the use of runway distance remaining signs providing pilots with direct visual cues on runway length remaining during a landing or takeoff man-

uever [FAA, 1991]. This research is currently addressing pilot behaviors as the runway length is changed to further enhance the validity and realism of the model. Section 7.2.3 describes future experiments to be carried out at the FAA Technical Facility in Oklahoma City to model this important parameter.

CHAPTER 3

Optimization Model and Solution Algorithms

The capacity enhancement of a runway by minimizing weighted average ROT (WROT) of an aircraft mix by locating exits optimally is the primary focus of this Chapter. WROT is the sum of individual ROT weighted with the landing frequency of aircraft comprising the aircraft mix. The individual ROT (IROT) of an aircraft is defined as time interval from the instance at which the aircraft passes over the runway threshold to the clearance of the runway. This time interval can be broken down into two components: 1) deceleration time to reach designated exit and 2) turnoff time. The deceleration time accounts for the flying time from the runway threshold to touchdown point and the ground running time from the touchdown point to the designated exit. The turnoff time accounts for the duration of the turning maneuver from the beginning of the turn to the complete clearance of runway.

3.1 Mathematical Model

In the previous chapter, an estimation scheme for the aircraft deceleration distance and time was developed. Suppose there are R types of aircraft in an aircraft mix, and K environmental scenarios are considered. Since the purpose of the optimization is to find a set of exit locations that minimizes the weighted sum of expected IROT's of the aircraft mix, the objective function should be:

$$\text{Minimization} \sum_{r=1}^{R} \sum_{k-1}^{K} w_r p_k E[\text{IROT}]_{rk} \qquad (3.1)$$

where w_r is the proportion of aircraft type r, and p_k is the chance of scenario k occurring.

The expected value of IROT is indexed by 'rk' because IROT should be estimated for each aircraft type and environmental scenario. Suppose N is the total number of exits to be built. Notice that $IROT_{rk}$ is a function of exit locations or decision variables $(x_1,...,x_N)$. Obviously, x_i's lie on the runway. Hence, $0 \le x_i \le$ runway length (or RL), for i=1,...,N. If we index x_i in an increasing order, then $0 \le x_1 \le .. \le x_N \le RL$. A distance restriction is usually imposed on two adjacent exits for identification and safety reasons. Let the minimum distance between two adjacent exits be D_{min}. Then constraints $x_{i+1} - x_i \ge D_{min}$, for i=1,...,N-1 should be added. The resultant mathematical model for optimal exit location problem is

$$\text{WROT: Min} \sum_{r=1}^{R} \sum_{k=1}^{K} W_r p_k E[IROT;(x_1,...,x_N)]_{rk}$$

$$\text{Subject to } x_{i+1}-x_i \ge D_{min}, \text{ for } i=1,...,N-1$$

$$x_1 \ge 0 \, , \, x_N \le RL \qquad \textbf{(3.2)}$$

3.1.1 Individual Runway Occupancy Time (IROT) Estimation

As stated in Chapter 2, deceleration distances and corresponding deceleration times are generated for each aircraft via Monte Carlo simulation. Suppose we have S deceleration distance data and S corresponding deceleration time data for each aircraft type. Define d^s and t^s as the s^{th} deceleration distance and corresponding deceleration time for s= 1,...,S. That is, an aircraft reaches the given exit speed at the distance d^s consuming t^s in the s^{th} landing trial. Since the same argument can be applied to all the aircraft type comprising the aircraft mix., the index 'rk' describing the aircraft type and surface condition is omitted. For instance, the terms, d^s and t^s, will be used in this section instead of using d^s_{rk} and t^s_{rk} as deceleration distance and time of aircraft type r, surface condition k and landing trial s.

For a given (rk) aircraft-surface condition combination, the expected IROT is calculated by averaging the ROT's of S landing trials. That is,

$$E[IROT;(x_1,...x_N)]=\frac{1}{S}\sum_{s=1}^{S} IROT^s(x_1,...x_N) \qquad \textbf{(3.3)}$$

where
$IROT^s(x_1,...,x_N)$=individual ROT given the exit locations $x_1,...x_N$ on landing trial s.

For the computation of $IROT_s(x_1,...,x_N)$, it is necessary to establish an exit assignment principle. The exit assignment principle employed in REDIM 2.0 follows the basic principle of exit suitability without preferential consideration to gate location issues. Following a realistic aircraft operational guideline, an aircraft is assigned to the first exit among

which are located beyond the deceleration distance, d^s. For example, if d^s is placed between $(i-1)^{th}$ and i^{th}, then the aircraft makes a turnoff using the i^{th} exit on the landing trial s.

The deceleration adjustment scheme discussed in Section 2.3.1 is also necessary for the computation of $IROT^s(x_1,...,x_N)$. Suppose an aircraft is assigned to the i^{th} exit. Then t^s, time for reaching d^s, is known directly from the simulation data, but the extra time for running the extra distance (x_i-d^s) is unknown. This extra time is computed based on the deceleration adjustment scheme. Let δt^s be the extra time for reaching assigned exit at s^{th} landing trial.

The last consideration for computation of $IROT^s(x_1,...,x_N)$ is turnoff time. Using internal turnoff algorithms, the turnoff time of an aircraft type is computed based on the geometry REDIM 2.0 generated for that aircraft type. If the turnoff geometry, however, varies, the turnoff time varies too. It is not unusual that different aircraft are assigned to a same exit. The geometry for an exit should accommodate the critical aircraft among which are assigned to that exit. This implies that non-critical aircraft need more turnoff time, because they have to execute a turnoff along with a geometry of larger radii of curvature. Approximation of turnoff time for a given geometry is performed by simulating the aircraft's nose gear changes in position along with a given geometry for every.1 second and tracing the corresponding wingtip position. Let t_{off}^s be the turnoff time at s^{th} landing trial.

$$IROT^s(x_1,...,x_N)=\sum_{i=1}^{N+1}(t^s+\delta t^s+toff^s)\, I_{(x_{i-1},x_i]}(d^s) \tag{3.4}$$

where

$$I_R(d)=\begin{cases}1, \text{ the variable d belongs to range R}\\ 0, \text{ otherwise}\end{cases}$$

$x_0=0$ (runway threshold)
$x_{N+1}=RL$ (runway length)

Notice that a 90^o angled exit is assumed to exist at the end of the runway whose location is denoted by x_{N+1}. An aircraft which misses the last high speed exit has to move forward up to the end of runway and execute a turnoff using the 90^o exit.

3.2 Dynamic Programming (DP) Formulation

We now present a continuous DP formulation for Problem WROT with the standard notation and terminology suggested by Hiller and Liebermann (1986).

Stages:
Stage, n, corresponds to a situation in which up to n exits can be located to the right (farther from runway threshold) of the last exit already located. For n =1,..,N, (N-n) exits are assumed to have been constructed from the threshold of the runway. Stage 0 is a dummy initial stage.

States:
The state, s_n, at stage n represents the location of the rightmost (farthest from the runway threshold) exit currently located. For n=N, $s_N = \{-D_{min}\}$ (which means an imaginary exit location of $-D_{min}$ ahead of runway threshold). For any other stage n =1,..,N-1, s_n would take a value in $\{s; (N-n)*D_{min} \le s \le RL\}$.

Decisions:
At any stage n and state s_n, the decision, d_n, corresponds to the location of next exit to be constructed to the right of s_n. Let '$d_n = 0$' mean that no more exits will be constructed to the right of currently located exits. Then the possible value of d_n are 0 and $\{d; (N-n)*D_{min} + D_{min} \le d \le RL\}$ for n=1,...,N.

With the stages, states, and decisions as defined above, we are able to proceed for further formulation of immediate cost, stage and state transition function, and the recursive formula.

Immediate return function:
The return function $c_n(s_n,d_n)$ is the 'immediate' cost incurred at stage n by making decision d_n in state s_n. This cost corresponds to the sum of ROT's of aircraft which miss $(N-n)^{th}$ exit and are able to execute a turnoff using $(N-n+1)^{th}$ exit. For any given values of s_n and d_n,

$$c_n(s_n,d_n) = \begin{cases} \infty, & \text{if } (d_n-s_n)<D_{min} \text{ and } d_n \neq 0 \\ \sum_{r=1}^{R}\sum_{k=1}^{K} w_r p_k IROT_{rk}(s_n,d_n), & \text{if } (d_n-s_n)\ge D_{min} \text{ and } d_n \neq 0 \\ 0, & \text{if } d_n = 0 \end{cases} \quad (3.5)$$

where

$$IROT_{rk}(s_n,d_n)=\sum_{s=1}^{S}(t^s_{rk}+\delta t^s_{rk}+toff^s_{rk})\, I_{(s_n,d_n]}(d^s_{rk}) \tag{3.6}$$

and

$$I_R(d)=\begin{cases}1, \text{ the variable d belongs to range R}\\ 0, \text{ otherwise}\end{cases} \tag{3.7}$$

The definitions of t^s_{rk},δt^s_{rk} and $toff^s_{rk}$ are same as in Section 3.1 except the additional subscript 'rk' representing an aircraft type r and environmental scenario k. Equation 3.6 implies that $IROT_{rk}(s_n,d_n)$ is the sum of ROT of aircraft r in environmental scenario k whose deceleration distance (d^s_{rk}) falls between s_n and d_n out of S landing trials.

Stage transition function:
Given a stage n and having made a decision d_n, the next stage the process transition to is given by

$$t_n(d_n)=\begin{cases}(n-1), \text{ if } d_n\#0\\ 0, \quad \text{if } d_n=0\end{cases} \tag{3.8}$$

State transition function:
Given a stage n and state s_n, and having made a decision d_n, the following state in stage $t_n(d_n)$ would be

$$S_{T_n}(d_n)\equiv\tau_n(s_n,d_n)=\begin{cases}d_n, \text{ if } d_n\neq 0\\ s_n, \text{ if } d_n=0\end{cases} \tag{3.9}$$

Backward recursive formula:
Let $f_n^*(s_n)$ be the optimal accumulated return function for a given input state s_n at stage n. Then this function is given recursively by

$$f^*_n(s_n)=\underset{d_n=0 \text{ or } s_n+D_{min}\le d_n\le RL}{\text{minimum}}\left[\, c_n(s_n,d_n)+f^*_{t_n(d_n)}(\tau_n(s_n,d_n))\,\right] \tag{3.10}$$

where the initial condition is given by

$$f_0^*(s_0)=\sum_{r=1}^{R}\sum_{k=1}^{K}\sum_{s=1}^{S} w_r p_k(t_{rk}^s+\delta t_{rk}^s+toff_{rk}^s)\, I_{(s_0,RL]}(d_{rk}^s) \tag{3.11}$$

Notice that the subscript '0' means the stage 0,which is the dummy initial stage, and s_0 means the location of the last high speed exit. The initial condition, $f^*_0(s_0)$ is the sum of ROT's of all aircraft landings which miss the last high speed exit and execute a turnoff using 90° angled exit located at the end of the runway.

To validate the DP approach for the Problem WROT, let the objective function in Eq. 3.2 be the global return function. That is,

$$R_N\{r_N(s_N,d_N),...,r_1(s_1,d_1)\}=\sum_{r=1}^{R}\sum_{k-1}^{K} w_r p_k E[IROT;(x_1,...,x_N)]_{rk} \tag{3.12}$$

Now notice that s_n and d_n are the locations of the (n-1) th and nthexit, respectively. The immediate return function at each stage n, for n=1,...,N, can be stated as:

$$r_n(s_n, d_n)=c_n(s_n, d_n)+I_{(N)}n\, f_0^*(s_0) \tag{3.13}$$

where

$$I_{(N)}d = \begin{cases} 1, \text{ if } n=N \\ 0, \text{ otherwise} \end{cases}$$

(See Eqs.3.5 and 3.11.)

Then

$$R_N\{r_N(s_N,d_N),...,r_1(s_1,d_1)\}=\sum_{n=1}^{N} r_n(s_n,d_n) \tag{3.14}$$

Since the global return function is obviously **separable** and **monotonic non-decreasing** function of the immediate return function, r_n, the principle of optimality holds. Hence, the

DP approach for the Problem WROT is valid.

3.2.1 Algorithmic Development

Beginning with stage 1, the DP algorithm proceeds recursively through stage N using the recursive formula (Eq. 3.10). At any stage n in this process, the state s_n corresponds to the location of the rightmost exit among already constructed (the $(N-n)^{th}$ exit) and the decision d_n corresponds to the location of the next exit (if decision d_n=0, no more exits will be constructed). Since the state space and decision space are continuous over the real line from 0 to RL, the optimal decision, d^*_n, and the corresponding optimal intermediate return function $f^*_n(s_n)$ should be expressed as functions of s_n at every stage n. The exact solution may be found on a specific problem with given values of N, R, K and the deceleration distances (d^s) and deceleration times (t^s) for all r=1,..,R, k=1,..,K and s=1,..,S. However, a generalized solution algorithm cannot be derived because of the structure of the objective function of the problem and the continuous state and decision spaces. If the candidate generation scheme developed during the Phase I is applied to this problem, the continuous DP formulation is converted as a discrete DP formulation without loss of optimality (Refer to Sherali et al, 1990). This approach, however, is impractical for implementing on a PC, because it generates too many candidate locations.

An approximation algorithm is derived by discretizing the line segment from 0 to RL with arbitrary search intervals. Suppose the exits can be located among the points generated by discretizing the runway with a certain search interval, say 25m, instead of any point on the runway. Then, the possible values of s_n and d_n for each stage n can be enumerated. For every possible s_n, we find $f^*_n(s_n)$ via Eq.3.10 over all possible values of d_n in a backward search manner. The corresponding optimal decision d^*_n is stored along with the value of $f^*_n(s_n)$. At final stage N, the value of $f^*_N(s_N)$ (= $f_N^*(0)$) gives the optimal objective function value of the Problem WROT. The optimal exit locations $x_1,..,x_N$ can be found by tracing the optimal decisions from d^*_1 to d^*_N using stage and state transition functions.

Now let I be the total number of search intervals over the entire runway. At each stage, we have I states and I decisions at worst case. For every single stage-state-decision combination, O(RKS) computations are involved. Thus, the algorithm is of polynomial complexity $O(NRKSI^2)$.

3.3 Comparison of Phase II and Phase I Optimization Approaches:

First of all, a basic principle behind Phase I approach is that each aircraft type should be assigned to an designated exit. By assigning each aircraft type to an designated exit, the variations of ROT for each aircraft is expected to be reduced although the average is expected to increase. In Phase II, an aircraft type is allowed to be assigned to two or more exits resulting in less average ROT with higher variations. Because of this difference in assignment principle, the amount of data and the computational efforts are increased significantly. The optimization in phase I was performed analyzing the influence of different exit locations on each aircraft type in an aggregate manner, while the optimization in Phase II

analyses the influence of the different exit locations on each landing trial. If we consider S landing trials for each aircraft, the computational efforts of phase II model is increased as S times of that of Phase I model.

The second difference is the characteristic of the solution (the optimal exit locations). The optimization scheme of Phase II produces a range of optimal solutions while that of Phase I resulted in a deterministic turnoff solution (i.e., point solution). Range solutions are achieved by repeating the simulation and the optimization several times. At each repetition, the simulation generates a different set of deceleration distance data and the optimization is performed based on the different set of data. For instance, a typical solution of this Phase II model might look like (475-525, 1650-1700, 2100-2175) instead of deterministic exit locations (500, 1700, 2150). The range solution reflects the fact that slight differences in exit locations do not affect significantly the average ROT thus giving airport designers more flexibility while planning runway improvements.

CHAPTER 4

Turnoff Geometric Design Compatibility Issues

This chapter addresses important lateral and longitudinal constraint issues that arise naturally while locating runway turnoffs. The lateral constraints are exemplified by limited distances from runway centerline to a taxiway centerline whereas longitudinal constraints deal with possible conflicts between neighboring turnoffs.

4.1 Runway Lateral Constraints and Their Assessment

A problem arising naturally from the placement of medium and high-speed turnoffs on a runway is the potential risk of executing turning maneuvers at high or moderate speeds in the presence of other aircraft ground traffic on nearby taxiways. About 190 airports in United States have implemented FAA standard high-speed geometries [FAA, 1981]. As many of these facilities were originally planned in the late forties and fifties they adopted lateral taxiway design standards that were not necessarily compatible with the lateral requirements of high speed turnoffs. Many of these facilities have separation distances between runway and parallel taxiway centerlines of only 122 m. (400 ft.). These distances are, in general, inadequate to expedite aircraft from an arrival runway at high speed unless a different turnoff design philosophy is adopted and smaller turnoff angles are used replacing existing 30 Deg. geometric standards. A 122 m. separation distance between the runway and a parallel taxiway leaves pilots with very little room for decelerating an aircraft on the turnoff tangent and this might well be one of the contributing factors in the poor use of existing high speed runway turnoffs at various airports [Koenig, 1978; Ruhl, 1990]. The main safety consideration in this regard is the little deceleration time pilots will have in bringing in their aircraft to a reasonable taxiing speed once a turnoff is taken near its design speed.

FIGURE 4.1 **Generalized Turnoff Geometry.**

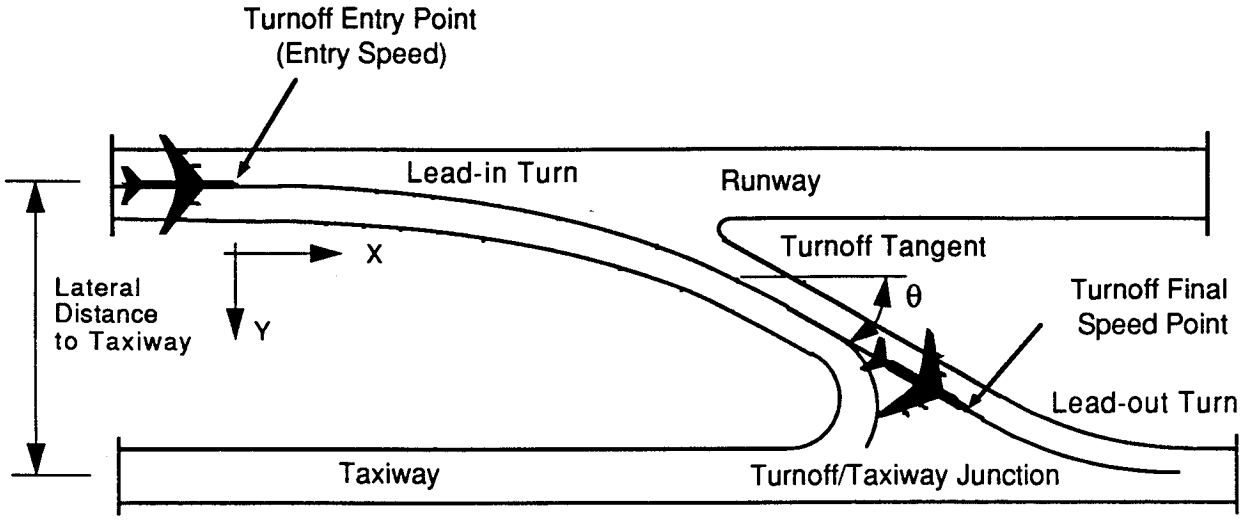

In order to illustrate this lets consider a heavy aircraft of the type of a Boeing 747-400 as it takes a standard FAA 30 Degree angle geometry at 26.7 m/s (60 MPH) which is considered to be the design speed for this turnoff [Horonjeff et al., 1961]. Figure 4.1 illustrates the general layout of a high speed turnoff showing two distinct radii of curvature associated with two curves called lead-in and lead-out turns. Using continuous simulation it is possible to derive lateral distance-speed plots to understand the aircraft kinematic behavior. Figure 4.2 illustrates four different curves representing four deceleration rate values on the tangent portion of the turnoff. All curves were derived using a turnoff entry speed (V_{exit}) of 26.7 m/s at the point of intersection of the turnoff geometry and the runway centerline. In these computer simulations the assumed free roll deceleration on the curve was -0.375 m/s^2 as this value was measured experimentally by Horonjeff et al. in 1961 using a large transport aircraft (KC-135) on 548.8 m. (1800 ft.) centerline radius curves [Horonjeff et al., 1961].

In Figure 4.2 the abscissa represents the lateral distance of the aircraft nose gear measured from the runway centerline. For design purposes one would have to add the lateral range distance associated with a lead-out radius (see Fig. 4.1) corresponding to the expected final speed as the aircraft enters the parallel taxiway. From Figure 4.2 it can be observed that existing FAA standards for a 30 degree turnoff will assume that pilots decelerate at about -0.75 m/s^2 on the tangent in order to reach the entrance point of a 122 m. (800 ft.) radius curve at around 17.9 m/s which is the design speed for this radius of curvature according to well accepted standards [Horonjeff et al., 1961]. The lateral distance from the runway centerline is about 150 m. thus resulting in an effective runway to taxiway centerline distance of 183 m. (600 ft.) once the lateral distance of a 244 m. (800 ft.) lead-out radius is added. Figure 4.3 represents the minimum recommended lateral distances mea-

FIGURE 4.2 **Aircraft Speed vs. Lateral Distance Traveled on a Standard FAA Acute Angle (30 degrees) Runway Turnoff at 26 m/s Design Speed.**

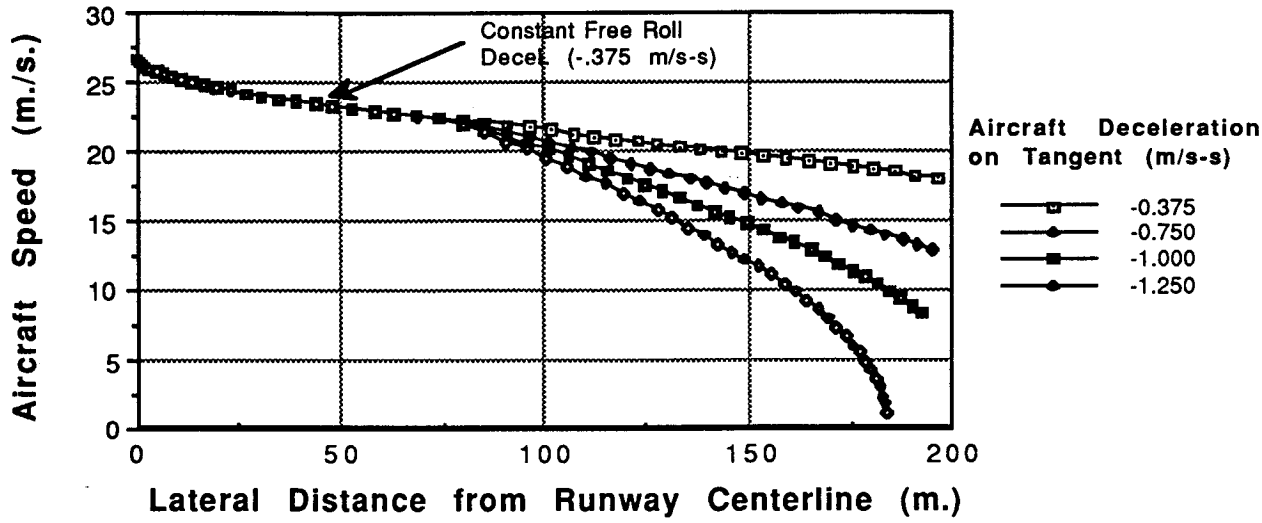

FIGURE 4.3 **Recommended Runway to Taxiway Separation Criteria for Standard FAA 30 Degree, Acute Angle Geometries.**

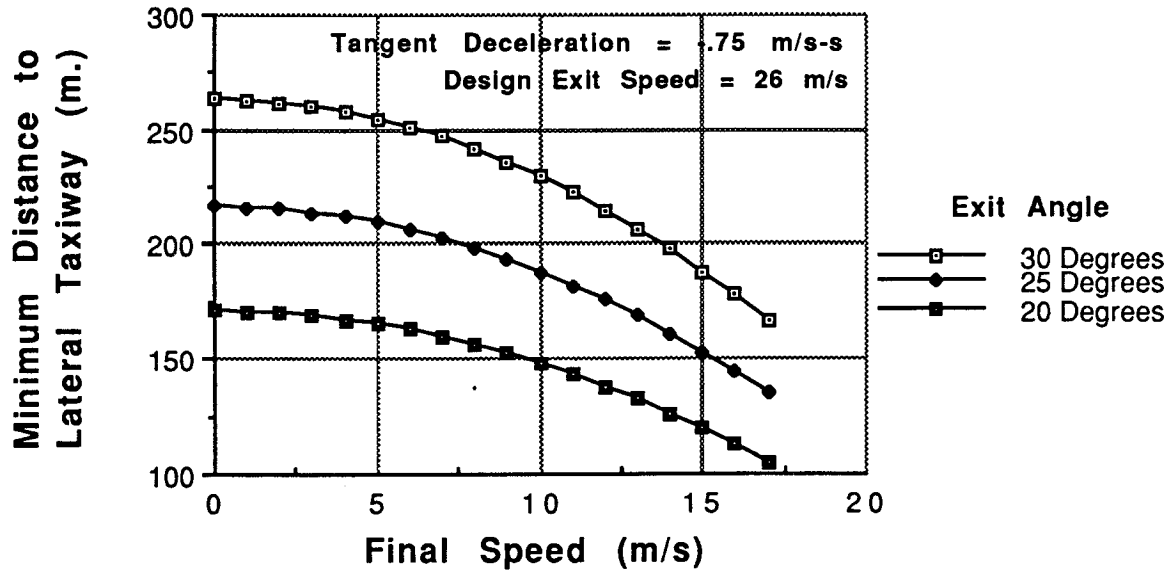

sured from runway to taxiway centerlines for geometries using a 548.8 m. (1800 ft.) as centerline radius of curvature and three different exit angles, θ.

Figure 4.3 was derived using a constant -.75 m/s^2 deceleration on the tangent with a third order time lag mechanism to represent a delayed braking schedule. Note that values shown in this figure represent distances between runway and taxiway centerlines and could be used for design standardization for future airport projects. The net effect of reducing the exit angle, θ, is a corresponding reduction in the minimum lateral space requirements needed to implement high speed turnoff geometries. Taking as a reference point an exit speed of 26 m/s it can be seen that a reduction of 23% in the lateral distance requirement is possible if the exit angle is reduced from 30 to 20 degrees (e.g., from 183 m. for $\theta = 30$ degrees to 141 m for $\theta = 20$ degrees). It is expected that all previous assumptions usually will hold under low visibility and wet pavement conditions as pilots act with conservatism and take high speed turnoffs at lower entry speeds. One important pilot uncertainty could be the "right-of-way dilemma" associated with an aircraft exiting at high speed near a taxiway junction. If pilots fear that taxiway traffic might pose a collision risk they might be unwilling to take a high-speed turnoff near their design exit speed unless visibility conditions allow easy verification of potential ground traffic. Some of the human factor implications related to the design of high speed turnoffs are addressed in Section 4.3 of this report.

The implications of taxiway proximity cannot be taken lightly in this respect as there is some evidence that in many of the existing airport facilities having small lateral distances between a runway and taxiway centerlines cannot productively use a standard 30 degree angle turnoff [Koenig, 1978; Ruhl. 1990]. The prospect of using a modified 30 degree turnoff with a 427 m. entrance spiral (1400 ft.) as stipulated in FAA AC 150/5300-13 increases the pilots' capability to decelerate an aircraft to more comfortable speeds before reaching the turnoff-taxiway junction as the curved portion of the turnoff increases in length as that of the standard 30 degree geometry (see Figs. 4.2 and 4.4).

Figure 4.4 illustrates this point showing four deceleration curves where the tangent deceleration schedule has been varied from -0.375 to -1.25 m/s^2 for a modified FAA acute angle, 30 degree angle geometry with a 427 m. entrance spiral. From the simulation results shown in Fig. 4.4 one can see that the minimum distance between a runway and a parallel taxiway centerline for this geometry should be 183 m. (150 m.to the entrance of the second 122 m. radius of curvature arc) as this will result in an entry speed of 17 m/s (37.9 MPH) at the taxiway/turnoff junction using zero braking throughout the tangent portion of the turnoff (i.e., -.375 m/s^2 deceleration. If some braking is allowed on the tangent section of the turnoff (say -0.75 m/s^2) a reduction in the distance to the parallel taxiway could be possible down to 145 m. (476 ft.) maintaining a 17 m/s final speed at the lead-out turn point of curvature. Deceleration rates on tangents of up to 0.75 m/s^2 would seem acceptable for well designed turnoffs although further simulator testing is needed to confirm this point. This deceleration rate is about half of that used on the runway by most transport-type aircraft. It is interesting to note that several airports have implemented the modified acute angle high speed exit with lateral distances of only 122 mts (400 ft.) as this

FIGURE 4.4 **Aircraft Speed vs. Lateral Distance Traveled on a Modified FAA 30 Deg. Runway Turnoff with a 427 m. (1400 ft.) Entrance Spiral.**

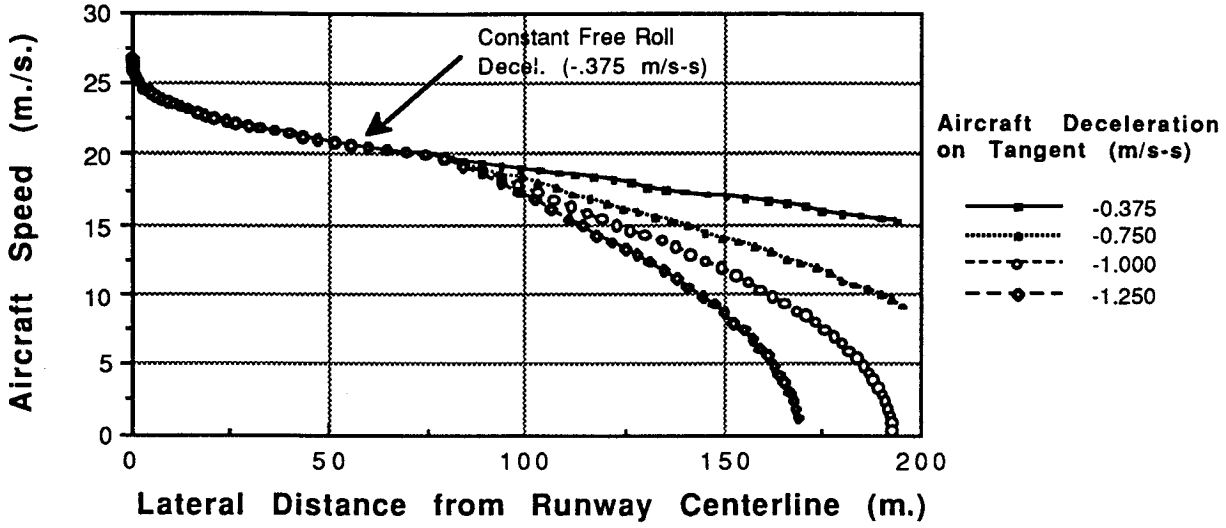

FIGURE 4.5 **Recommended Runway to Taxiway Separation Criteria for Modified FAA Acute Angle Geometry with 427 m. (1400 ft.) Spiral.**

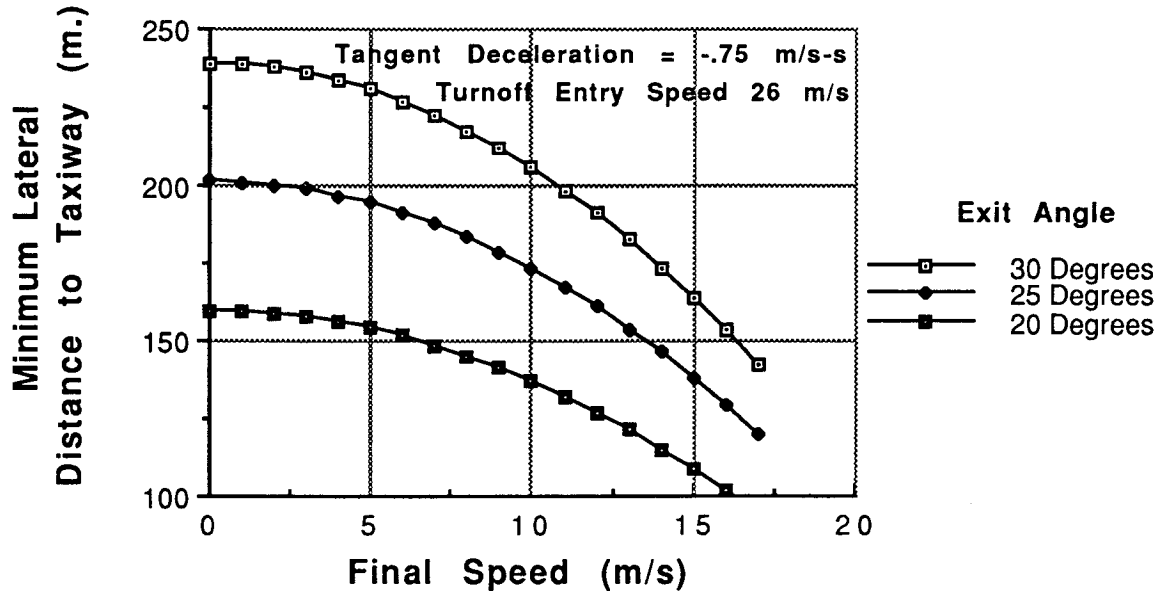

complies with current design standards for precision runways serving aircraft in approach category C and up to design group IV (i.e., wingspans between 36 and 52 m.).

Figures 4.5 depicts graphically minimum recommended lateral distances between runway and taxiway centerlines for a modified, acute angle high speed turnoff with a 427 m. (1400 ft.) entrance spiral. This figure summarizes computer simulation results used to establish minimums for lateral spacing separations for various exit angles and final exit speeds. Note that turnoff entry speed and deceleration on the tangent turnoff portion have been maintained constant at 26 m/s and -0.75 m/s^2, respectively.

4.1.1 Turnoff Entry Speed Limitations

Here we examine the limitations on turnoff entry speed as they apply to existing and newly proposed turnoff geometries (designated REDIM generated geometries hereon). The idea is to find the limitations on turnoff entry speeds that will yield realistic final speeds at the taxiway/turnoff junction. The derivation of these results was made possible with the use of simple aircraft equations of motion in a two-dimensional plane with a third order delay in the deceleration rate equation to realistically simulate pilot time lags in the application of brakes on the tangent section of the turnoff trajectory. The applicable equations of motion during a turnoff maneuver are shown in Equations 4.1 through 4.6 which were solved numerically using a continuous simulation language to estimate precisely the minimum lateral distance requirements from runway to taxiway centerlines to satisfy turnoff entry speed requirements.

$$x_t = x_{t-1} + \int_{t-1}^{t} V_t \cos\theta_t \, dt \qquad (15.1)$$

$$y_t = y_{t-1} + \int_{t-1}^{t} V_t \sin\theta_t \, dt \qquad (15.2)$$

$$V_t = V_{t-1} + \int_{t-1}^{t} a_t \, dt \qquad (15.3)$$

$$a_t = \begin{cases} -a_{\text{curve entrance}} & \text{if } \theta_t < \theta_{\text{turnoff}} \\ \text{delay}^{3\text{rd}} \begin{cases} -a_{\text{tangent}} \\ -a_{\text{final curve}} \end{cases} & \text{if } \theta_t \geq \theta_{\text{turnoff}} \\ & \text{if } \dot{\theta}_t < 0 \end{cases} \tag{15.4}$$

$$\theta_t = \theta_{t-1} + \int_{t-1}^{t} \dot{\theta}_t \, dt \tag{15.5}$$

$$\dot{\theta}_t = \begin{cases} f(R) & \text{for standard FAA Turnoffs} \\ f(R, I_{zz}, \mu_{side}) & \text{for standard REDIM-Generated Turnoffs} \end{cases} \tag{15.6}$$

In these equations θ_t is the instantaneous aircraft heading, a_t is the instantaneous aircraft acceleration, x_t and y_t are the cartesian coordinates of the aircraft (the nose wheel has been used as reference position), v_t is the aircraft nose wheel tangential velocity and $d\theta/dt$ is the rate of change of the aircraft heading angle.

Figure 4.1 shows the turnoff nomenclature and illustrates the meaning of the entry and final turnoff points. Note that the turnoff entry point is defined as the intersection of the runway and turnoff centerlines whereas the turnoff final point is the intersection of the tangent portion of the turnoff and the point of curvature of the lead-out centerline curve. The selection of this final turnoff point was based on the assumption that an aircraft reaching this point should be capable of negotiating the lead-out turn at a prescribed speed. Current high speed FAA turnoff designs specify lead-out turn centerlines of 244 m. (800 ft.) which translate to a design speed of 17.9 m/s (40 MPH). If a double back trajectory is provided, however, the final turnoff speed is reduced considerably (probably below 6 m/s) as aircraft have to negotiate smaller radius of curvature on the double back (i.e.,50 m. radius typical).

Figures 4.6 through 4.8 illustrate entry speed turnoff limitations for the largest and most critical commuter aircraft (TERP B category) using the turning algorithms of REDIM [Trani and Hobeika et al., 1990] for three different exit angles ranging from 30 to 20 degrees. The interpretation of these is as follows:

Select a desired turnoff entry speed (V_{exit}) on the horizontal axis and a final speed at the turnoff-taxiway junction then estimate the minimum lateral distance to a parallel taxiway by reading off the ordinate axis. Taking as a numerical example an entry design turnoff speed of 25 m/s (56 MPH) and using a final speed of 17.5 m/s (39 MPH) it can be seen from Figure 4.6 that a minimum lateral separation of 122 m. (400 ft.) is required to execute the turn comfortably if the exit angle is maintained at 30 degrees. If the designer lowers the exit angle to 25 degrees a reduction in the lateral spacing requirement of 31 m. is

FIGURE 4.6 Recommended Runway to Taxiway Separation Criteria for Commuter Aircraft (TERP B) using REDIM Geometries (30 Deg. Exit Angle).

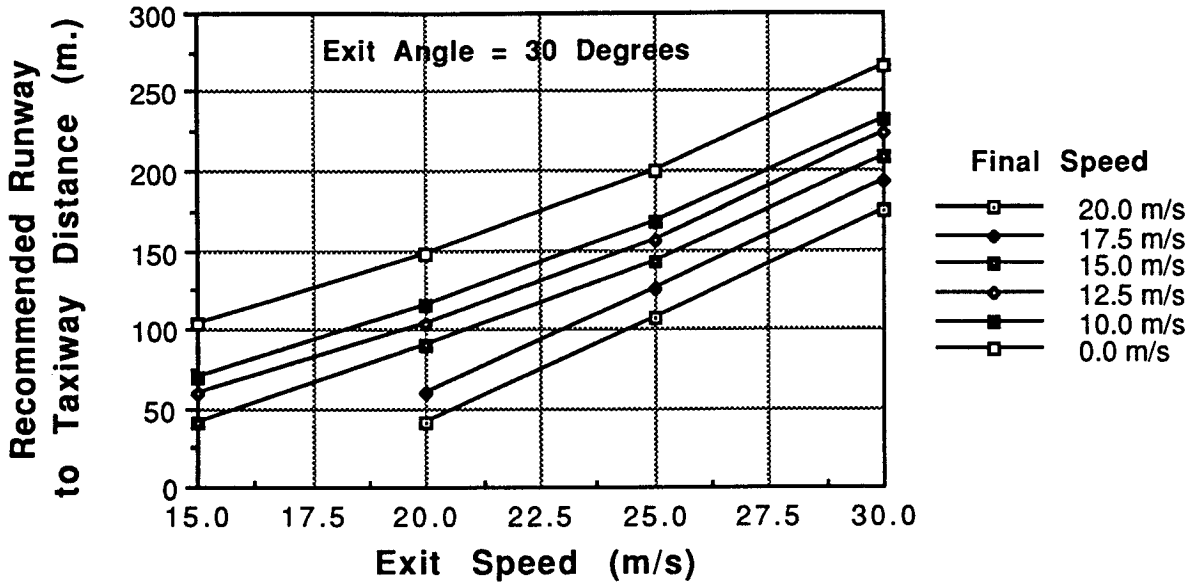

FIGURE 4.7 Recommended Runway to Taxiway Separation Criteria for Commuter Aircraft (TERP B) using REDIM Geometries (25 Deg. Exit Angle).

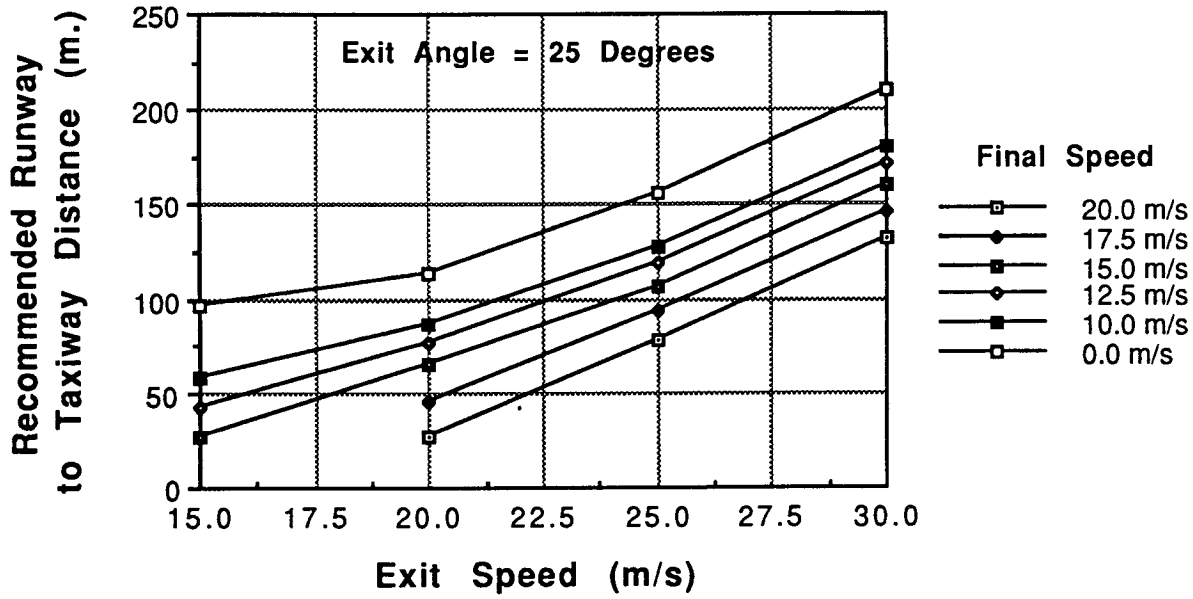

achieved necessitating only 91 m. (300 ft.) laterally to satisfy the same turnoff entry and final speed conditions. These curves are useful for design and planning purposes in the presence of lateral constraints.

Figures 4.9 through 4.11 illustrate the minimum lateral distance requirements for medium size transport aircraft classified under the TERP C category for ATC purposes. Figures 4.12 through 4.14 depict the same requirements for heavy transport aircraft (TERP D category). It should be emphasized that these plots were obtained modeling the pilot's deceleration time lag on the turnoff as a third order delayed system with a time constant of 0.5 seconds. A -0.75 m/s^2 deceleration rate on the turnoff tangent was also used in the computations. More details in this regard are provided in Section 4.1.3.

FIGURE 4.8 Recommended Runway to Taxiway Separation Criteria for Commuter Aircraft (TERP B) using REDIM Geometries (20 Deg. Exit Angle).

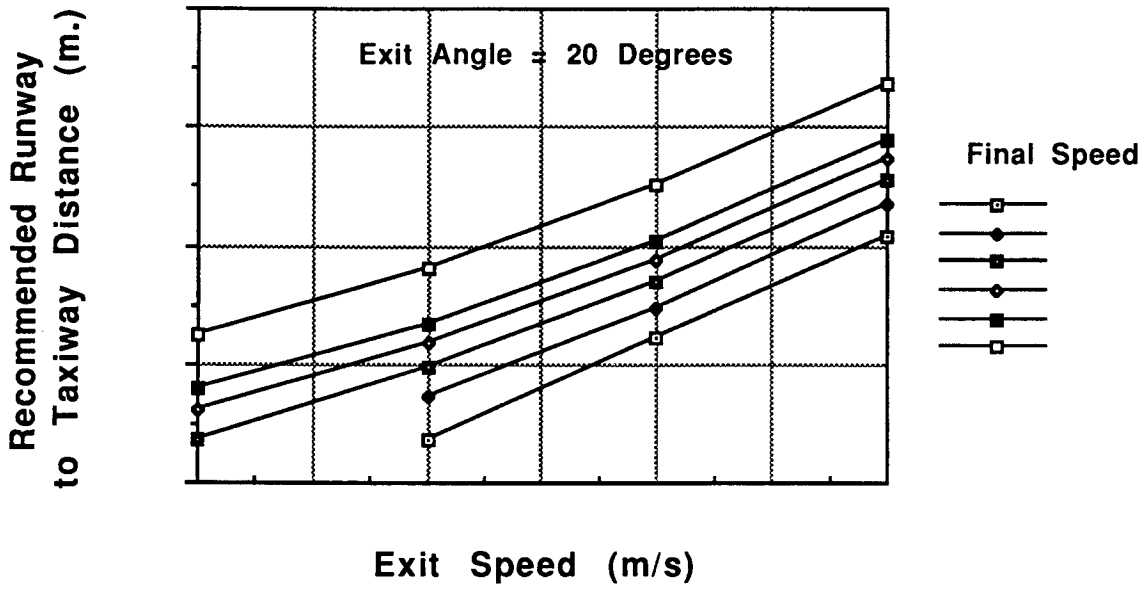

4.1.2 Pilot Visibility Issues at Taxiway and Runway Junctions

Aircraft visibility angles play an important role in everyday airport operations as pilots have limited capabilities to see outside objects from their cockpit eye level position. Visibility requirements in the horizontal and vertical planes are dictated by Federal Aviation Administration Regulations (FAR 25.277) and limited to a frontal visibility hemisphere covering 130 degrees from port and starboard cockpit reference points. Table 4.1 illus-

trates horizontal and vertical visibility characteristics for current transport aircraft [Boeing, 1988, 1989, 1990, 1991].

Note that low turnoff angles in general have an inherent drawback of leaving pilot with little horizontal visibility to assess potential traffic at turnoff/taxiway intersections. This problem could be mitigated with the use of automatic traffic signalization systems which are currently being tested by the FAA at John F. Kennedy airport.

The importance of these visibility angles should not be underestimated as aircraft pilots usually would like to maintain certain awareness of potential traffic while maneuvering near taxiway intersections.

TABLE 4.1 Horizontal and Vertical Visibility Angles for Various Aircraft.

Aircraft Name	Horizontal Visibility (degrees)	Vertical Visibility Up/Down (degrees)
Boeing 747-400[a]	147	37/34
Boeing 757-200	129	34/19
Boeing 727-200	134	24/33
Boeing 767-300	126	35/25
Boeing 737-200	133	24/33

a. Horizontal and perpendicular to longitudinal aircraft axis visibility angles increase as the head is displaced outward from reference cockpit position.

From the airport operational point of view these horizontal and vertical visibility angles should be considered in the geometric design of intersections between a taxiway and a runway and between runway turnoffs and taxiways as pilots will undoubtedly look for aircraft traffic at either side of the runway or taxiway while executing crossing maneuvers. A desirable feature of the new designs is that they should provide enough crew awareness of aircraft traffic on runways being crossed and taxiway intersections without special aircraft maneuvers that will increase crew workload. The motivational factors guiding pilots in their assessment of intersections should be examined in flight simulations to verify some of these behaviors.

4.1.3 Pilot Reaction Times and Turnoff Deceleration Schedule

In deciding the design exit speed of a turnoff geometry one has to pay careful attention to the aircraft operational stopping criteria before reaching a turnoff/taxiway intersection or in some extreme cases a holding line (i.e., when a closely-spaced parallel runway is present). For many airports in the U.S, the small lateral separation between runways or between runways and parallel taxiways makes this issue one of great relevance as aircraft

FIGURE 4.9 **Recommended Runway to Taxiway Separation Criteria for Medium Transport Type Aircraft (TERP C) using REDIM Geometries (30 Deg. Exit Angle).**

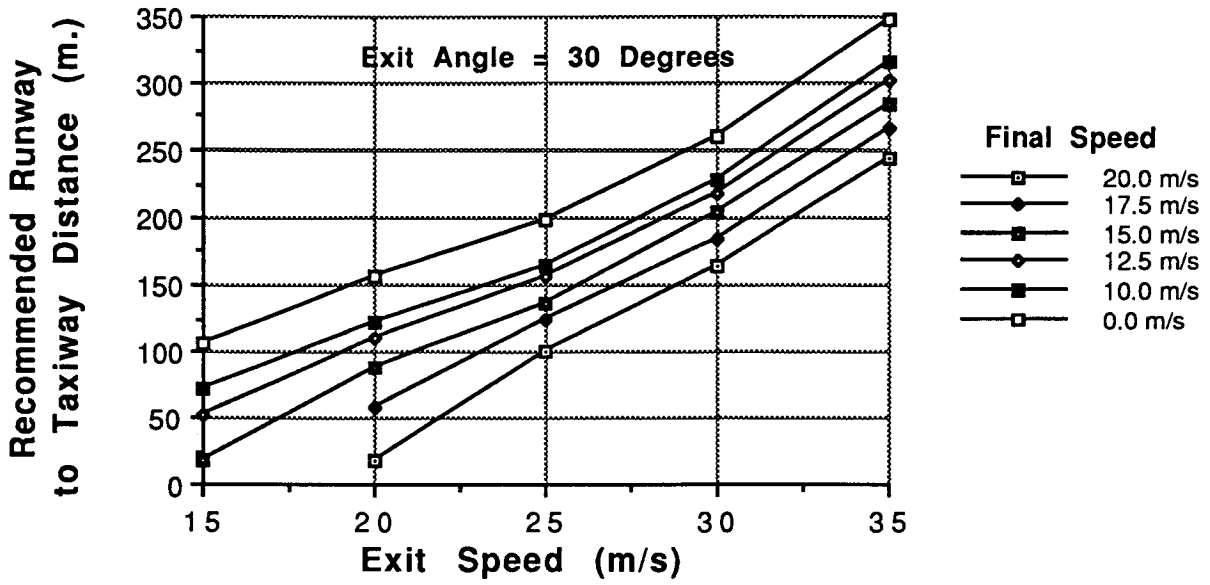

FIGURE 4.10 **Recommended Runway to Taxiway Separation Criteria for Medium Transport Type Aircraft (TERP C) using REDIM Geometries (25 Deg. Exit Angle).**

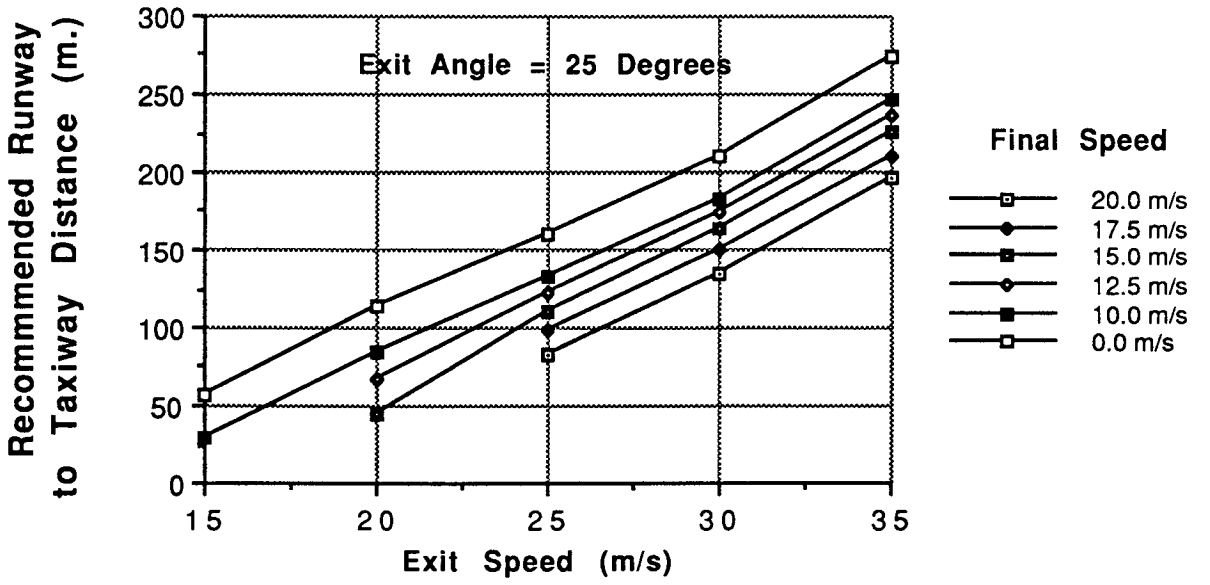

FIGURE 4.11 **Recommended Runway to Taxiway Separation Criteria for Medium Transport Type Aircraft (TERP C) using REDIM Geometries (20 Deg. Exit Angle).**

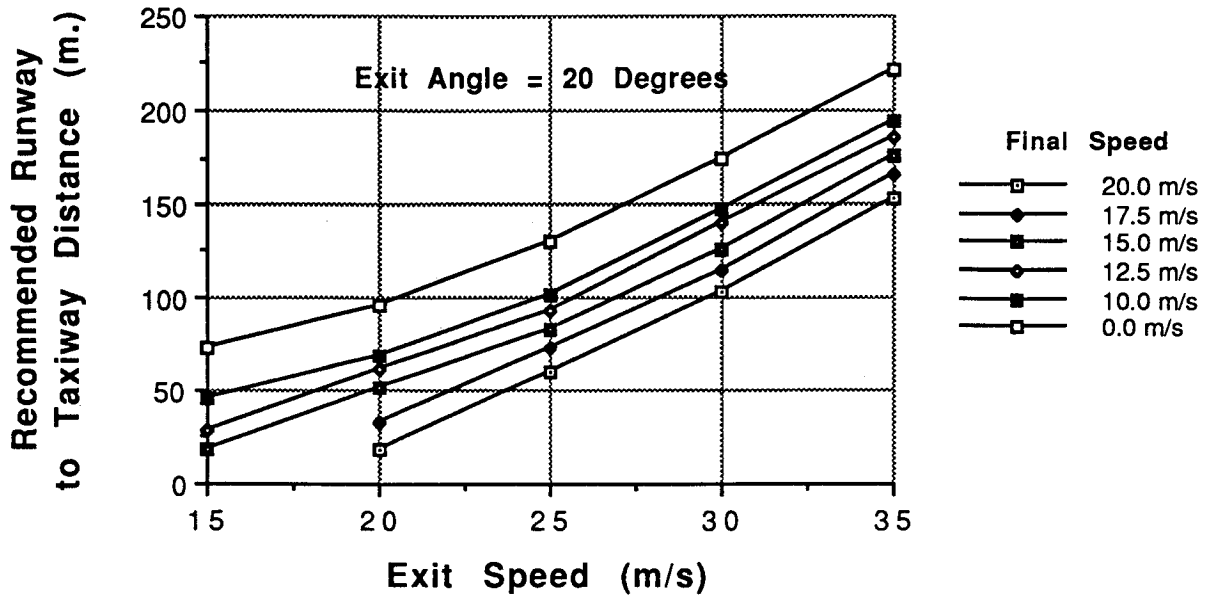

FIGURE 4.12 **Recommended Runway to Taxiway Separation Criteria for Heavy Transport Type Aircraft (TERP D) using REDIM Geometries (30 Deg. Exit Angle).**

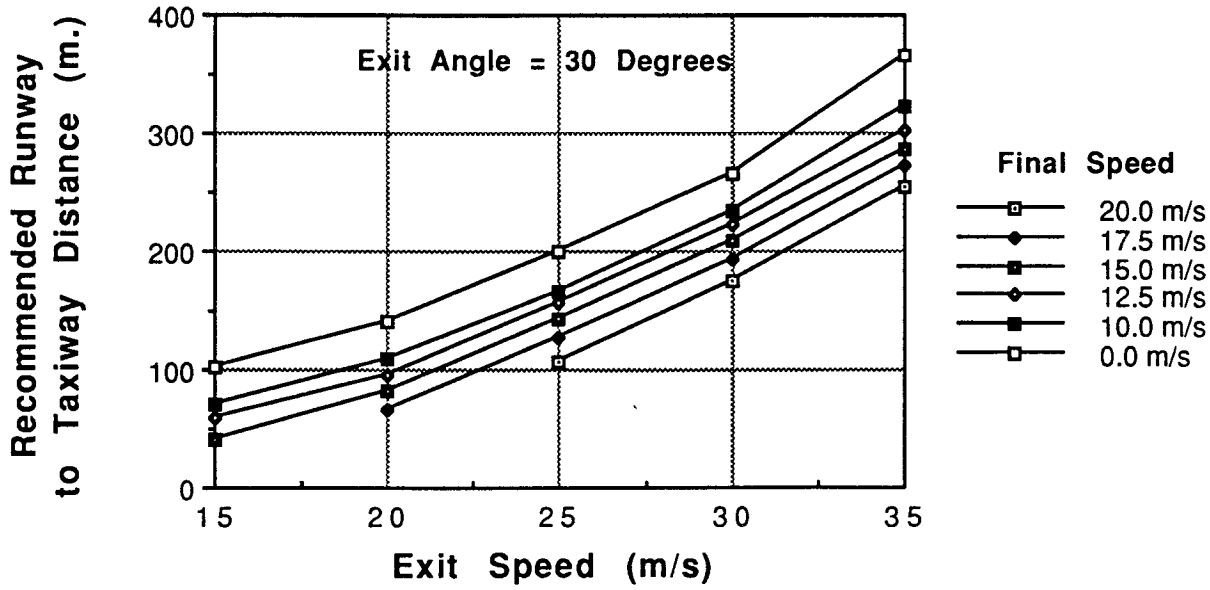

FIGURE 4.13 Recommended Runway to Taxiway Separation Criteria for Heavy Transport Type Aircraft (TERP D) using REDIM Geometries (25 Deg. Exit Angle).

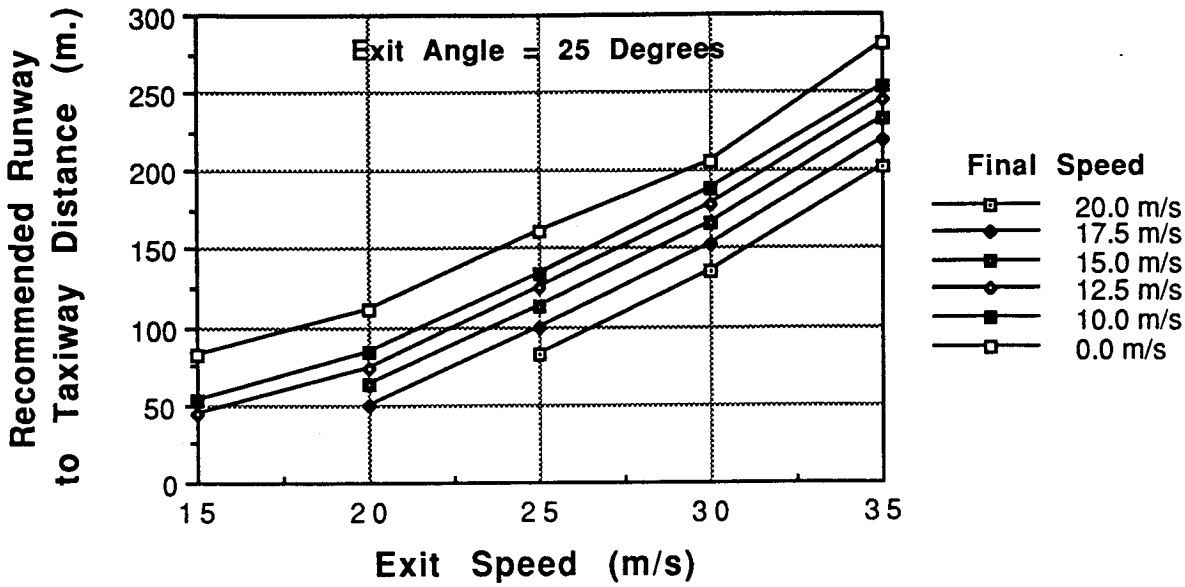

FIGURE 4.14 Recommended Runway to Taxiway Separation Criteria for Heavy Transport Type Aircraft (TERP D) using REDIM Geometries (20 Deg. Exit Angle).

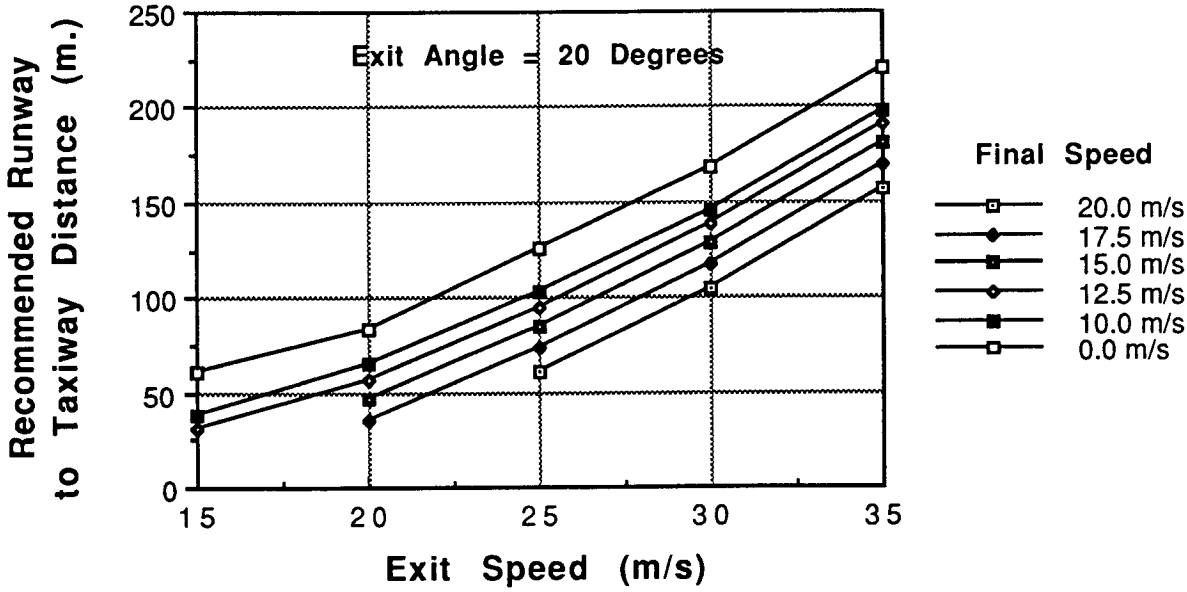

landing on a runway and taking a high-speed turnoff have to decelerate quickly on the turnoff to reach a manageable speed at the start of the lead-out turn (Fig. 4.1) or sometimes it might be forced to stop at a holding line position before crossing an active parallel runway. The influence of pilot behavior on a turnoff is of paramount importance to determine lateral distance thresholds associated with new rapid runway design turnoffs. Figures 4.2 and 4.3 depict results for standard FAA geometries that could be used as guidelines to determine the suitability of these turnoffs under lateral constrained scenarios.

The implications of selecting a particular turnoff geometry are very obvious as each one possesses various degrees of curvature consuming various lateral range distances over time. For example, a standard 30 degree, acute angle FAA turnoff geometry we can see from Figure 4.2 that a heavy aircraft decelerating at -0.75 m/s2 requires 150 m. laterally to decelerate to comfortable speeds after taking the turnoff at the design speed of 26.7 m/s (60 m.p.h.). These plots account for typical pilot time lags in the application of braking on the tangent portion of the turnoff and they could be used as guidelines for design of future runway facilities.

4.1.4 Junction Maneuvering Speeds

The assumptions regarding turnoff speeds at turnoff intersections and junctions have to be based upon the safe and expeditious ground operations.Current junction designs for FAA 30 degree angle geometries dictate a lead-out turn radius of 244 m. (800 ft.) equating to a design entry speed of 17 m/s (40 m.p.h.). This speed can only be used if the aircraft is assumed to follow the lead-out turn path. When a double back option is available the entry speed for even the largest radius of curvature (i.e., 52 m. for design group VI) would only allow average taxiing speeds of 5-8 m./s. (11-17 m/p.h.) depending upon the maneuverability and size of the aircraft.The 45 degree angle geometry has a 37 m. (120 ft.) lead-out radius thus allowing at most a regular taxiing speed of 8 m/s.

4.2 Runway Longitudinal Constraints

Runway turnoff geometries designed for high exit speed require large downrange distances between the runway/turnoff to turnoff/taxiway intersection points (see Figure 4.15) for their implementation. A modified 30 degree angle turnoff geometry with a 427 m. (1400 ft.) transition spiral requires 670 m. (2198 ft.) between points of intersection. Large downrange turnoff requirements have the potential drawback of limiting the number of turnoff geometries that could be implemented at a runway facility. The main concern in REDIM 2.0 is the possible negative effect of conflicts arising between adjacent dissimilar turnoffs. REDIM 2.0 turnoff conflict resolution algorithms check for the proximity of "neighboring" solutions before declaring any turnoff geometry as being optimally located. This intelligent mode of operation is active in REDIM 2.0 for two of the four runway analysis modes (i.e., design and improvement cases) as these could result in conflicts between neighboring candidate turnoff solutions. The reader should be aware that for any type of turnoff geometry there are three well defined types of constraints to be investigated before

a turnoff is a viable exit candidate on any runway: 1) geometric, 2) operational and 3) obstacle free zone separation minima. Currently REDIM 2.0 addresses the first two constraints as they are usually the most dominant in realistic airport scenarios.

The geometric constraint refers to minimum lateral separation dictated exclusively by the physical shape of the turnoff. For example the minimum desirable geometry of a standard 30 degree FAA acute angle turnoff would consists of a lead-in turn followed immediately by a lead-out turn (see Fig. 4.15) without a tangent segment. This minimal configuration still requires a lateral separation between a runway and taxiway centerlines of 106 m. (350 ft.) with no double back and 167 m. (550 ft.) with a double back if aircraft design group V standards are used.

The operational constraint refers to minimum lateral separation dictated exclusively by the entry and final speeds on the turnoff. The standards proposed in REDIM 2.0 are those derived in this research using computer aircraft simulations and shown graphically in Figures 4.2 through 4.14. In general, the operational requirements to meet entry and final speeds on the turnoff dominate over the geometric design requirements. However, for low exit angles and moderate speeds this rule might not hold true.

Obstacle free zone operation minima standards refer to those rules where the minimum separation between a runway and a taxiway or a runway is dictated by obstacle free zone (OFZ) regulations. Cases like this arise when a close-parallel runway is present from that being analyzed and where full stopping criteria needs to be enforced before reaching the parallel runway at a holding line position. This phenomena is illustrated in Fig. 4.15 depicting a hold line to exists between runways 1 and 2 in order to comply with OFZ rules. Currently, REDIM does not implement OFZ checks but the user can verify OFZ compliance by checking Advisory Circular 150/5300-13. A zero final speed in the turnoff design parameters could be used to estimate minimum lateral separation criteria up to a holding line as shown in Fig. 4.15.

FIGURE 4.15 Turnoff Geometry Dictated by Separation Minima Constraints.

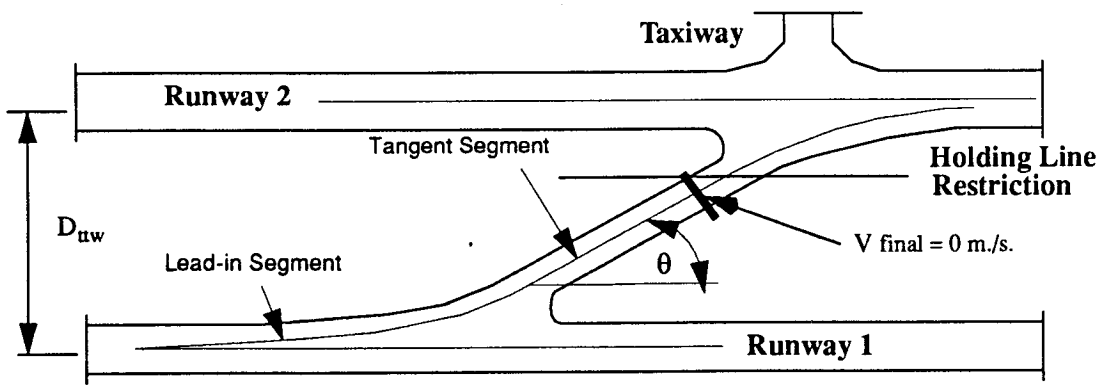

The conflict resolution algorithm implemented uses knowledge of existing and proposed new geometries in terms of their longitudinal and lateral space requirements (Figure 4.13). This topic is covered in the following section.

4.2.1 Characterization of Existing Turnoff Geometries

Five standard geometries are characterized in this section with aim of establishing guidelines for neighboring turnoff resolution. The turnoff characterization is executed by defining any turnoff geometry in terms of three basic segments: 1) lead-in turn, 2) tangent segment and 3) lead-out turn. Figure 4.16 illustrates these segments for a generalized turnoff geometry. The definition of each segment is made in terms of suitable radii and turnoff angles complying with FAA design group criteria used in airport design [FAA, 1989]. Table 4.2 defines the longitudinal and minimum lateral space requirements, labeled D_{long} and D_{lat}, for four standard turnoff FAA geometries and for the recently proposed "wide throat" turnoff [Carr, 1981].

FIGURE 4.16 General Turnoff Segmentation for D_{long} and D_{lat} Characterization.

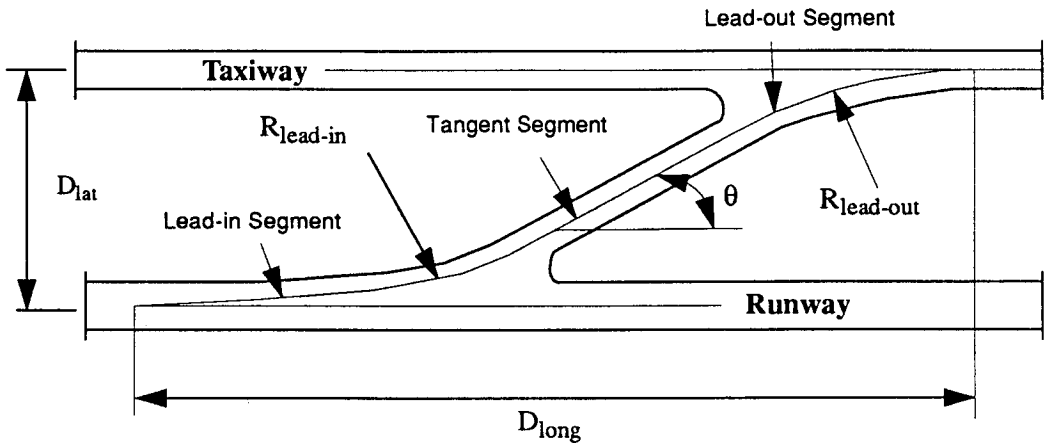

Table 4.3 defines the same equations in English units. The minimum lateral separation distance between a runway and taxiway centerlines, D_{lat}, is provided in REDIM as a geometric check to see whether particular turnoff is feasible for a given distance between centerlines, D_{ttw}, provided by the user.Note that for some geometries two values of D_{lat} are usually provided since the minimum lateral space requirement could be dictated by either the lead-out geometry or by the "double back" geometry if present. Taking as an example the standard 30 degree acute angle geometry it is seen that a minimum separation between runway and parallel taxiway centerlines is 159 m. (521 ft.) if a double back geometry is used and a transport aircraft classified in design group IV as critical design vehicle (see Table 4.4). Using the same critical aircraft the minimum lateral separation between runway and taxiway centerlines, from a geometric stand point alone, without a double back is 106 m. (349 ft.). The second distance, however, would violate existing

FAA separation criteria which for this type of vehicle requires 122 m. (400 ft.) as the minimum D_{lat}. Table 4.4 contains radii dimensions pertaining to each aircraft design group classification as well as accepted FAA separation criteria used in airport design. These values are used with equations contained in Tables 4.2 and 4.3. Note that for a wide throat

TABLE 4.2 Geometric Characterization of Existing Runway Turnoffs (Metric System).

Turnoff	Longitudinal Space (D_{long}) in meters	Minimum Lateral Space (D_{lat})
90 Deg. Angle	R[a] + 137.2	R + 76.2
45 Deg. Angle (θ=45)	244 (sin θ) + 37 (sin θ) + [D_{ttw}[b] - D_{lat}] / tan θ	244 (1- cos θ) + 37 (1- cos θ)
30 Deg. Angle (θ=30)	549 (sin θ) + 244 (sin θ) + [D_{ttw} - D_{lat}] / tan θ + 61	549 (1- cos θ) +244 (1- cos θ) or R (1+ cos θ) + 73.5
30 Deg. Angle with 427 m. Spiral Curve (θ=30)	244 (sin θ) + [D_{ttw} - D_{lat}] / tan θ + 415	244 (1- cos θ) + 73.5 or R (1+ cos θ) + 73.5 (double back)
"Wide Throat"	R[c] + 300	122

a. R varies according to the aircraft design group classification (see Table 4.4).
b. D_{ttw} is the distance from runway to taxiway centerlines.
c. R varies from 122 m. to 52 m. depending upon D_{ttw} (see Table 4.5 for suggested values)

TABLE 4.3 Geometric Characterization of Existing Runway Turnoffs (English System).

Turnoff	Longitudinal Space (D_{long}) in feet	Lateral Space (D_{lat}) in feet
90 Deg. Angle	R[a] + 450	R + 250
45 Deg. Angle (θ=45)	800 (sin θ) + 120 (sin θ) + [D_{ttw}[b] - D_{lat}] / tan θ	800 (1- cos θ) + 120 (1- cos θ)
30 Deg. Angle (θ=30)	1800 (sin θ) + 800 (sin θ) + [D_{ttw} - D_{lat}] / tan θ + 61	1800 (1- cos θ) +800 (1- cos θ) or R (1+ cos θ) + 241 (double back)
30 Deg. Angle with 1400 ft. Spiral Curve	800 (sin θ) + [D_{ttw} - D_{lat}] / tan θ + 1360	800 (1- cos θ) + 241 or R (1+ cos θ) + 241 (double back)
"Wide Throat"	R[c] + 984	400

a. R varies according to the aircraft design group classification (see Table 4.4).
b. D_{ttw} is the distance from runway to taxiway centerlines.
c. R varies from 400 ft. to 170 ft. depending upon D_{ttw} (see Table 4.5 for suggested values)

geometry values of ending radii, R are suggested in Table 4.5. These values were derived from an original wide throat geometry with a 122 m. (400 ft.) distance between centerlines. The values in Table 4.5 reflect a discrete radii tapering between a 122 m. (400 ft.) radius corresponding to a 167 m. lateral separation distance between runway and taxiway centerlines to a 52 m. (170 ft.) radius whenever D_{ttw} exceeds 213 m. (700 ft.). Appendix A shows in detail the geometrics associated with this turnoff.

TABLE 4.4 **Turnoff Parameters for Various Aircraft Design Groups and Approach Categories C and D [FAA, 1989].**

Parameter	Group I	Group II	Group III	Group IV	Group V	Group VI
Radius, R (m./ft.)	(23/75)	(23/75)	(31/100)	(46/150)	(46/150)	(52/170)
Fillet Radius (m./ft.)	(18/60)	(17/55)	(17/55)	(24/80)	(26/85)	(26/85)
FAA Separation Distance to Taxiway CI (m./ft.)	120[a] (400)	120 (400)	120 (400)	120 (400)	120[b] (400)	180 (600)

a. The Federal Aviation Administration advisory circular 150/5300-13 rounds-off distances to those shown in this table.
b. This standard applies to airport elevations less than 410 m. (1345 ft.). Increase to 135 m. (450 ft.) for airfield elevations between 410 m. and 2000 m. (1345 - 6560 ft.) and 150 m. (500 ft.) for airfield elevations above 2000 m. (6560 ft.).

TABLE 4.5 **Recommended Lead-out Radii for Wide Throat Geometry.**

D_{uw} m. (ft.)	< 168 (550)	168 - 191 (550 - 625)	192- 213 (625 - 700)	> 213 > 700
Radius m (ft.)	122 (400)	91 (300)	61 (200)	52 (170)

4.3 Characterization of REDIM Generated Turnoff Geometries

The characterization of REDIM generated turnoff geometries is executed through continuous simulation of the aircraft trajectory until the aircraft has reached the tangency point of the lead-out turn segment. Figure 4.16 illustrates geometrically the procedures to estimate D_{long} and D_{LAT} for a generalized REDIM turnoff trajectory. Equations 4.1 through 4.6 also apply in this case and thus are integrated forward in time to describe the full turnoff trajectory accounting for aircraft inertia and nose gear side friction coefficient constraints. Using this procedure a variable radii of curvature geometry results and thus it is necessary for every aircraft to be treated independently for this analysis. Since the conflict resolution

only applies for the improvement and design cases and is usually executed prior to the optimization procedures it is necessary to determine D_{long} and D_{lat} in terms of a critical aircraft. The critical aircraft is usually determined from the aircraft mix selected by the user. Once a critical aircraft is found the continuous simulation procedure is executed to derive unique values for D_{long} and D_{lat}.

4.4 Turnoff Conflict Resolution Procedures

Once the characterization of a turnoff has been made in terms of its minimum lateral and longitudinal space requirements it is possible to establish rules to verify whether or not two adjacent turnoff geometries will conflict with each other. The procedure is executed only for the design and improvement cases as these two program run modes require the user to select a number of exits to be constructed on an existing or new runway. Figure 4.17 illustrates possible scenarios where neighboring turnoff geometries could become a potential problem.

Figure 4.17(a) represents a generalized existing runway with two exits, i and (i+1) located d_1 and d_2 from runway threshold. Each exit is characterized by longitudinal dimensions $D_{long\ (i)}$ and $D_{long\ (i+1)}$, respectively. A distance denoted as $D_{available}$ is available for constructing a new rapid runway geometry. Note that the control points defining distance $D_{available}$ are the intersection point of the tangent of exit (i) plus a small distance called e_{min} and the ending point of the neighboring exit (i+1) designated d_3. If the user wants to add new rapid runway exits to this scenario the program estimates $D_{availabe}$ for every pair of adjacent exits in order to estimate which gaps are feasible to place a new exit geometry with user defined parameters V_{exit} and θ. The reader should recall that a user has already specified turnoff exit parameters such as exit and final speeds for new exits which are used to characterize each possible new turnoff to be constructed.

Once the longitudinal characterization of candidate turnoffs has been completed resulting in a specific D_{long} for the new candidate turnoff geometry this distance is compared with $D_{available}$ to ascertain which runway "gaps" are feasible candidates to locate optimal turnoffs. Figure 4.17(b) illustrates a possible rapid runway exit designated Exit (i) located between exits (i-1) and (i+1) with characteristic length $D_{long\ (i)}$. Note from this figure that a distance called Δd represents the range of possible locations for exit (i) in order to avoid conflicts with neighboring exits (i-1) and (i+1). This procedure when applied to the improvement case scenario reduces the ranges of feasible solutions substantially thus reducing the computational effort in the optimization procedure.

Figure 4.17(c) illustrates an unfeasible turnoff placement scenario where the new turnoff (i) clearly exceeds the distance available for turnoff locations between exits (i-1) and (i+1). Note that two overlapping segments denoted Δd_1 and Δd_2 arise in this case thus making the placement of exit (i) impossible within the longitudinal space limitations shown. Possible courses of action to follow would be: 1) to reduce the design speed for exit (i) in order to shorten the length D_{long}, 2) to increase the exit angle in order to also reduce the longitudinal distance taken by the turnoff, and 3) to close one of the standard

FIGURE 4.17 Sample Turnoff Conflict Resolution Scenarios.

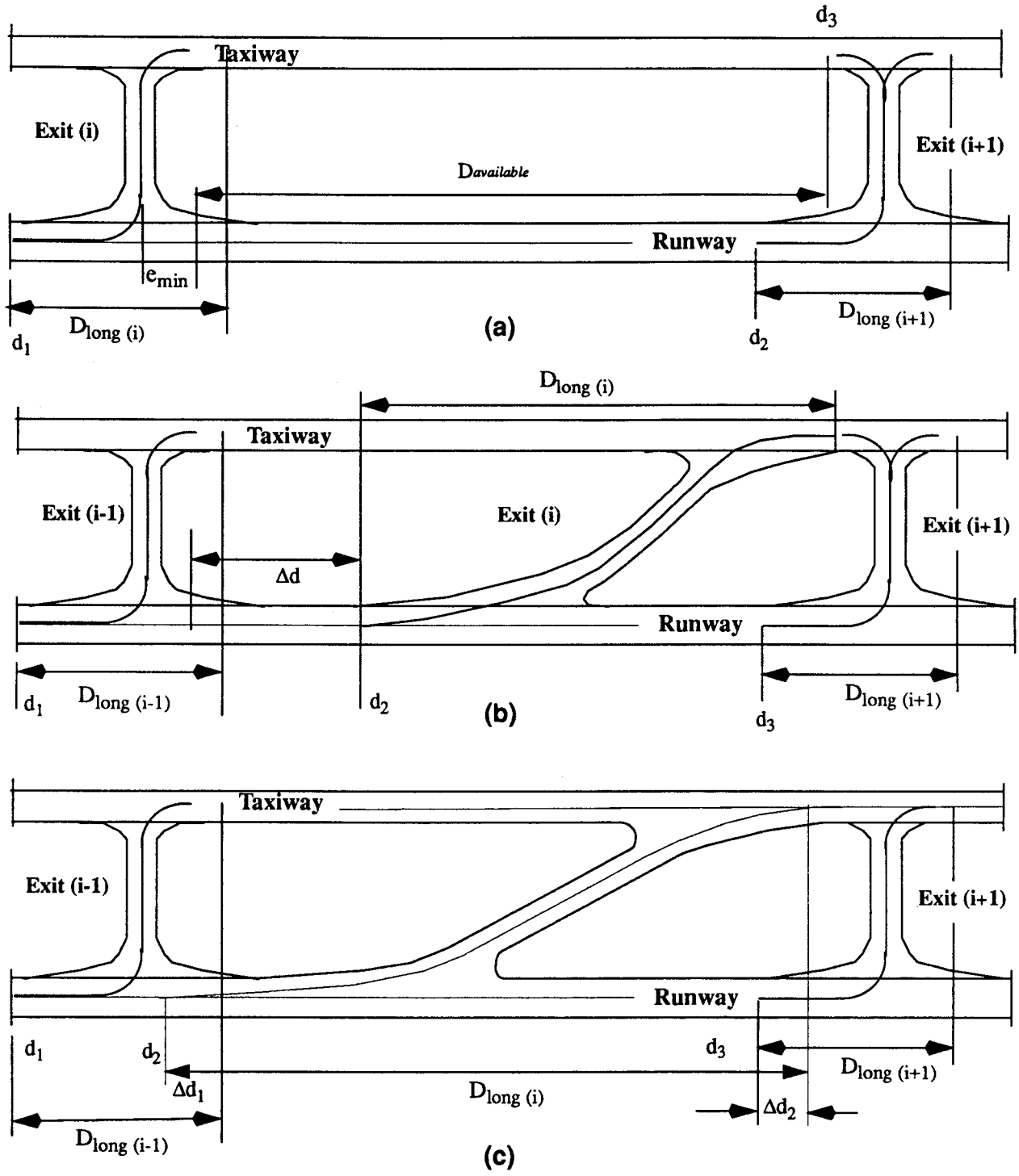

90 degree turnoff geometries thus allowing the placement of the rapid runway turnoff (i). Obviously, each alternative presents some problems that should be carefully evaluated by the analyst.

CHAPTER 5

REDIM 2.0 Software Package

This chapter describes the software package developed as part of this research project. The model described here is termed Runway Exit Design Interactive Model version 2 (REDIM 2.0). The model can be run on any IBM or compatible computer with EGA graphic capabilities. Due to the intensive computations related with the stochastic event generation and optimization procedures of the program, a computer with an INTEL 80286 microprocessor and a math coprocessor constitute the minimum desired configuration. REDIM 2.0 will run in machines not having a math coprocessor but the running times are considerably larger than those equipped with a math coprocessor.

5.1 Model Structure

REDIM 2.0 structure is depicted graphically in Figure 5.1. The model is comprised of four well defined modules: 1) Input, 2) Simulation, 3) Optimization and 4) Output. The modules interact with three data files containing aircraft related information (master and working files) and an output file generated after the end of each run. The following paragraphs describe in some detail the peculiarities of each module and the input/output structure of the program.

5.2 Main Menu

The "Main Menu" placed at the top level of the flow chart has five modes: 1) "Edit", 2) "Analysis", 3) "Output", 4) "Print", and 5) "Quit". The Main Menu always appears at the top of the computer screen. The 'edit' mode invokes the procedures of Input

FIGURE 5.1 **REDIM 2.0 Modular Breakdown.**

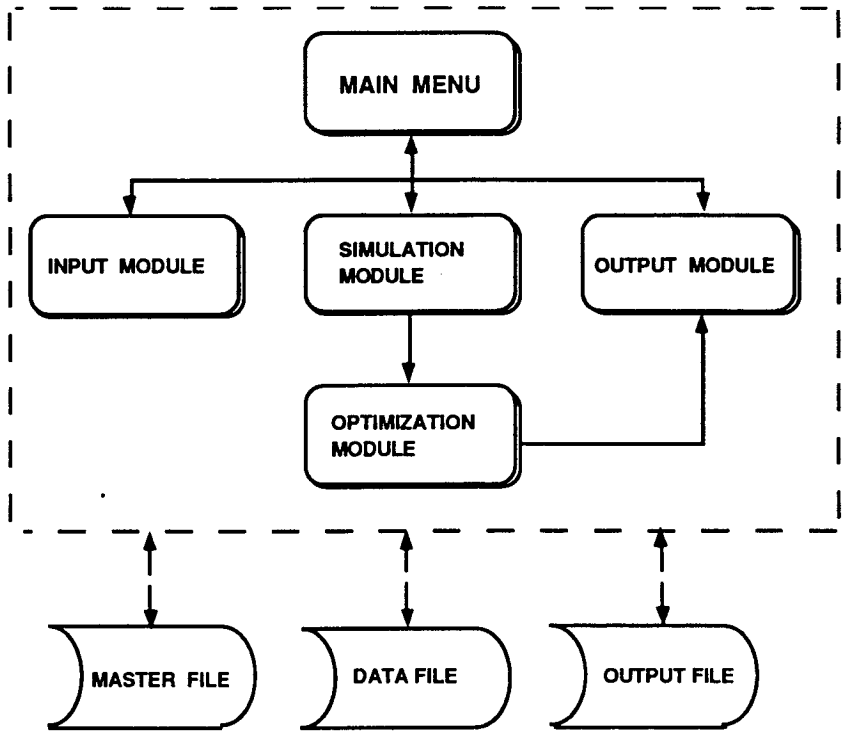

Module, where the user may edit the Data File or Master File. The 'analysis' mode invokes the analysis procedures. REDIM 2.0 provides four types of analyses: 'design,' 'improvement,' 'evaluation' and 'individual.' The 'output' mode connects the user with output module where the user may view the various output screens.

5.3 Input Module

The Input Module comprises a series of interactive screens that allow the user to input and edit data necessary for the analysis portion of the program (i.e. Simulation and Optimization Modules). This module is controlled by menus or key-stroke commands such as "Esc" key.

Input data is classified into six broad categories: 1) analysis type and related data, 2) aircraft mix, 3) airport operational data, 4) airport environmental data, 5) runway gradients and 6) surface conditions. All of these are necessary for the analysis, and should be saved in a 'Working Data File' specified by the user with an arbitrary name. For the convenience of the user, all predefined aircraft characteristics are kept in a Master Data File named "MASTREV.DAT" and are transferred to the Working Data File automatically if necessary.

5.3.1 Data Classification

In REDIM 2.0. there are three kinds of data needed for analysis: 1) input data, 2) constant data, and 3) calculated data. Among these kinds of data, constant data and calculated data are determined in the Simulation and Optimization Module. Input data is provided by the user via the Input Module and its user-friendly screens. The input data is classified into six categories as mentioned previously. The following paragraphs define the categories in more detail.

Analysis Type and Related Data

The program provides the user with four choices for the type of analysis to be performed. For each type of analysis, there are some specific accompanying data needed to execute the model properly. "Design" analysis asks the user to input the number of new exits, the lateral distance between the runway and the parallel taxiway, the exit angle, the speed at the junction of exit and taxiway and the exit speed of each aircraft category. "Evaluation" analysis requires the information on the existing exit configuration including the number of existing exits, the locations and the types, the entry speed for each existing exit and availability. For the "improvement" analysis, the user has to input all the data above. The "individual" mode requires only the aircraft type and surface condition.

Aircraft Mix

In this category, the percentages of the aircraft comprising the airport population mix are included. The maximum number of aircraft for a mix is restricted as twenty because this number seems to be a practical limit and because the memory requirements of the software should not exceed 640k dictated by the DOS operating system.

Airport Operational Data

In this category, the free roll time between the touchdown and the beginning of braking, the free roll time between the end of braking and the beginning of turn off are included. A safety factor for the impending skidding condition is also part of this category.

Airport Environmental Data

The following parameters are included in this category: wind speed, wind direction, airport elevation, airport temperature, runway orientation and runway width. This will affect the optimal placement of turnoffs, since they have effect on airport landing roll performance.

Runway Gradient

In this category, runway length, and the effective gradient for every one tenth of runway are included. The runway gradient affects the effective aircraft deceleration used in the kinematic equations of motion. This effect, although small for landing opera-

tions, is considered for the sake of model completeness

Weather

The relative frequency of dry and wet runway surface conditions are included in this category. The percentages should reflect the expected conditions predominant at the airport facility.

5.3.2 Data Input Method

In the Input Module, there are three different input methods used: 1) menu input, 2) line input, and 3) table input. Menu input arises when the user selects his choice among the list displayed on the screen using the arrow keys and enter key. The flow in the program is controlled by the menu input method. The main menu, edit menu for working data file, edit menu for master data file, selection of a analysis type, etc. are the examples of the menu input method. Line input occurs when the user puts a numerical value like runway length or a string datum like a data file name at the position specified on a screen. The user inputs file names (data and/or output file), the number of exits, etc. using this method. Table input is similar to line input. However, table input is used in order to get several numerical data on the same screen, while line input is used in order to get one numerical or string datum on a line. By the table input method the user inputs aircraft mix data, exit speeds etc.

5.3.3 Procedures in Input Module

If the user selects 'Edit' from the Main Menu, the program shows the user 'Edit Menu' which offers the user with two choices: 'Edit Data File' and 'Edit Master File.'

Editing the Data File

This portion of the program allows the user to modify existing data file. If the user selects this mode from the Edit Menu, the list of the data categories, which are explained in Section 5.3.1, are shown on the screen. The user may select one from the list, and then modify the values of data items in that category.

Editing the Master File

While the function of "Edit Data" mode is editing the working data file, the function of "Edit Master File" is editing the master data file which keeps the aircraft names and their geometric characteristics. If "Edit Master File" mode is selected, the Edit Menu for master data file appears. In this menu, there are two choices: 1) "Add a New Aircraft" and 2) "Change some Specific Data." If the user chooses the first, he/she has to select one out of five aircraft categories (TERPS A-E) and input the new aircraft name. Then a screen for editing aircraft characteristics appears. If the user opts for the second choice, he/she has to select one aircraft category and one aircraft name included in the

category selected. Then a screen for editing aircraft characteristics appears.

5.4 Analysis Types and Their Input/Output Relationships

As stated earlier, the user can select one of four types of analysis: 1) design of a new runway system, 2) improvement of an existing runway system, 3) evaluation of an existing runway system and 4) analysis of individual aircraft landing performance.

The 'design' option assumes a hypothetical situation with no exits on the runway. The number of new exits and the design exit speed for each aircraft category are inputs for this type of analysis. The results are 1) optimal exit locations, 2) aircraft assignment to the new exits, 3) the weighted average ROT which is minimized by the optimal exit locations, and 4) turnoff geometries of the exits.

The 'improvement' option assumes that a few exits would be added to an existing runway. This analysis requires the number of new exits which will be constructed and all information on the existing exits, which includes 1) the number of existing exits, 2) the locations and types of existing exits and 3) availability of existing exits. The design exit speed for each aircraft category is also required. The results are similar in nature to those of the 'design' option. The only difference is that this option takes into account the existing exits as well as the new exits for aircraft assignment

The purpose of 'evaluation' option is to estimate the average ROT of a given aircraft mix assuming only existing exits are utilized. All information on the existing exits are required for this analysis. The aircraft assignment to the existing exit and the resultant average ROT are the major outputs of this analysis, while the user may view the geometry of the existing exits.

The 'individual' option is added in Phase II research for analyzing the landing behavior of an aircraft in more detail. The aircraft type and surface condition are the inputs for this analysis. The five percentile values (95%, 90%, 80%, 70% and 50%) of landing distance and ROT are the found for six exit speeds.

5.5 Computational Modules

The Simulation Module and the Optimization Module are the collections of subroutines made for computations. These computational modules are responsible for the aircraft landing roll dynamic simulation so as to generate turnoff locations for each aircraft and the dynamic programming optimization so as to decide the exit locations. For example, the Simulation Module involves the subroutines for aircraft dynamics and the subroutines for random number generation from the truncated normal distribution. The Optimization Module includes the subroutines for exit candidate generation and for the dynamic programming algorithm. The details of these computations are described in Chapters 2 and 3.

5.6 Output Module

The function of the Output Module is to present the analysis results in graphical form or tabular forms. Three types of analysis, 'design', 'improvement' and 'evaluation' share the same formats of the output, which are 'Aircraft Assignment and ROT Table,' 'ROT Statistics,' 'Exit Locations,' 'Exit Centerline Comparison,' and 'Exit Geometry.' The 'Aircraft Assignment and ROT Table' shows exit utilizations of each aircraft type and the corresponding ROT's. The 'ROT Statistics' shows the average ROT for each aircraft type and the grand average ROT of the aircraft mix in a bar chart format. The 'Exit Locations' presents the runway and the taxiway and the exits graphically on a scale. The 'Exit Centerline Comparison' plots the x-y coordinates of turnoff centerlines of the exits selected by the user on a scaled plane. The 'Exit Geometry' shows the complete geometry and the specifications of the exits selected by the user.

The fourth type of analysis ('individual') has only a form of output where the deceleration distances and ROT's of an aircraft type are presented for six different exit speeds and for five percentile values. Here, the percentile value means the proportions of aircraft landings to execute a turnoff at a given exit location.

5.7 Working Data File

REDIM 2.0 relies upon user selected information detailing the airport environmental and operational features as well as on aircraft data contained in the Master Data File. Since it is likely that many users would like to incorporate their own data under several runway scenario conditions the provision of a Working Data File is necessary to avoid critical changes to the Master Data File supplied with the program. Once the user inputs the aircraft mix data, pertinent aircraft data is duplicated from the Master Data File to a user Working Data File.Every run is then executed using the Working Data File from which modifications can be carried out.

5.8 Master Data File

The Master Data File contains aircraft characteristics necessary to execute the simplified aircraft landing simulation procedures used in REDIM 2.0. The data file lists aircraft parameters used in the internal computations. Among these are: wing span, empty operational weight, load on main gear, maximum landing weight, wheelbase, etc.

5.9 Printing a Summary Report

REDIM 2.0 provides the user with a summary report containing relevant input and output data at the touch of a single keystroke. This printout can be obtained from the

Main Menu or the Output Module.The organization of the summary report is shown in Table 5.1.

TABLE 5.1 REDIM 2.0 Summary Report Contents.

Report Section	Sub-Section	Remarks
I) Input Data Summary	I.1) Analysis Type and Existing Exits	Contains locations, type and entry speed parameters of every turnoff modeled in the current scenario
	I.2) Aircraft Mix and Aircraft Characteristics	Summarizes aircraft population mix entered for current scenario and the aircraft characteristics extracted from the working data file
	I.3) Airfield Operational Data	Lists current values for skid safety factor and the desired minimum separation between adjacent turnoff locations
	I.4) Environmental Data	Contains values of wind speed, runway orientation, temperature and runway width used in current run
	I.5) Runway Gradients	Lists for every tenth of runway length the local horizontal gradient
II) Analysis Results	II.1) Average ROT	Lists the weighted average runway occupancy time obtained for the current run
	II.2) Aircraft Assignment/ROT Table	Assigns aircraft percentages to every exit location for every runway surface condition
	II.3) Turnoff Centerline Geometries	Lists X-Y coordinates of every new or existing turnoff geometry

5.10 Print-Screen Output Capabilities

In order to convey more information to the user REDIM 2.0 incorporates two fast assembly language routines to capture any output screen that needs to be printed. The model provides only two types of printer drivers at this time one for HP-compatible laser printers and another one for Epson compatible dot matrix printers. Output screens can be readily obtained while the user is reviewing the output module screens.

5.11 Model Computational Aspects

In order to provide good measures of dispersion in REDIM 2.0 the model is executed over five trial sets using randomized seeds and twenty replications per trail per aircraft/runway surface condition. This implies that every aircraft/runway surface condition combination is actually executed one hundred times in order to get good estimates of the probability density function describing the aircraft landing roll kinematic behavior. The most intensive computational algorithm in REDIM 2.0, however, is the optimization of exit locations consuming approximately 80% of the CPU time needed to execute a typical analysis. The reader should be aware that the computational effort varies dramatically with the various factors such as the runmode selected (e.g., design, improvement or analysis of runways), the number of exits selected, the runway length, and the mix index. The most prominent factor being the run mode selected. The design mode is the most computationally intensive of all running modes available in REDIM 2.0 as this mode deals with the optimal placement of turnoffs on a new runway where usually no longitudinal constraints have been specified.

5.12 Hardware Requirements

Suggested hardware requirements to model realistic runway scenarios with REDIM 2.0 are as follows:

- IBM or compatible personal computer with a 80286 or 80386 microprocessors
- A math coprocessor
- EGA or VGA color monitor
- HP laser printer or Epson FX-80 dot-matrix printer
- 1 MB minimum of Random Access Memory

Due to the intensive computations during the optimization and dynamic simulation procedures using a Monte Carlo simulation approach a math coprocessor is highly recommended as it will speed up the computation time by a factor of 2 (typically). A computer using the 80386 microprocessor is highly recommended as this will also reduce the computational time substantially.

CHAPTER 6

REDIM Applications

This chapter deals with specific applications of REDIM 2.0 to six runways located at six airports around the United States.Airports selected for this study were: 1) Philadelphia International (Camden), 2) Baltimore Washington International (BWI), 3) Boston Logan International, 4) Washington National, 5) Kennedy International and 6) Newark Airports. These airports were selected by FAA as representative applications were REDIM could payoff as a runway turnoff location and design tool. The analysis was aimed at a selected runway at each airport with the intention to evaluate the predictive capabilities of REDIM 2.0 as well as to test possible improvements to existing facilities in order to reduce runway occupancy time.

6.1 Philadelphia International Airport

Philadelphia International Airport has 2 closely-spaced runways oriented East-West (09-27) and an intersecting runway oriented near a North-South direction (17-35). Figure 6.1 illustrates a simple schematic of the current facility. Runway 17-35 is of particular interest at this airport for our analysis. This runway has a length of 1664 m. (5640 ft.) and width of 46 m. (150 ft.) and serves primarily general aviation operations. The layout shown in Fig. 6.1 illustrates clearly the position of the main and general aviation terminals.

Tables 6.1 and 6.2 list the existing turnoff locations for runways 17 and 35, respectively including the type of exit and their associated exit design speeds according to well accepted standards. Table 6.3 contains pertinent information regarding the aircraft population mix used in this analysis. It should be emphasized that all operations assumed for this runway are those of business jets, commuter and general aviation aircraft.

Table 6.4 illustrates typical runway occupancy time results in an assignment/ROT table for-

mat. This table contains individual aircraft-type runway occupancy time (ROT) for two different airfield surface conditions, dry and wet. Percentages shown in this table represent the percent of aircraft of type i that will exit through runway exit j and surface condition k as shown in the table. To illustrate this point consider the case of a small general aviation aircraft such as a Cessna 172. According to Table 6.4 one hundred percent of the vehicles of this type will take exit 2 (labeled W) located 690 meters from runway threshold 17.

TABLE 6.1 Turnoff Data for Runway 35 at Philadelphia International.

Taxiway No.	Taxiway Designation	Location m. (ft.)	Taxiway Type (Degrees)	Design Speed m./s. (m.p.h.)
1	A	406 (1332)	90	8 (17.8)
2	E	731 (2397)	45	17.9 (40)
3	W	975 (3196)	> 90	6.7 (15.0)
4	H	1056 (3462)	60	8 (17.8)
5	K	1584 (5194)	90	8 (17.8)
6	L	1644 (5393)	90	8 (17.8)

TABLE 6.2 Turnoff Data for Runway 17 at Philadelphia International.

Taxiway No.	Taxiway Designation	Location m. (ft.)	Taxiway Type (Degrees)	Design Speed m./s. (m.p.h.)
1	K	81 (266)	90	8 (17.8)
2	W	690 (2264)	45	17.4 (40)
3	E	974 (3196)	45	17.4 (40)
4	A	1299 (4261)	90	8 (17.8)
5	AA	1644 (5393)	90	8 (17.8)

FIGURE 6.1 **Schematic of Philadelphia International Airport (Camden).**

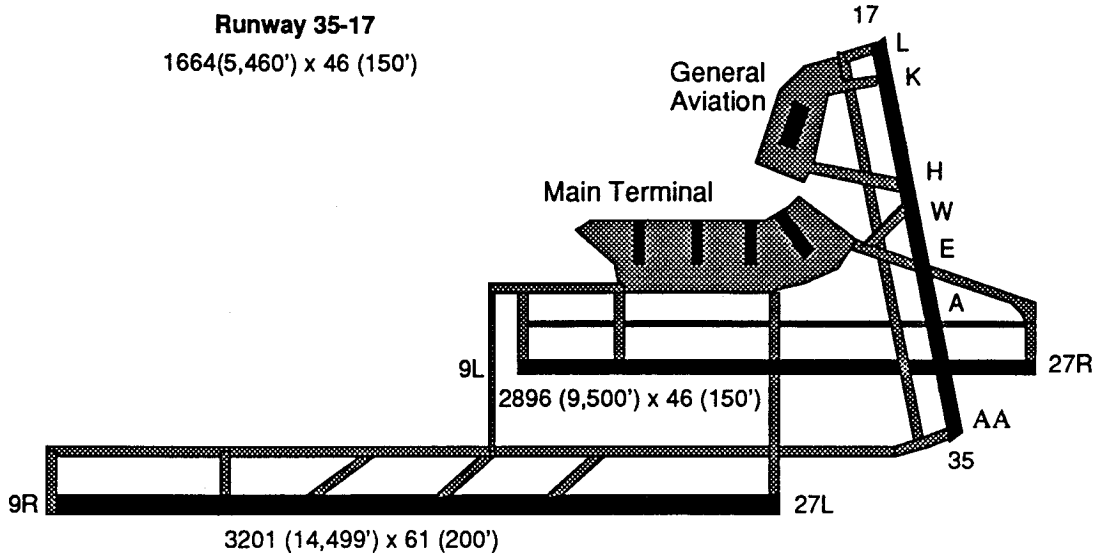

TABLE 6.3 **Aircraft Mix at Philadelphia International for Runway 35-17.**

Aircraft Number	Aircraft Type	Percent of the Total Mix (%)	Aircraft Number	Aircraft Type	Percent of the Total Mix (%)
1	Cessna 172	12	6	Cessna 550	3
2	Cessna 208	8	7	Gulsftream IV	2
3	EMB 120	18	8	Beechcraft B300	4
4	Saab 340	12	9	Learjet 31	4
5	SW 227	20	10	DHC-8	17

TABLE 6.4 **Runway Occupancy Time Results for Runway 35 at Philadelphia International Airport.**

Exit Number Exit Code[a] Exit Loc. Exit Type	1 Open 406 90 Deg.	2 Open 731 45 Deg.	3 Open 975 90 Deg.	4 Open 1056 90 Deg.	5 Open 1584 90 Deg.	6 Open 1644 90 Deg.
CE-172						
Dry ROT	27.8	35.2				
(%)	(71.0)	(29.00)				
Wet ROT	28.1	35.2				
(%)	(46.0)	(54)				
CE 208						
Dry ROT	23.5	31.1				
(%)	(2.0)	(98.0)				
Wet ROT		31.1				
(%)		(100.0)				
BE-300						
Dry ROT		27.7	35.9			
(%)		(30.0)	(70.0)			
Wet ROT		28.1	35.6			
(%)		(3.0)	(97.0)			
Saab 340						
Dry ROT			35.6	44.3	62.8	
(%)			(54.0)	(4.0)	(42.0)	
Wet ROT			36.3		63.3	
(%)			(5.0)		(95.0)	
SA 227						
Dry ROT		26.8	44.0	60.9		
(%)		(9.0)	(1.0)	(97.0)		
Wet ROT				60.6		
(%)				(100.0)		
EMB 120						
Dry ROT			34.2	44.0	60.8	
(%)			(2.0)	(1.0)	(97.0)	
Wet ROT					60.6	
(%)					(100.0)	
CE-550						
ROT		27.7	35.9			
(%)		(66.0)	(36.0)			
Wet ROT		28.1	35.9			
(%)		(13.0)	(87.0)			

TABLE 6.4 Runway Occupancy Time Results for Runway 35 at Philadelphia International Airport.

Exit Number Exit Code[a] Exit Loc. Exit Type	1 Open 406 90 Deg.	2 Open 731 45 Deg.	3 Open 975 90 Deg.	4 Open 1056 90 Deg.	5 Open 1584 90 Deg.	6 Open 1644 90 Deg.
Learjet-31						
Dry ROT		27.1	35.0			
(%)		(8.0)	(92.0)			
Wet ROT			34.7	61.3		
(%)			(99.0)	(1.0)		
DCH-8						
Dry ROT		30.7	38.6			
(%)		(4.0)	(96.0)			
Wet ROT			38.4	67.6		
(%)			(94.0)	(6.0)		
Gulfstream IV						
Dry ROT			31.3	43.2		
(%)			(30.0)	(70.0)		
Wet ROT				42.1		
(%)				(100.0)		
Weighted Average Runway Occupancy Time						**41.5 seconds**

a. The exit code designates whether or not a runway exit is included in this analysis run. REDIM 2.0 offers the analyst the option of retaining all runway exits or just those selected by the user.

From this analysis it is concluded that weighted average runway occupancy time of 41.5 seconds is typical for this runway facility. This value in fact represents a good service time for a medium size runway with a predominantly small aircraft population. It can be seen from Table 6.4 a good utilization of all runway exits with the exception of exit 5 (located at 1584 m.) which is used about 1% of the total time (i.e., combining the utilization of commuter aircraft).Judging from the results obtained it is possible to improve the existing condition of this runway by adding a seventh exit between taxiways "hotel" and "kilo" at an intermediate position to reduce the high ROT values obtained for some commuter aircraft under wet pavement conditions. The addition of a single medium speed, forty five degree angle geometry between taxiways "hotel" and "kilo" reduces the WAROT value from 41.5 to 39.0 seconds. The location of this new taxiway

6.2 Baltimore-Washington International Airport

Baltimore Washington International general layout is shown in Figure 6.2. Runway 15L-33R, a 1524 m. (5000 ft.) general aviation runway, was selected for this analysis. Tables 6.5 and 6.6 contain pertinent runway turnoff information used in our analysis. Note that presently four usable runway exits are available for both northflow and southflow operations. Taxiway "Mike" (M) forms an obtuse angle with the runway centerline for southflow operations and thus has been modeled with some penalty in the design exit speed for runway 15L use (see Table 6.5). Table 6.7 illustrates the aircraft population mix used in this analysis. Note the large number of general aviation, business and commuter aircraft. Table 6.8 shows the assignment table results obtained using REDIM 2.0. The weighted average runway occupancy time for this runway is 52.3 seconds.

FIGURE 6.2 Schematic of Baltimore Washington International Airport Runway 15L-33R.

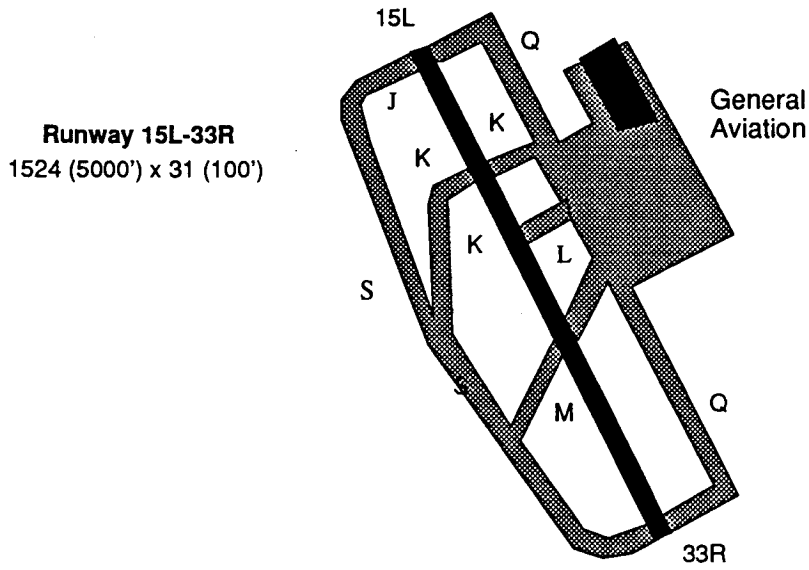

TABLE 6.5 Turnoff Data for Runway 15L at Baltimore Washington Airport.

Taxiway No.	Taxiway Designation	Location m. (ft.)	Taxiway Type (Degrees)	Design Speed m./s. (m.p.h.)
1	K	400 (1313)	90	8 (17.8)
2	L	648 (2125)	90	8 (17.8)
3	M	1143 (3750)	135	6.7 (15)
4	S	1506 (4938)	90	8 (17.8)

TABLE 6.6 Turnoff Data for Runway 33R at Baltimore Washington Airport.

Taxiway No.	Taxiway Designation	Location m. (ft.)	Taxiway Type (Degrees)	Design Speed m./s. (m.p.h.)
1	M	419 (1375)	45	17.4 (40)
2	L	877 (2875)	90	8 (17.8)
3	K	1047 (3435)	90	8 (17.8)
4	J	1506 (4938)	90	8 (17.8)

TABLE 6.7 Aircraft Mix at Baltimore Washington International.

Aircraft Number	Aircraft Type	Percent of the Total Mix (%)	Aircraft Number	Aircraft Type	Percent of the Total Mix (%)
1	Cessna 172	5	7	Cessna 550	7
2	Cessna 208	3	8	Grumman IV	3
3	Saab 340	14	9	Cessna 650	4
4	SW 227 "Metro"	18	10	Learjet 31	4
5	British Aero. 31	13	11	Beechcraft B-58	3
6	DeHavilland DHC-8	15	12	Embraer 120	11

TABLE 6.8 **Runway Occupancy Time Results for Runway 15L-33R at BWI International Airport.**

Exit Number Exit Code[a] Exit Loc. Exit Type	1 Open 400 90 Deg.	2 Open 648 90 Deg.	3 Open 1143 90 Deg.	4 Open 1506 90 Deg.
CE-172				
Dry ROT	27.8	37.9)		
(%)	(52.0)	(48.0)		
Wet ROT	28.1	38.3		
(%)	(22.0)	(78.0)		
CE 208				
Dry ROT		32.6		
(%)		(100.0)		
Wet ROT		32.7		
(%)		(100.0)		
BE-58				
Dry ROT		31.2	49.3	
(%)		(4.0)	(96.0)	
Wet ROT			49.8	
(%)			(100.0)	
Saab 340				
Dry ROT			50.3	59.8
(%)			(89.0)	(11.0)
Wet ROT			51.1	60.4
(%)			(26.0)	(74.0)
EMB-120				
Dry ROT			48.4	57.0
(%)			(19.0)	(81.0)
Wet ROT				57.8
(%)				(100.0)
SA-227				
Dry ROT			46.9	
(%)			(100.0)	
Wet ROT			47.2	
(%)			(100.0)	
BAe-31				
Dry ROT			47.4	57.5
(%)			(98.0)	(2.0)
Wet ROT			48.0	57.4
(%)			(44.0)	(56.0)

TABLE 6.8 Runway Occupancy Time Results for Runway 15L-33R at BWI International Airport.

Exit Number Exit Code[a] Exit Loc. Exit Type	1 Open 400 90 Deg.	2 Open 648 90 Deg.	3 Open 1143 90 Deg.	4 Open 1506 90 Deg.
CE-550				
Dry ROT			48.3	
(%)			(100.0)	
Wet ROT			48.6	
(%)			(100.0)	
CE-650				
Dry ROT			47.7	
(%)			(100.0)	
Wet ROT			47.9	
(%)			(100.0)	
Learjet-31				
Dry ROT			47.0	
(%)			(100.0)	
Wet ROT			47.4	
(%)			(100.0)	
DHC-8				
Dry ROT			53.7	
(%)			(100.0)	
Wet ROT			54.4	
(%)			(100.0)	
G1159C				
Dry ROT			41.0	
(%)			(100.0)	
Wet ROT			41.5	
(%)			(100.0)	
Weighted Average Runway Occupancy Time (WAROT)				**52.3 sec.**

a. The exit code designates whether or not a runway exit is included in this analysis run. REDIM 2.0 offers the analyst the option of retaining all runway exits or just those selected by the user.

6.3 Boston Logan International Airport

Boston Logan International Airport has three main runways as shown in Figure 6.3. The runway of interest in this case is runway 09-27 having a total length of 2134 meters (7000 ft.) and four exit locations as shown in Tables 6.9 and 6.10. Table 6.11 contains pertinent information regarding the aircraft mix operating at this facility. Once again the main users of this runway are commuter and general aviation aircraft. Table 6.12 illustrates the ROT/ exit assignment table for the baseline scenario showing a weighted average runway occupancy time (WAROT) of 50.3 seconds. Using the same aircraft mix but landings on runway 27 the weighted average ROT value obtained is 49.3 seconds. This small difference is due to the better location of taxiway "Echo" (i.e., 1423 m. from threshold on runway 27) for the large commuter population used in the problem.

TABLE 6.9 Turnoff Data for Runway 27 at Logan International Airport.

Taxiway No.	Taxiway Designation	Location m. (ft.)	Taxiway Type (Degrees)	Design Speed m./s. (m.p.h)
1	D	262 (860)	45	17.4 (40)
2	C	936 (3070)	60	8 (17.8)
3	E	1423 (4666)	30	26.9 (60)
4	S	2097 (6877)	90	8 (17.8)

TABLE 6.10 Turnoff Data for Runway 09 at Logan International Airport.

Taxiway No.	Taxiway Designation	Location m. (ft.)	Taxiway Type (Degrees)	Design Speed m./s. (m.p.h.)
1	E	749 (2456)	>90	6.7 (15)
2	C	1198 (3930)	60	8 (17.8)
3	D'	1872 (6140)	>90	6.7 (15)
4	D	2097(6877)	90	8 (17.8)

Figure 6.3 Boston Logan International Airport Configuration.

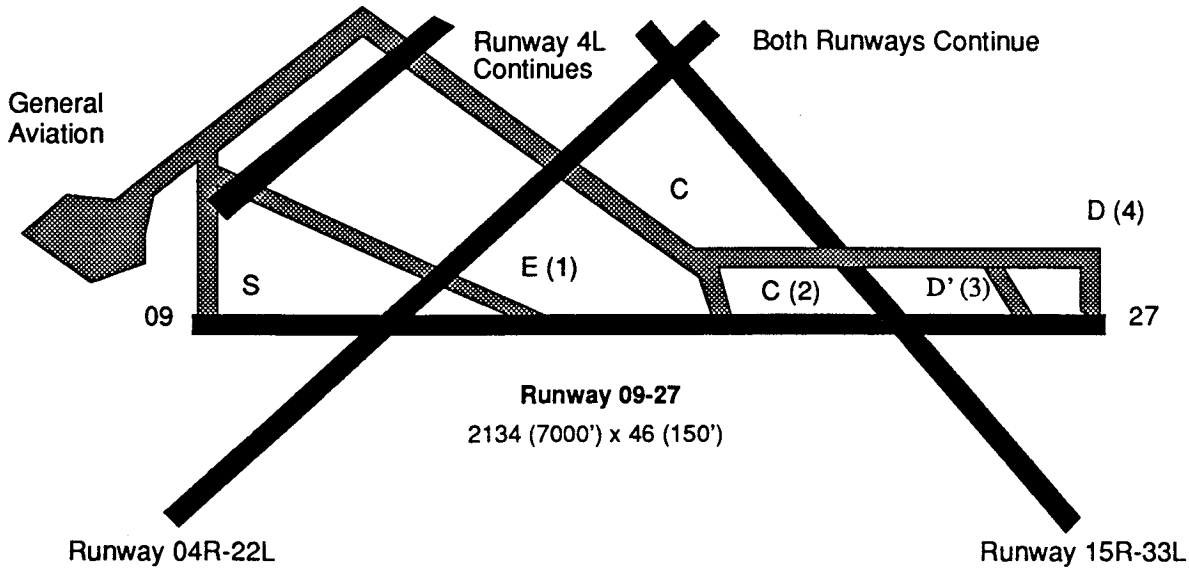

Numbers in parenthesis denote the taxiway number used for identification in the text.

TABLE 6.11 Aircraft Mix at Boston Logan International Airport.

Aircraft Number	Aircraft Type	Percent of the Total Mix (%)	Aircraft Number	Aircraft Type	Percent of the Total Mix (%)
1	Cessna 172	8.0	6	SA 227	15.0
2	Cessna 208	6.0	7	Saab 340	21.0
3	Piper PA-38-112	8.0	8	CE 650	4.0
4	Piper PA-32-301	4.0	9	Learjet 31	7.0
5	EMB 120	17.0	10	DHC-8	12.0

TABLE 6.12 **Runway Occupancy Time Results for Runway 09 at Boston Logan International Airport.**

Exit Number Exit Code[a] Exit Loc. Exit Type	1 Open 749 45 Deg.	2 Open 1198 90 Deg.	3 Open 1872 90 Deg.	4 Open 2097 90 Deg.
PA-38-112				
Dry ROT	41.0			
(%)	(100.0)			
Wet ROT	41.7			
(%)	(100.0)			
PA-32-301				
Dry ROT	38.1			
(%)	(100.0)			
Wet ROT	38.4			
(%)	(100.0)			
CE-172				
Dry ROT	41.5			
(%)	(100.0)			
Wet ROT	42.1			
(%)	(100.0)			
CE-208				
Dry ROT	36.5			
(%)	(100.0)			
Wet ROT	36.7			
(%)	(100.0)			
SAAB-340				
Dry ROT		49.5	72.8	
(%)		(96.0)	(4.0)	
Wet ROT		49.7	72.9	
(%)		(57.0)	(43.0)	
EMB-120				
Dry ROT		47.3	70.4	
(%)		(66.0)	(34.0)	
Wet ROT		48.2	70.9	
(%)		(5.0)	(95.0)	
SA-227				
Dry ROT	34.8	48.0		
(%)	(8.0)	(92.0)		
Wet ROT		48.2		
(%)		(100.0)		

TABLE 6.12 Runway Occupancy Time Results for Runway 09 at Boston Logan International Airport.

Exit Number Exit Code[a] Exit Loc. Exit Type	1 Open 749 45 Deg.	2 Open 1198 90 Deg.	3 Open 1872 90 Deg.	4 Open 2097 90 Deg.
CE-650				
Dry ROT	34.4	48.0		
(%)	(8.0)	(92.0)		
Wet ROT		48.2		
(%)		(100.0)		
Learjet-31				
Dry ROT	34.1	47.5		
(%)	(3.0)	(97.0)		
Wet ROT		47.4		
(%)		(100.0)		
DHC-8				
Dry ROT		53.3		
(%)		(100.0)		
Wet ROT		53.7		
(%)		(100.0)		
Weighted Average Runway Occupancy Time (WAROT)				**50.3 secs.**

a. The exit code designates whether or not a runway exit is included in this analysis run. REDIM 2.0 offers the analyst the option of retaining all runway exits or just those selected by the user.

6.4 Washington National Airport

Washington National Airport is one of the busiest in the nation considering the total area available for aircraft ground operations. Three intersecting runways comprise this airport and the subject of this analysis is runway 15-33 primarily used by business and commuter operations (see Figure 6.4). Table 6.10 shows that runway 15-33 has three main turnoffs: "Juliett" (J), "Mike" (M) and "Foxtrot" (F) located at 495, 1106 and 1572 meters away from threshold 15, respectively. For modeling purposes the intersection of runways 15-33 and 18-36 has been considered as a possible turnoff since taxiway "India" (I) is located at a short distance from the intersection point thus making it possible for some operations arriving on runway 15 to exit through this point. Table 6.11 lists a typical aircraft mix operating at this facility and used for the analysis and Table 6.12 summarizes the assignment of aircraft to each available runway exit. It is seen from Table 6.12 that the expected value of ROT for runway 15 is 51.25 seconds. The WAROT for runway 33 increases to 52.8 seconds using the same aircraft mix.

FIGURE 6.4 Schematic of Washington National Airport.

Runway 18-36
2094 (6,870') x 46 (150')

Runway 15-33
1582 (5,189') x 46 (150')

Runway13-21
1373 (4506') x 46 (150')

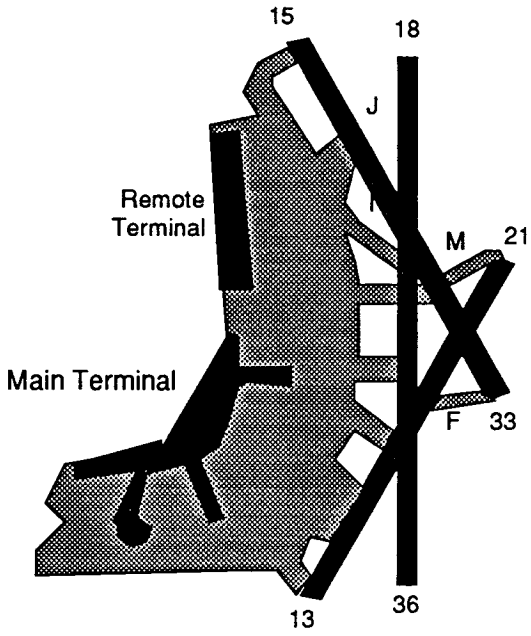

TABLE 6.13 Turnoff Data for Runway 15 at Washington National Airport.

Taxiway No.	Taxiway Designation	Location m. (ft.)	Taxiway Type (Degrees)	Design Speed m./s. (m.p.h.)
1	J	495 (1624)	45	17.4 (40)
2	M	1106 (3629)	90	8 (17.8)
3	F	1572 (5157)	90	8 (17.8)

TABLE 6.14 Turnoff Data for Runway 33 at Washington National Airport.

Taxiway No.	Taxiway Designation	Location m. (ft.)	Taxiway Type (Degrees)	Design Speed m./s. (m.p.h.)
1	M	466 (1528)	90	8 (17.8)
2	J	980 (3215)	90	8 (17.8)
3	I	1560 (5117)	45	8 (17.8)

TABLE 6.15 Aircraft Mix at Washington National Airport.

Aircraft Number	Aircraft Type	Percent of the Total Mix (%)	Aircraft Number	Aircraft Type	Percent of the Total Mix (%)
1	Piper PA-46-310	2.0	6	Boeing DHC-7	10.0
2	Beechcraft Be-59	3.0	7	Cessna CE 550	5.0
3	Beechcraft 300	4.0	8	Learjet 31	6.0
4	Saab 340	27.0	9	Boeing DHC-8	25.0
5	Embraer EMB-120	15.0	10	Gulfstream IV	3.0

TABLE 6.16 **Runway Occupancy Time Results for Runway 15 at National Airport.**

Exit Number Exit Code[a] Exit Loc. Exit Type	1 Open 495 90 Deg.	2 Open 1106 90 Deg.	3 Open 1560 90 Deg.
PA-46-310P			
Dry ROT	25.4		
(%)	(100.0)		
Wet ROT	25.5	53.5	
(%)	(89.0)	(11.0)	
BE-58			
Dry ROT		46.8	
(%)		(100.0)	
Wet ROT		46.9	
(%)		(100.0)	
BE-300			
Dry ROT		45.8	
(%)		(100.0)	
Wet ROT		45.7	
(%)		(100.0)	
Saab 340			
Dry ROT		46.4	61.8
(%)		(76.0)	(24.0)
Wet ROT		47.3	62.4
(%)		(14.0)	(86.0)
EMB-120			
Dry ROT		45.1	60.0
(%)		(13.0)	(87.0)
Wet ROT			59.8
(%)			(100.0)
DHC-7			
Dry ROT		50.5	
(%)		(100.0)	
Wet ROT		45.7	
(%)		(100.0)	
CE-550			
Dry ROT		44.2	
(%)		(100.0)	
Wet ROT		44.3	
(%)		(100.0)	

TABLE 6.16 Runway Occupancy Time Results for Runway 15 at National Airport.

Exit Number Exit Code[a] Exit Loc. Exit Type	1 Open 495 90 Deg.	2 Open 1106 90 Deg.	3 Open 1560 90 Deg.
Learjet-31			
Dry ROT		44.2	
(%)		(100.0)	
Wet ROT		44.3	
(%)		(100.0)	
DHC-8			
Dry ROT		50.0	
(%)		(100.0)	
Wet ROT		50.4	65.9
(%)		(99.0)	(1.0)
G1159C (G IV)			
Dry ROT		38.3	
(%)		(100.0)	
Wet ROT		38.6	
(%)		(100.0)	
Weighted Average ROT (WAROT)			**51.25 secs.**

a. The exit code designates whether or not a runway exit is included in this analysis run. REDIM 2.0 offers the analyst the option of retaining all runway exits or just those selected by the user.

C-2

6.5 New York Kennedy International Airport

New York's JFK International Airport is at the heart of the most trafficked area in the United States. Runway 13R-31L, a 4442 meter long runway with large displaced thresholds on both sides, was selected for this analysis. Figure 6.5 illustrates the configuration for runway 13R-31L and its eight exit locations. Tables 6.17 and 6.18 show all turnoff locations, designators and turnoff types as well as the assumed exit design speeds. The aircraft population operating at J.F.K. International is mainly composed of medium and large transport aircraft as shown in Table 6.19. The runway occupancy time/aircraft assignment table is illustrated in Table 6.20. The baseline analysis shows an expected value of ROT of 54.3 seconds. This value, although higher than those obtained previously, is in fact good considering the large proportion of heavy aircraft landing on this runway.

FIGURE 6.5 Schematic of New York JFK Runway 13R-31L.

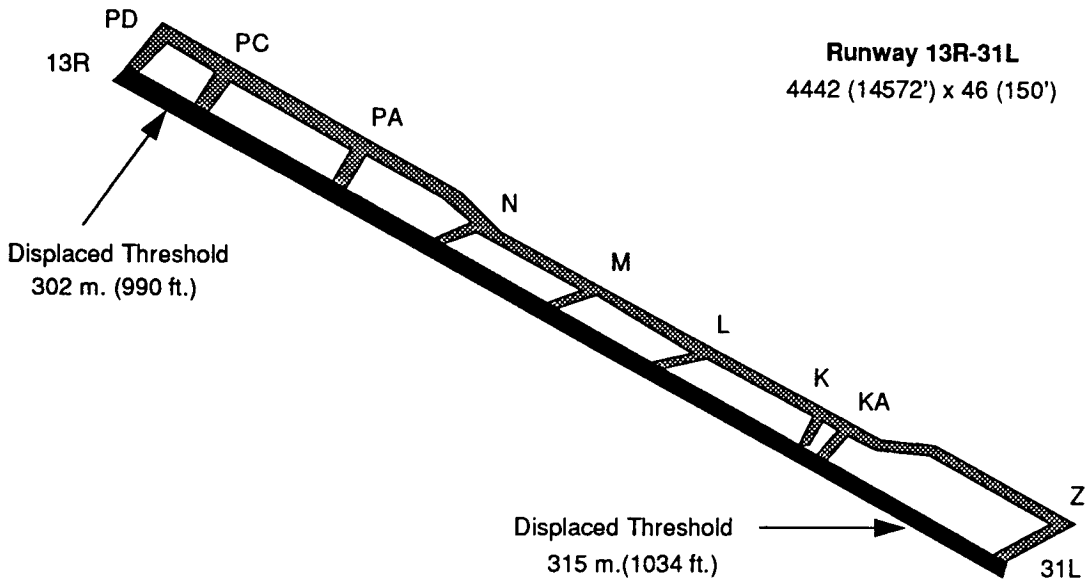

TABLE 6.17 Turnoff Data for Runway 13R at Kennedy International Airport.

Taxiway No.	Taxiway Designation	Location m. (ft.)	Taxiway Type (Degrees)	Design Speed m./s. (m.p.h.)
1	C	95 (312)	90	8 (17.8)
2	PA	838 (2749)	90	8 (17.8)
3	N	1417 (4648)	45	17.4 (40)

TABLE 6.17 Turnoff Data for Runway 13R at Kennedy International Airport.

Taxiway No.	Taxiway Designation	Location m. (ft.)	Taxiway Type (Degrees)	Design Speed m./s. (m.p.h.)
4	M	1898 (6225)	45	17.4 (40)
5	L	2607 (8551)	45	17.4 (40)
6	KA	3189 (10560)	90	8 (17.8)
7	Z	4114 (13493)	45	17.4 (40)
8	K	3491 (11449)	>90	6.7 (15)

TABLE 6.18 Turnoff Data for Runway 31L at Kennedy International Airport.

Taxiway No.	Taxiway Designation	Location m. (ft.)	Taxiway Type (Degrees)	Design Speed m./s. (m.p.h.)
1	D	4416 (14485)	90	8 (17.8)
2	C	4020 (13184)	90	8 (17.8)
3	A	3305 (10842)	90	8 (17.8)
4	N	2697 (8847)	90	8 (17.8)
5	M	2141 (7025)	90	8 917.8)
6	L	1560 (5118)	90	8 (17.8)
7	K	978 (3209)	90	8 (17.8)
8	KA	899 (2949)	90	8 (17.8)

TABLE 6.19 Aircraft Mix at Kennedy International Airport.

Aircraft Number	Aircraft Type	Percent of the Total Mix (%)	Aircraft Number	Aircraft Type	Percent of the Total Mix (%)
1	Saab 340	4.0	7	MD-82	5.0
2	Airbus A310-300	9.0	8	Boeing 757-200	3.0
3	Boeing 767-300	11.0	9	Boeing 747-200	14.0
4	Fokker F-100	1.0	10	DC-10-30	7.0
5	Boeing 727-200	32.0	11	Lockheed L1011	8.0
6	Boeing 737-300	5.0	12	DC-8-73	1.0

TABLE 6.20 Runway Occupancy Time Results for Runway 13L-31R at New York International Airport.

Exit Number Exit Code Exit Loc. Exit Type	1 Open 95[a] 90 Deg.	2 Open 838 90 Deg.	3 Open 1417 90 Deg.	4 Open 1898 90 Deg.	5 Open 2607 90 Deg.	6 Open 3189 90 Deg.
Saab 340						
Dry ROT			50.3			
(%)			(100.0)			
Wet ROT			49.5			
(%)			(100.0)			
A-310-300						
Dry ROT			45.9			
(%)			(100.0)			
Wet ROT			45.8	58.5		
(%)			(94.0)	(6.0)		
B-767-300						
Dry ROT			45.7	58.2		
(%)			(97.0)	(3.0)		
Wet ROT			45.8	58.5		
(%)			(57.0	(43.0)		
Fokker-100						
Dry ROT			45.7			
(%)			(100.0)			
Wet ROT			45.5			
(%)			(100.0)			

TABLE 6.20 Runway Occupancy Time Results for Runway 13L-31R at New York International Airport.

Exit Number Exit Code Exit Loc. Exit Type	1 Open 95[a] 90 Deg.	2 Open 838 90 Deg.	3 Open 1417 90 Deg.	4 Open 1898 90 Deg.	5 Open 2607 90 Deg.	6 Open 3189 90 Deg.
B-727-200						
Dry ROT			45.4			
(%)			(100.0)			
Wet ROT			45.4	58.4		
(%)			(77.0)	(23.0)		
B-737-300						
Dry ROT			45.6			
(%)			(100.0)			
Wet ROT			45.3	56.9		
(%)			(99.0)	(1.0)		
MD-83						
Dry ROT			45.5			
(%)			(100.0			
Wet ROT			45.5	58.2		
(%)			(88.0)	(12.0)		
B-757-200						
Dry ROT			46.3			
(%)			(100.0)			
Wet ROT			46.1			
(%)			(97.0)			
B-747-400						
Dry ROT			47.4	59.0	76.5	
(%)			(1.0)	(98.0)	(1.0)	
Wet ROT				58/8	77/7	
(%)				(69/0)	(31/0)	
L-1011						
Dry ROT			44.4	56.9		
(%)			(86.0)	(14/		
Wet ROT			44.5	57/2		
(%)			(28.0)	(72.0)		
DC-8-73						
Dry ROT			48.0	61.1		
(%)			(27.0)	(73.0)		
Wet ROT			48.4	(99.0)		
(%)			(1.0)			
Weighted Average Runway Occupancy Time (WAROT)						**54.3 secs.**

a. Distances are measured from the runway displaced threshold.

6.6 Newark International Airport

Newark International Airport has a total of three runways with two closely spaced parallel runways oriented North-South and a smaller intersecting East-West runway (11-29) which is the subject of this analysis. Figure 6.6 illustrates a simple schematic of runway 11-29 showing seven exit locations identified in Tables 6.21 and 6.22. Runway has an approximate length of 1945 m. and width of 46 m. and serves primarily general aviation, business and commuter aircraft operations as shown in Table 6.23.Although primarily a general aviation runway the aircraft mix shown in Table 6.23 includes narrow body and a single wide body aircraft to illustrate typical ROT times under extreme airport operating conditions such as strong crosswinds present on the primary runways.The weighted average ROT value expected for this population is around 46.3 seconds which speaks well about the availability of existing exits. Table 6.24 also illustrates that REDIM 2.0 stochastic landing roll algorithms are sensitive to closely located exits as depicted by the spread in exit utilization for the Boeing 727-200. Note that if medium size transport aircraft were to use this runway exits "sierra", "romeo", "papa", and "zulu" would be used.

TABLE 6.21 Turnoff Data for Runway 11 at Newark Airport.

Taxiway No.	Taxiway Designation	Location m. ft.	Taxiway Type (Degrees)	Design Speed m./s. ft./s.
1	V	333 (1093)	90	8 (17.8)
2	U	563 (1845)	90	8 (17.8)
3	T	800 (2623)	>90	6.7 (15)
4	S	1073 (3521)	30	8 (17.8)
5	R	1185 (3886)	90	8 917.8)
6	P	1303 (4274)	30	8 (17.8)
7	Z	1659 (5440)	90	8 (17.8)
8	N	1925 (6314)	90	8 (17.8)

TABLE 6.22 Turnoff Data for Runway 29 at Newark Airport.

Taxiway No.	Taxiway Designation	Location m. (ft.)	Taxiway Type (Degrees)	Design Speed m./s. (m.p.h.)
1	P	784 (2571)	90	8 (17.8)
2	R	741 (2429)	90	8 (17.8)
3	S	859 (2817)	90	8 (17.8)
4	T	1155 (3789)	30	26.9 (60)
5	U	1348 (4420)	90	8 (17.8)
6	V	1584 (5197)	30 (90)	26.9 (60)
7	W	1880 (6168)	90	8 (17.8)

TABLE 6.23 Aircraft Mix at Newark Airport.

Aircraft Number	Aircraft Type	Percent of the Total Mix (%)	Aircraft Number	Aircraft Type	Percent of the Total Mix (%)
1	Cessna CE 208	2.0	7	Airbus A-300-600	6.0
2	Beechcraft BE- 58	2.0	8	Fokker 100	3.0
3	Embraer EMB-120	13.0	9	Boeing 727-200	21.0
4	SA-227 Metro	15.0	10	Boeing 737-300	10.0
5	Learjet 31	3.0	11	MD-80	17.0
6	Boeing DHC-8	8.0			

FIGURE 6.6 **Schematic of Newark International Airport Runway 11-29.**

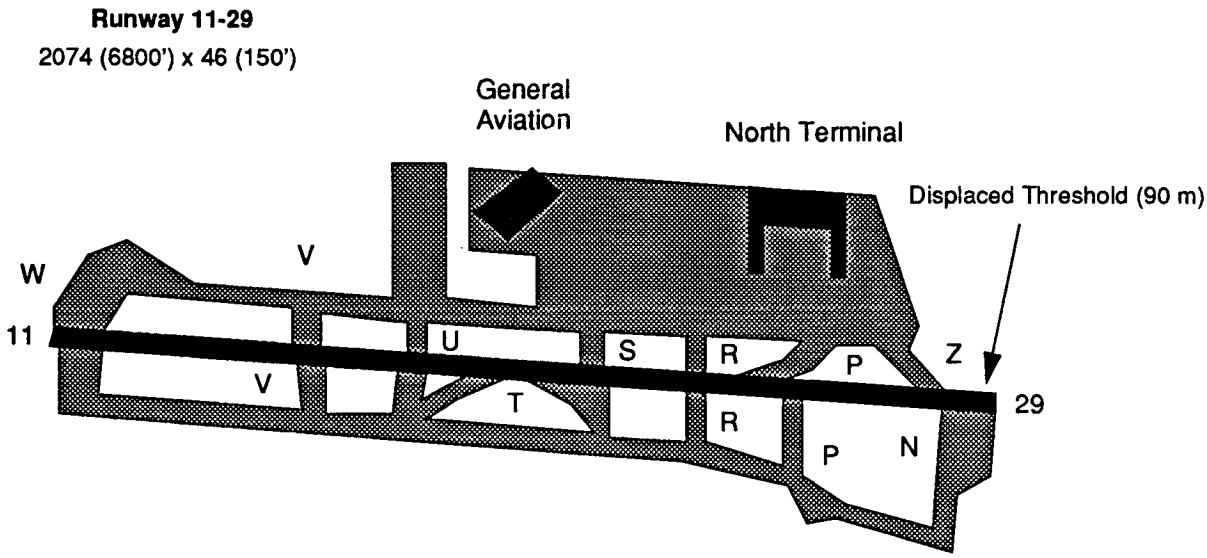

TABLE 6.24 **Runway Occupancy Time Results for Runway 11-29 at Newark International Airport.**

Exit Number Exit Code[a] Exit Loc. Exit Type	1 Open 333 90 Deg.	2 Open 563 90 Deg.	3 Open 800 90 Deg.	4 Open 1073 30 Deg.	5 Open 1185 90 Deg.	6 Open 1303 30 Deg.	7 Open 1659 90 Deg.
CE-208							
Dry ROT		29.0					
(%)		(100.0)					
Wet ROT		29.2					
(%)		(100.0)					
BE-58							
Dry ROT			37.2	44.8			
(%)			(99.0)	(1.0)			
Wet ROT			37.8	44.5			
(%)			(71.0)	(29.0)			
EMB-120							
Dry ROT				41.9		48.4	
(%)				(55.0)		(45.0)	
Wet ROT				42.8		48.3	62.2
(%)				(2.0)		(86.0)	(12.0)

TABLE 6.24 Runway Occupancy Time Results for Runway 11-29 at Newark International Airport.

Exit Number Exit Code[a] Exit Loc. Exit Type	1 Open 333 90 Deg.	2 Open 563 90 Deg.	3 Open 800 90 Deg.	4 Open 1073 30 Deg.	5 Open 1185 90 Deg.	6 Open 1303 30 Deg.	7 Open 1659 90 Deg.
SA-227							
Dry ROT			35.6	42.4			
(%)			(22.0)	(78.0)			
Wet ROT			36.4	42.3			
(%)			(2.0)	(99.0)			
Learjet-31							
Dry ROT			35.4	42.7			
(%)			(16.0)	(84.0)			
Wet ROT			36.5	42.5			
(%)			(1.0)	(99.0)			
DHC-8							
Dry ROT			41.4	46.7			
(%)			(1.0)	(99.0)			
Wet ROT				46.6			
(%)				(100.0)			
A-300-600							
Dry ROT				42.6	46.1	48.4	57.6
(%)				(13.0)	(8.0)	(76.0)	(3.0)
Wet ROT						48.4	59.2
(%)						(56.0)	(43.0[b])
Fokker-100							
Dry ROT				41.4	44.0	47.4	
(%)				(90.0)	(8.0)	(2.0)	
Wet ROT				41.5	44.8	47.5	
(%)				(32.0)	(1.0)	(49.0)	
B-727-200							
Dry ROT				42.2	45.3	47.7	56.9
(%)				(6.0)	(12.0)	(78.0)	(4.0)
Wet ROT					46.0	47.8	58.0
(%)					(1.0)	(47.0)	(52.0)
B-737-300							
Dry ROT				41.2	44.1	47.1	
(%)				(86.0)	(8.0)	(6.0)	
Wet ROT					41.3	45.1	47.5
(%)					(18.0)	(12.0)	(70.0)

TABLE 6.24 Runway Occupancy Time Results for Runway 11-29 at Newark International Airport.

Exit Number Exit Code[a] Exit Loc. Exit Type	1 Open 333 90 Deg.	2 Open 563 90 Deg.	3 Open 800 90 Deg.	4 Open 1073 30 Deg.	5 Open 1185 90 Deg.	6 Open 1303 30 Deg.	7 Open 1659 90 Deg.
MD-80							
Dry ROT				42.0	44.8	47.8	56.7
(%)				(21.0)	(11.0)	(66.0)	(2.0)
Wet ROT				42.6		47.8	57.8
(%)				(1.0)		(69.0)	(28.0[c])
Weighted Average Runway Occupancy Time (WAROT)							46.3 s.

a. The exit code designates whether or not a runway exit is included in this analysis run. REDIM 2.0 offers the analyst the option of retaining all runway exits or just those selected by the user.

b. One percent of the Airbus A-310 would take exit "zulu" located 1925 m. from threshold (not shown in table) with an expected value of ROT of 66.0 seconds.

c. Two percent of the McDonnell Douglas MD-80's would take exit "zulu" located 1925 m. from threshold (not shown in table) with an expected value of ROT of 65.2 seconds.

6.7 Seattle-Tacoma International Airport

Seattle-Tacoma International Airport has two closely-spaced (i.e., 244 m. away from centerlines) runways oriented North-South (16-34). Runway 16R is the subject of interest in this analysis. Figure 6.7 illustrates a simple schematic of runways 16R-34L and 16L-34R showing four exit locations identified in Tables 6.25 and 6.26. Runway 16R-34L has an approximate length of 2840 m. and width of 46 m. (150 ft.) and serves all classes of vehicles including heavy jets and general aviation aircraft.Table 6.27 shows the aircraft population mix used for this analysis with an equivalent mix index of 81.5. Table 6.28 shows the baseline ROT table results for the existing facility with an estimated weighted average runway occupancy time of 56.4 seconds using four existing runway exits. ROT reductions of up to 7 seconds are possible for this runway configuration if two new moderate design speed exits (i.e., FAA standard acute angle turnoffs) are placed at ranges 1310-1400 m. and 2100-2160 m. from runway 16R threshold. Note that this particular runway configuration has an added constraint in the form of a closely-spaced parallel runway which requires operations on 16R-34L to hold short of runway 16L-34R before a runway crossing maneuver is authorized. This fact would restrict the use of these two new turnoffs to speeds below 20 m/s as pilots would likely bring their aircraft to full stop prior to crossing runway 16L-34R.

TABLE 6.25 Turnoff Data for Runway 16R at Seatac International Airport.

Taxiway No.	Taxiway Designation	Location m. ft.	Taxiway Type (Degrees)	Design Speed m./s. ft./s.
1	C3	920 (3018)	45	8 (17.8)
2	C2	1145 (3756)	135	6.7 (14.9)
3	C9	1785 (5855)	30	20.0 (44.6)
4	C11	2808 (9210)	90	8 (17.8)

TABLE 6.26 Turnoff Data for Runway 34L at SeaTac International Airport.

Taxiway No.	Taxiway Designation	Location m. (ft.)	Taxiway Type (Degrees)	Design Speed m./s. (m.p.h.)
1	C9	830 (2722)	150	5 (16.4)
2	C2	1510 (4952)	30	20 (44.6)
3	C3	1810 (5937)	135	6.7 (14.9)

TABLE 6.26 Turnoff Data for Runway 34L at SeaTac International Airport.

Taxiway No.	Taxiway Designation	Location m. (ft.)	Taxiway Type (Degrees)	Design Speed m./s. (m.p.h.)
4	C1	2808 (9210)	90	8(17.8)

TABLE 6.27 Aircraft Mix at SeaTac International Airport.

Aircraft Number	Aircraft Type	Percent of the Total Mix (%)	Aircraft Number	Aircraft Type	Percent of the Total Mix (%)
1	PA-38-112	1.0	9	A-300-600	1.4
2	CE 208	1.0	10	B 767-300	1.0
3	CE 402C	4.0	11	B 727-200	19.0
4	EMB-120	2.0	12	B 737-300	12.4
5	SA 227	12.0	13	MD-83	12.0
6	BAe-31	10.2	14	B 747-200B	3.0
7	DHC-7	4.0	15	L 1011	3.1
8	CE 550	4.1	16	DC-8-73	3.0

FIGURE 6.7 **Schematic of Sea-Tac International Airport Runway 16R-34L.**

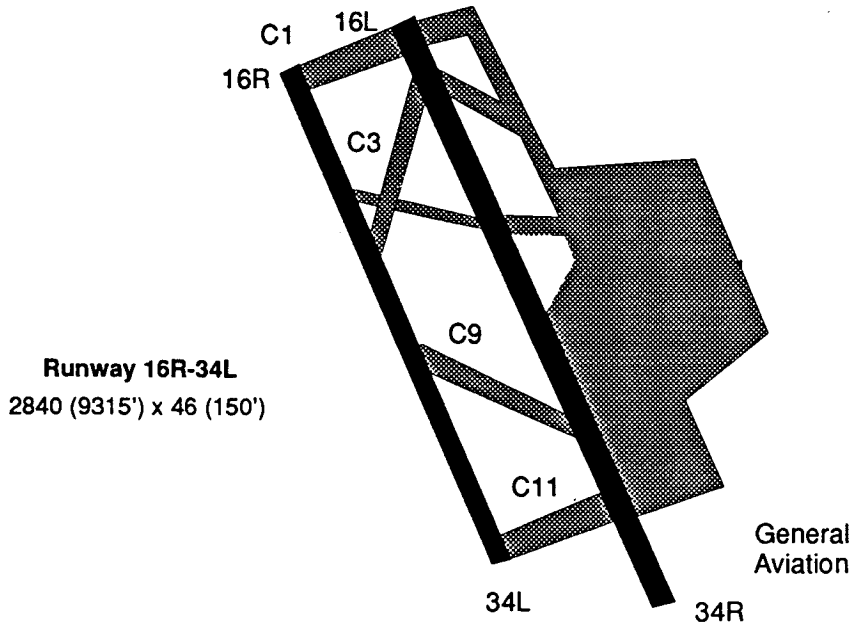

TABLE 6.28 **Runway Occupancy Time Results for Runway 16R at Seattle-Tacoma International Airport.**

Exit Number Exit Code[a] Exit Loc. Exit Type	1 Open 958 45 Deg.	2 Open 1150 90 Deg.	3 Open 1787 30 Deg.	4 Open 2807 90 Deg.
PA-38-112				
Dry ROT	47.8			
(%)	(100.0)			
Wet ROT	48.0			
(%)	(100.0)			
CE 208				
Dry ROT	44.2			
(%)	(100.0)			
Wet ROT	44.2			
(%)	(100.0)			
EMB 120				
Dry ROT		46.0	64.6	
(%)		(29.0)	(71.0)	
Wet ROT			64.4	
(%)			(100.0)	

TABLE 6.28 **Runway Occupancy Time Results for Runway 16R at Seattle-Tacoma International Airport.**

Exit Number Exit Code[a] Exit Loc. Exit Type	1 Open 958 45 Deg.	2 Open 1150 90 Deg.	3 Open 1787 30 Deg.	4 Open 2807 90 Deg.
SA 227				
Dry ROT	38.8	43.3		
(%)	(99.9)	(1.0)		
Wet ROT	38.5	44.9		
(%)	(82.0)	(18.0)		
BAe-31				
Dry ROT	38.7	45.3	64.0	
(%)	(8.0)	(89.0)	(3.0)	
Wet ROT		45.6	64.6	
(%)		(49.0)	(51.0)	
DHC-7				
Dry ROT	44.6			
(%)	(100.0)			
Wet ROT	44.4			
(%)	(100.0)			
CE-550				
ROT	40.5			
(%)	(100.0)			
Wet ROT	40.2			
(%)	(100.0)			
DHC-8				
Dry ROT	43.7	51.4		
(%)	(96.0)	(4.0)		
Wet ROT	43.9	52.0		
(%)	(47.0)	(53.0)		
A-300-600				
Dry ROT		45.7	64.4	
(%)		(9.0)	(91.0)	
Wet ROT			63.8	
(%)			(100.0)	
B 767-300				
Dry ROT		46.8	64.4	
(%)		(1.0)	(99.0)	
Wet ROT			62.8	
(%)			(100.0)	

TABLE 6.28 Runway Occupancy Time Results for Runway 16R at Seattle-Tacoma International Airport.

Exit Number Exit Code[a] Exit Loc. Exit Type	1 Open 958 45 Deg.	2 Open 1150 90 Deg.	3 Open 1787 30 Deg.	4 Open 2807 90 Deg.
B 727-200				
Dry ROT		44.7	63.6	
(%)		(5.0)	(95.0)	
Wet ROT			63.0	
(%)			(100.0)	
B 737-300				
Dry ROT	38.8	43.5	63.3	
(%)	(4.0)	(75.0)	(21.0)	
Wet ROT		44.4	63.5	
(%)		(19.0)	(81.0)	
MD-83				
Dry ROT		44.3	63.8	
(%)		(16.0)	(84.0)	
Wet ROT			63.5	
(%)			(100.0)	
B 747-200B				
Dry ROT			61.8	73.3
(%)			(98.0)	(2.0)
Wet ROT			61.3	75.0
(%)			(49.0)	(51.0)
L 1011-500				
Dry ROT			62.6	
(%)			(100.0)	
Wet ROT			61.4	
(%)			(100.0)	
DC-8-73				
Dry ROT			64.5	
(%)			(100.0)	
Wet ROT			63.6	93.4
(%)			(95.0)	(5.0)
Weighted Average Runway Occupancy Time (seconds)				**56.43 s.**

a. The exit code designates whether or not a runway exit is included in this analysis run. REDIM 2.0 offers the analyst the option of retaining all runway exits or just those selected by the user.

Intentionally Left Blank

CHAPTER 7 Phase III Research Topics

This chapter addresses two important issues that will be part of Phase III of this research project: 1) the potential capacity gains as a result of the use of rapid runway turnoffs and 2) flight simulation experiments needed to calibrate the computer model developed. The descriptions given here are important as they constitute a natural extension to the topics discussed in the previous six chapters of this report. Phase III comprises several field studies to calibrate and complement the development of the REDIM 2.0.

7.1 Potential Capacity and Delay Improvements Using Rapid Runway Turnoff Geometries

The improvements derived from the use of optimally located geometries require external assessment from macroscopic simulation packages where aircraft terminal airspace and ground operation are simulated and conflicts between arrivals, departures, special operations (i.e., touch-and-go and ground transfers) are resolved. Currently few models encompass all these operations at the same time and probably SIMMOD is the best tool to address airport capacity and delay. SIMMOD, however, does not have the capability to emulate high speed turnoff operations and consequently cannot be used to assess preliminary gains in this respect. To address in some detail this important issue the Center for Transportation Research has developed a simple runway operations computer model to estimate capacity and delay gains using high speed turnoffs on a single runway.

The RUNSIM model (Runway Simulation) is programmed in SIMSCRIPT II.5 and models individual arrival and departure aircraft operations to estimate queues at taxiway holding positions and at terminal airspace nodes [Nunna, 1991]. The model includes the logic necessary to allocate aircraft operations to ten different types of runway exit geometries

including REDIM-generated high speed turnoffs. RUNSIM complements the results of REDIM 2.0 and estimates global statistics for arrival and departure operations. The main outputs to this model are the delays incurred by each aircraft arrival and departure operation. In order to demonstrate this a single runway airport scenario was used in order to verify arrival and departure delays under mixed aircraft operations. Using this model it can be shown that airport operations show reductions in the amount of departure delays observed. The fictitious scenario is shown in Fig. 7.1 where an existing 3000 m. runway with four turnoffs is used as baseline scenario.

FIGURE 7.1 Airport Topology for Capacity and Delay Analysis.

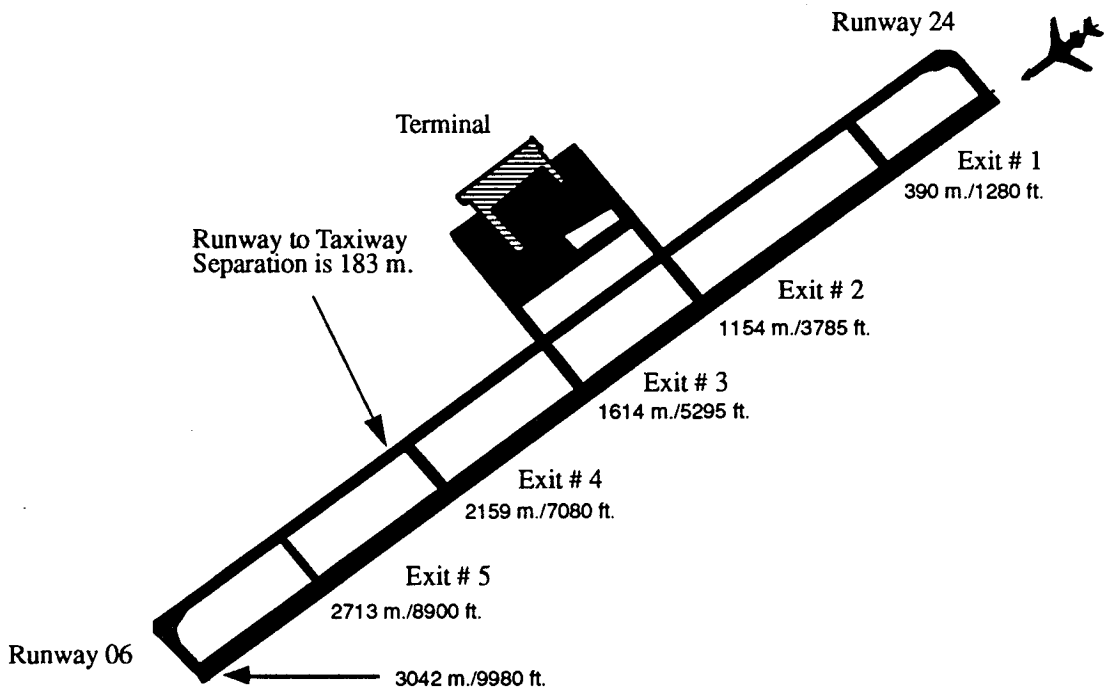

7.1.1 Simulation Results Using Existing Air Traffic Control Rules

Under existing air traffic control conditions the interarrival separations under IFR conditions follow a 6/5/2.5 nautical mile rule. The simulations were carried out from the final approach fix for arrivals and from the gate for departures to simplify the analysis. An aircraft mix representative of a large hub airport facility was also used in these simulations. Several input parameters were varied from the "baseline scenario" to test the sensitivity of the model when the number of exits and their types are varied.

FIGURE 7.2 Arrival Delay Curves for Various Airport Scenarios.

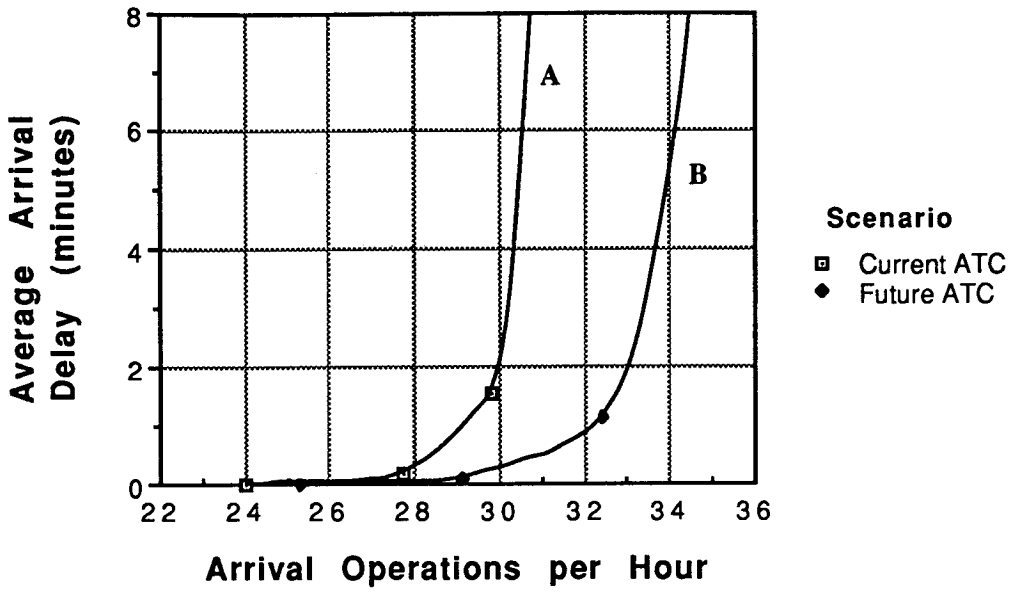

FIGURE 7.3 Departure Delay Curves for Various Airport Scenarios.

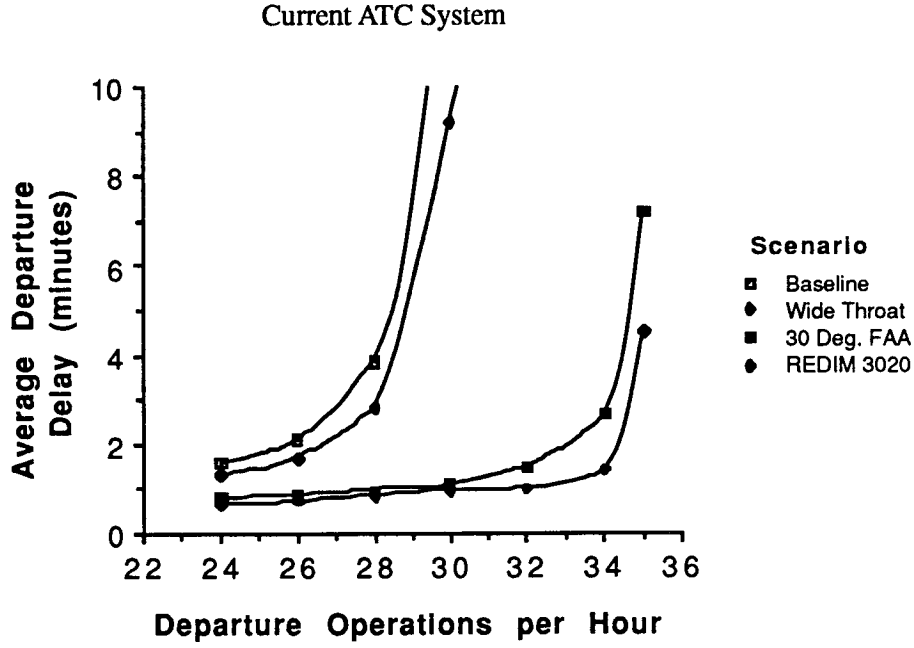

Data for arrival and departure rates was assumed to follow a poisson distribution. The interarrival and interdeparture times were varied from 125 seconds to 150 seconds to test the sensitivity of the runway delay to varying demand rates. In this range the total arrival delay is very sensitive to the demand rate because the demand is reaching the arrival capacity of the runway. The model however, is flexible enough to allow any combination of interarrival and interdeparture times. Due to the stochasticity of the model 500 arrivals and 500 departures were used per iteration to represent operations over a long period of time. Air traffic control time buffer data used were derived from observed values in ATC simulators [Credeur, 1989].

With this data, and for each interarrival time RUNSIM was run for five iterations to generate data for total delay for arrivals and departures, weighted average runway occupancy time (WAROT) and its standard deviation. The average values of these runs was used for plotting a demand versus average delay graph as shown in Figures 7.2 and 7.3. These figures illustrate that as the demand nears the ultimate capacity (i.e., capacity associated with an infinite delay) the total delay increases very rapidly. For the baseline scenario and an acceptable average delay of 4 minutes, the practical capacity for arrivals is 30.2 arrivals per hour under current ATC conditions. The resulting WAROT of the aircraft population is 54.5 seconds. In this study the effects of runway exit replacement are investigated to ascertain runway occupancy time gains possible with the implementation of standard high speed exits as well as REDIM generated geometries. The scenarios shown in Table 7.1 were investigated:

TABLE 7.1 Runway Scenarios Investigated for ROT Gain Analyses.

Scenario Number	Scenario	Runway Exits Description	Exit Speed (m/s)
1	Baseline	5 usable 90 degree runway exits (see Fig. 4.1)	8.00
2	Wide Throat	Replace exits 1 through 4 with four optimally located "wide throat" turnoffs	15.00
3	30 Degree Standard FAA	Replace baseline exits 1-4 with four optimally located 30 degree acute angle exits	23.00
4	30 Degree Modified Exit	Replace baseline exits 1-4 with four optimally located 30 degree, modified entrance acute angle exits (i.e., 427 m. entrance spiral)	26.00
5	REDIM 3030	Replace baseline exits 1-4 with four optimally located REDIM generated turnoffs with 30 m/s exit design speed	30.00
6	REDIM 3530	Replace baseline exits 1-4 with four optimally located REDIM generated turnoffs with 35 m/s exit design speed	35.00

Table 7.3 illustrates the possible gains in weighted average runway occupancy time ranging from 54.5 seconds for the baseline scenario down to 36.8 seconds for the implementation of REDIM high speed geometries designed for 35 m./s. and an exit angle of 20 degrees. The reader should notice that these improvements apply for a runway whose exit locations have been replaced by optimally located turnoff on each category. Note from Table 7.3 that as the exit design speed (i.e., entry turnoff speed) is increased the optimal locations shift closer to the threshold as one might expect.

A plot of the average interarrival delay per aircraft are shown in Fig. 7.2 (curve labeled A) corresponding to existing final approach ATC separation rules. This result is not surprising since, under current ATC conditions, the interarrival separation and not the ROT of the aircraft is the critical factor governing the capacity and delay. An important result from this capacity and delay analysis is that the average delay for departures decreased significantly for a fixed level of departure operations. Figure 7.3 illustrates this for four of the six configurations studied where a significant shift in the departure delay curve is observed as the design exit speed is increased. The reason behind this shift is the availability of more acceptable gaps for departures, an effect of decreased WAROT for a single runway under mixed aircraft operations.

TABLE 7.2 Aircraft Population Used for Capacity and Delay Analyses.

Aircraft	Percent Mix	TERP Classification	Aircraft	Percent Mix	TERP Classification
Cessna 208	3	A	Boeing 767	2	D
Saab 340	10	B	BAe-146	5	C
EMB 120	8	B	Boeing 727	15	C
SA 227	12	B	Boeing 737	15	C
Boeing 757	5	C	Grumman IV	3	C
Boeing 747	3	D	MD 11	2	D
CE 550	5	B	MD 83	12	C

TABLE 7.3 Summary of Turnoff Locations for Capacity and Delay Airport Scenarios.

Scenario Number	Scenario	Runway Exits Description Exit Location (m.) Exit Type						Weighted Average ROT (sec.)
		Exit # 1	Exit # 2	Exit # 3	Exit # 4	Exit # 5	Exit # 6	
1	Baseline	390 90 deg.	1154 90 deg.	1614 90deg.	2159 90 deg.	2713 90 deg.	3042 90 deg.	54.50
2	Wide Throat	390 90 deg.	950 WT	1225 WT	1425 WT	1900 WT	3042 90 deg.	51.20
3	30 Degree Standard FAA	390 30 deg.	950 30 deg.	1200 30 deg.	1400 30 deg.	1925 30 deg.	3042 90 deg.	44.63
4	30 Degree FAA Modified Exit[a]	390 90 deg.	900 30 deg. modified	1150 30 deg. modified	1350 30 deg. modified	1875 30 deg. modified	3042 90 deg.	43.00
5	REDIM 3020[b]	390 90 deg.	875 RE 3020	1125 RE 3020	1325 RE 3020	1825 RE 3020	3042 90 deg.	40.80
6	REDIM 3520[c]	390 30 deg.	825 RE 3520	1050 RE 3520	1250 RE 3520	1650 RE 3520	3024 90 deg.	36.80

a. The FAA modified 30 degree, acute angle geometry includes a 457 m. (1400 ft.) transition spiral.
b. The designation RE 3020 implies a high-speed exit designed for 30 m/s entry speed and a 20 degree exit angle.
c. The designation RE 3520 implies a high-speed exit designed for 35 m/s entry speed and a 20 degree exit angle.

7.1.2 Future Air Traffic Control Scenarios

The current ATC separation rules set by FAA is the critical parameter governing the delay at most airport facilities. By improving the technology in dealing with wake turbulence, improved radar technology for better air traffic control, the FAA proposes to decrease the interarrival separation to the values shown in Table 7.4. This scenario studies the effect of new ATC separation rules on capacity and delay. The model is run by changing the arrival separation to the new values and keeping the other values same as in "baseline scenario". Figure 7.3 shows the arrival delay relationship of this scenario, where the capacity (practical) has increased to 34.0 operations per hour, which is an increase of near 4 operations (arrivals) per hour as compared to the present rules.

Hence for REDIM exits to be more effective and to achieve a balance between the airspace arrival and runway practical capacities, the ATC separations have to be further decreased through the use of new technology. The ultimate goal is to allow smaller separations between adjacent arrivals and a corresponding reduction in the position errors of approaching aircraft. Nonetheless decreasing departure delays even under today's ATC

TABLE 7.4 **Current and Future ATC Aircraft Inter-Arrival Separation Criteria.**

Leading Aircraft	Current ATC Separation				Future ATC Separation		
	Trailing Aircraft				Trailing Aircraft		
	Small	Large	Heavy		Small	Large	Heavy
Small	2.5 (84)	2.5 (64)	2.5 (60)		2.0 (65)	2.0 (51)	2.0 (48)
Large	4.0 (131)	2.5 (64)	2.5 (60)		3.0 (98)	2.0 (51)	2.0 (48)
Heavy	6.0 (196)	5.0 (129)	4.0 (96)		5.0 (163)	4.0 (103)	3.0 (72)

Cell values represent separations and headways in **nautical miles** and **seconds**, respectively.
Assumed speeds: 1) 110 knots for small, 2) 140 knots for large and 3) 150 knots for heavy aircraft.

environment seems to offer operational advantages that will be further explored in Phase III of this research when more complex airport configurations will be studied.

7.2 Flight Simulation Experiments

This section summarizes the experiments to be conducted at Oklahoma City by the Federal Aviation Administration in conjunction with the University Center for Transportation Research (UCTR) at Virginia Tech. This study is to be conducted under terms of NASA Langley Contract 18147 Task 15. It is expected that this experiments will be performed as part of Phase III of the current research carried out by the UCTR for NASA and FAA.

The purpose of these experiments can be summarized as follows:

a) To assess the operational suitability of rapid runway turnoff geometries under closed loop pilot simulations.

b) To determine pilot responses to optimally-placed rapid runway turnoff locations.

The research being pursued forms part of the FAA ARD-200 Office to develop a computer program to minimize runway occupancy times under realistic airport scenarios (i.e., large aircraft populations using a single runway). The research being pursued by the UCTR is to develop an integrated computer model -REDIM- to execute the optimization of rapid runway turnoffs and at the same time describe turnoff geometries satisfying prescribed entry speed criteria. The proposed simulation effort will be a benchmark for the research team to validate some of the turnoff algorithms implemented in REDIM as well as some of the exit locations suggested by the model for a Boeing 727-200.

In order to execute these experiments in a more controlled fashion it is advised to divide the simulator experiences in three distinctive sets of experiments: 1) Turnoff geometry simulations, 2) Rapid runway exit locations including the turnoff geometries and 3) Aircraft landing roll behaviors with runway length variations. In this fashion the crew members will be able to replicate precisely the entry turnoff speeds and exit locations to be tested. The following paragraphs attempt to describe the experiments to be executed.

7.2.1 Turnoff Geometry Experiments

This part of the experiment will try to estimate the pilots' acceptance to various rapid runway turnoff geometries. The experiments will be conducted by exposing a selected group of pilots to eight different "new" geometry configurations and to the standard FAA acute angle geometry which will be used as baseline scenario. Each run will be subjectively evaluated by pilots to verify their assessment and this will be compared with time traces derived from the simulation runs. The turnoff geometries will be modified according to the following design parameters:

a) Turnoff Exit Angle

b) Turnoff Entry Speed

c) Turnoff Safety Factor

These conditions will be evaluated under wet pavement conditions if the simulator fidelity can appropriately represent this scenario. Parameters to be extracted in this stage are shown in Table 7.5 for further reference. It should be noticed that the turnoff geometries to be simulated will have variable turnoff widths according to a prescribed linear turnoff taper. It is expected that for each run the research team will have access to several variable time traces derived from the simulator using the Data File Collection System developed for the FAA Phase 2 simulator. These in turn will be used to correlate pilot's opinions and to ascertain possible difficulties with each geometry. The following variables are considered important in this correlation procedure and thus should be recorded as simulator outputs for further examination by the research team.

TABLE 7.5 Aircraft Simulator Variables to be Extracted for Turnoff Geometry Experiments.

1) Indicated Airspeed	11) Lateral Acceleration
2) Ground Speed	12) Ground Distance Travelled
3) Pressure Altitude	13) Pilot Eye Height
4) Yaw Angle	14) Rudder Pedal Force
5) Total Thrust	15) Column Force
6) Ground Distance	16) Wheel Force
7) Nose Gear Compression	17) Flap Angle
8) Left Gear Compression	18) Longitudinal Acceleration
9) Longitudinal Velocity	19) Longitudinal Wind Velocity
10) Lateral Velocity	20) Lateral Wind Velocity

These parameters will also be used to examine pilot's control actions as the turnoff is negotiated and establish measures of effectiveness to judge the adequacy of each turnoff. It is believed that a typical trace sampling rate of 2-3 measurements per second should be sufficient to establish a good database for further analysis. This would translate into 80-120 data points for every run assuming average 40 second turnoff geometry runs. These traces should be saved in magnetic media if possible for more detailed analyses by the research team.

Parametric variation of three geometry-related variables for two possible values results in eight turnoff geometry scenarios shown in Table 7.6 plus the baseline run. Using a simple replication of each scenario by a four-crewmember group results in a total of 36 simulations if a baseline turnoff scenario is also included. One of the most fundamental reasons to execute the geometry-related experiment in an individual fashion from that of the exit locations is to control with more accuracy the entry speeds at the point of curvature (P.C.) or turnoff starting point. Each simulation should be started few hundred meters from the turnoff point to allow pilots' adjustment and full situational awareness before entering the turnoff geometry (see Fig. 7.4).

TABLE 7.6 Turnoff Geometries to be Tested in the Boeing 727-200 Simulator.

Scenario	Exit Angle (Degrees)	Turnoff Safety (%)	Distance to Taxiway (m)	Entry Speed (m./sec.)
I	30	50	228	35
II	20	50	183	35
III	30	50	183	30
IV	20	50	183	30
V	30	100	228	35
VI	20	100	183	35
VII	30	100	183	30
VIII	20	100	183	30
Baseline	30	N/A	183	27

A simple dynamic model shows that a Boeing 727-200 (with Pratt & Whitney JT8D-15 engines) at maximum allowable landing weight could reach 35 m/s (78 MPH) in about 350 meters (1150 ft.) after brake release at takeoff thrust levels. This simulation is depicted graphically in Fig. 7.5 where the aircraft C.G. acceleration, velocity and downrange distance are shown as a function of time to assess the simulation time requirements in the aircraft acceleration process. This simulation was carried out using a point mass model with a nonlinear thrust lapse rate and rolling friction as a function of speed. The baseline flap angle used in the simulation was 30 degrees down consistent with the landing limitations of the aircraft at a maximum landing weight.

A more conservative distance of 550 - 600 mts. (1804 - 1970 ft.) could be used to locate the rapid runway test geometries from the point of brake release allowing each run to comfortably reach the maximum exit speed (i.e., 35 or 30 m/s at the intersection point

(see Fig. 7.4) even at a reduced throttle setting command schedule. Fig. 7.4 illustrates the expected simulation setting for these experiments and shows the relative magnitude of the segments to be programmed in the simulator software. In this simulation a first order lag schedule was used to model the throttle setting with a time constant of one second. This will produce an effective thrust response lag of 5 seconds to achieve a commanded thrust level (about 99.0% of the commanded thrust level). A sample result is shown in Fig. 7.6 with a time history of the "smoothed" throttle setting and corrected thrust responses throughout the aircraft acceleration maneuver.

From this analysis it is seen that a 5 second stabilization period (also called crew awareness time later on) is probably necessary before the crew is committed to execute the turnoff as this will give them time to verify the aircraft state variables versus those required by each experiment. This "crew exit awareness" time will also be necessary to ensure an engine steady-state response to a near thrust idle condition which would be typical of airline operations at near turnoff entry speeds. Moreover, this will also help the research team to observe pilot lag times, if any, in recognizing these new geometries.

FIGURE 7.4 **Turnoff Geometry Simulation Diagram.**

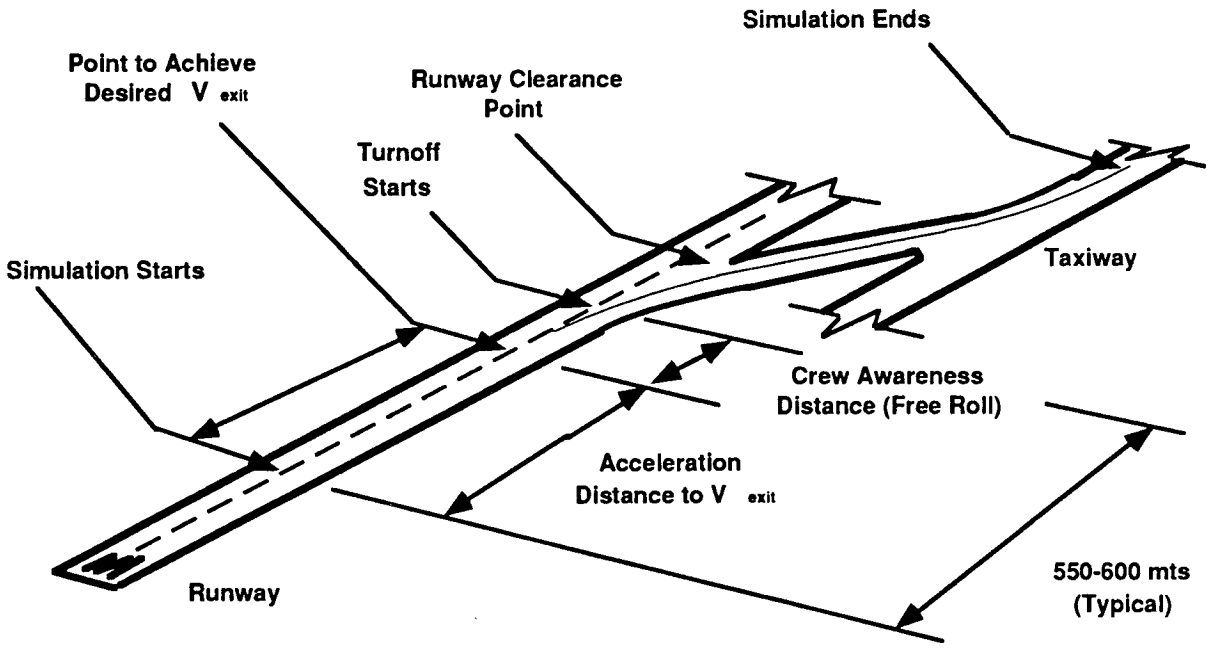

The end of each simulation run will be accomplished once the aircraft has reached the point of intersection of a parallel taxiway and the turnoff geometry being tested. The actual ending points will vary slightly to test lateral space constraints as some turnoff geometries will not allow safe deceleration at higher exit speeds unless the lateral spacing between the runway centerline and the parallel taxiway is increased. Table 7.7 illustrates all turnoff trials and their corresponding expected final speeds at the turnoff/taxiway junction. The main assumption in this model is that deceleration is only allowed during the

straight portion of the turnoff. Under real circumstances it is expected that pilots will be able to brake at about -0.75 to -1.00 m/s^2 during the straight segment of the turnoff while only rolling friction will be the only source of deceleration on the curved portion of the turnoff geometry. During the curved segments comprising the turnoff a conservative value of rolling friction deceleration has been assumed to be 0.375 m/s2. This number has been extracted from data obtained by Horonjeff et al. [Horonjeff et al., 1960] for a Boeing KC-135.

An example run of the expected state variables in the flight simulator is depicted in Fig. 7.7 where time traces of acceleration (AC_Path), aircraft heading angle (Sai) and aircraft speed (V_Path) are shown during a typical rapid runway turnoff maneuver. The deceleration trace shows very clearly the constant deceleration behavior during the curved portion of the turnoff whereas a first order model represents the braking effort expected from a pilot in terms of aircraft deceleration on the tangent portion of the turnoff.

This model once again assumes a maximum allowable landing aircraft mass (i.e., 72,200 kgs.) and the detailed equations of motion have been outlined in Trani et al. [Trani et al., 1990].

7.2.2 Runway Turnoff Location Experiments

This part of the experiment will try to estimate the pilots' acceptance to various rapid runway turnoff locations. The experiments will be conducted by exposing the same group of pilots to six different turnoff location/geometry configurations plus the standardized location determined from current FAA methods [FAA, 1989]. Once again each run will be subjectively evaluated by pilots to verify their assessment using questionnaires and this will be compared with time histories derived from the simulation runs.The turnoff locations will be modified according to the desired exit speed. Speeds of 30 and 35 m/s will be used as data points to asses the validity of the REDIM model assumptions under three different exit location scenarios labeled short, medium and long (see Table 7.8).This simulation will include a complete description of the final approach as well as the ground simulation as it is necessary to evaluate the complete landing roll performance. Table 7.8 illustrates the scenarios envisioned for this portion of the experiment.

The simulations will be conducted in a relatively long runway (i.e., 2750 mts. or more) to assess crew landing roll behavioral patterns under relatively unconstrained runway length conditions. The runs should be executed at near maximum landing weight conditions if possible (i.e., 72,000 kg for a typical B727-200) and the lowest flap angle setting permitted by this weight limitation. For every run it is expected that the number of exits should be kept to a minimum including the "new exit" being tested. One way to overcome this would be to locate neighboring exits at no less than 300 m. (985 ft) from the exit being tested during the particular run.

The turnoff location experiments will be complemented with two of the proposed turnoff geometries (i.e., turnoff geometries VI and VIII) in order to gain more insight on pilots responses and workload during the complete landing phase .

FIGURE 7.5 Expected Aircraft State Variables for a Turnoff Geometry Test.

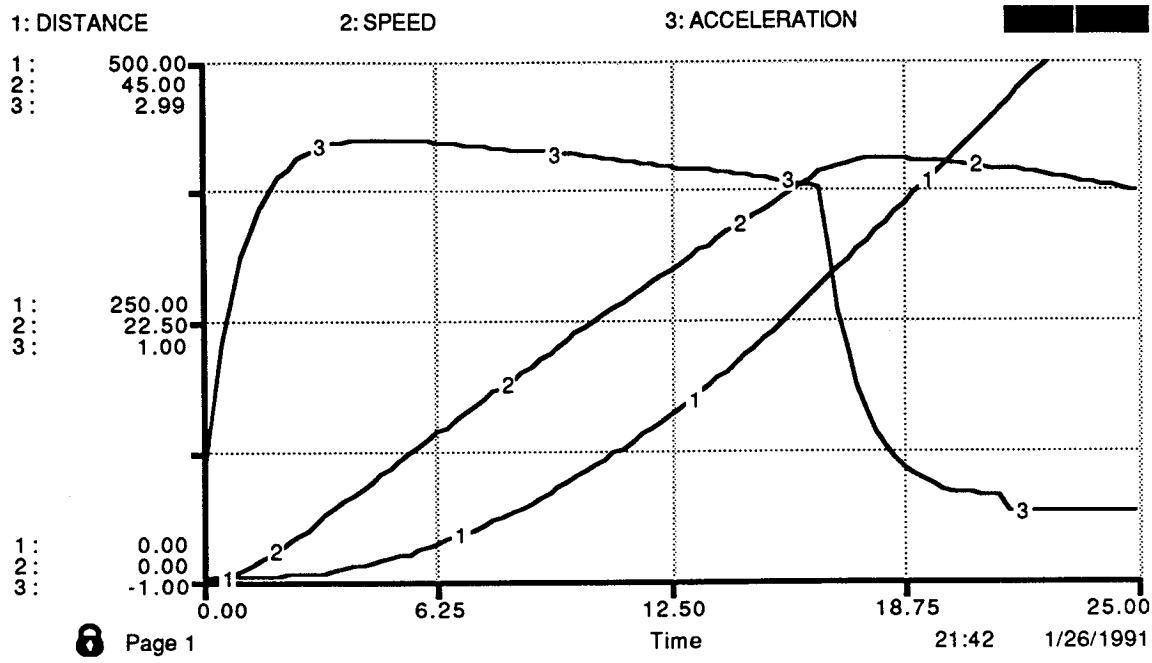

FIGURE 7.6 Aircraft Thrust Variables for a Typical Turnoff Geometry Test.

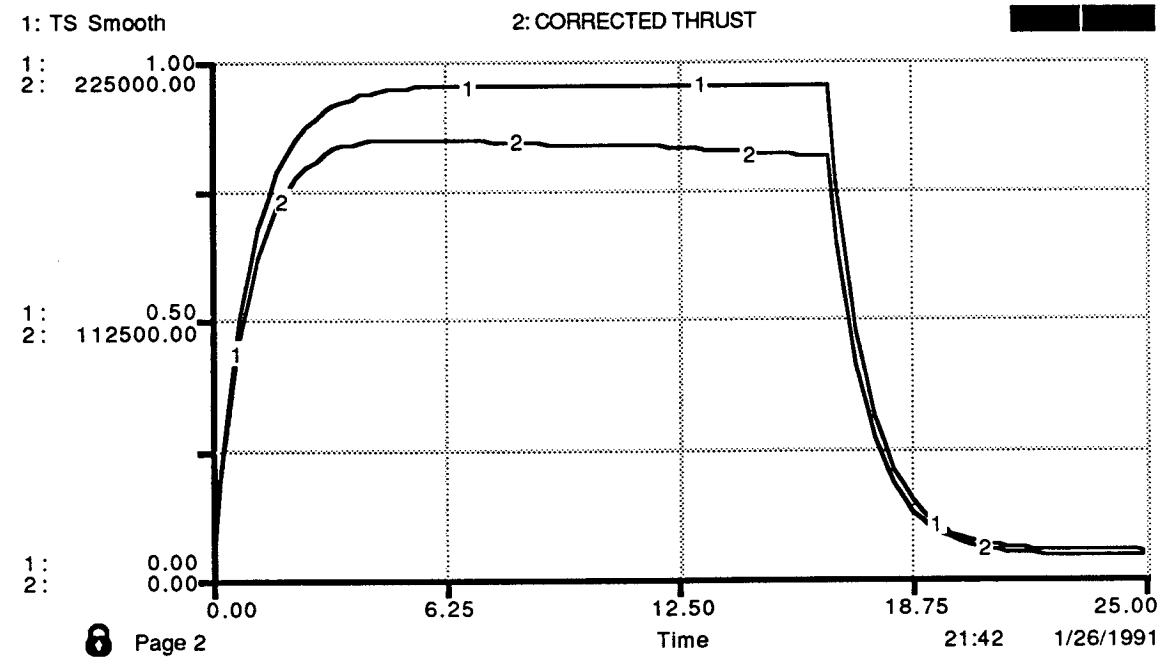

TABLE 7.7 Turnoff Geometries to be Tested in the Boeing 727-200 Simulator.

Scenario	Turnoff Angle (Deg)	Distance to Taxiway (m)	Turnoff Safety (%)	Entry Speed (m/s)	Final Speed (m./sec.)
I	30	228	50	35	18.4[1]
II	20	183	50	35	10.0[2]
III	30	183	50	30	10.0
IV	20	183	50	30	14.0
V	30	228[3]	100	35	19.2
VI	20	183	100	35	10.4
VII	30	183	100	30	14.4

1. Ending speed at the turnoff/taxiway junction.
2. Reaches taxiway speed (10 m/s) before reaching the turnoff/taxiway junction.
3. Proposed 228 mts. (750 ft.) lateral separation to parallel taxiway.

FIGURE 7.7 Aircraft Deceleration, Heading Angle and Speed Time Histories During a Turnoff.

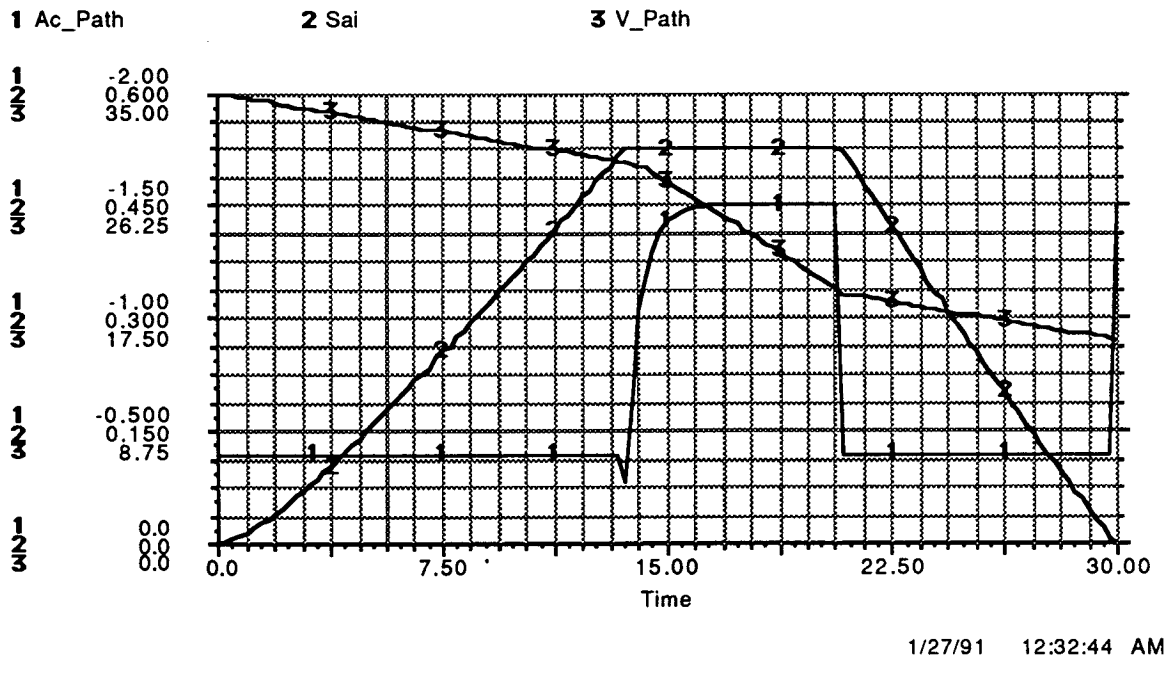

TABLE 7.8 Location/Geometry Scenarios to be Investigated (REDIM 2.0).

Scenario Number	Speed [(m/s)/knots]	Location (m.)	Location Description	Turnoff Geometry
I	35 / 68.0	1215	Short	II
II	35 / 68.0	1355	Medium	II
III	35 / 68.0	1496	Long	II
IV	30 / 58.3	1315	Short	IV
V	30 / 58.3	1450	Medium	IV
VI	30 / 58.3	1690	Long	IV
Baseline	27 / 52.3	1500[1]	Standard	Standard

1. Baseline Scenario value based upon a 1.52 m/s-s (5.0 ft/s-s) deceleration rate, touchdown location at 457.3 (1500 ft) and a 72 m/s (140 knot) approach speed.

In order to gain an appreciation of the complete landing roll dynamics and its influence in the runway turnoff location(s) it is expected that this portion of the experiment will include the complete landing roll maneuver and possibly portions of the final approach procedure as needed for flight training and starting setup of the simulator. Table 7.9 illustrates the variables considered important in the experiments to determine the suitability of REDIM proposed turnoff geometries.

TABLE 7.9 Aircraft Simulator Variables for Turnoff Location/Geometry Experiments.

1) Indicated Airspeed	11) Vertical Velocity
2) Ground Speed	12) Longitudinal Acceleration
3) Radio Altitude	13) Lateral Acceleration
4) Yaw Angle	14) Pitch Angle
5) Roll Angle	15) Total Thrust
6) Ground Distance	16) Rudder Pedal Force
7) Nose Gear Compression	17) Flap Angle
8) Left Gear Compression	18) Ground Distance Travelled
9) Longitudinal Velocity	19) Spoiler Deployed Flag
10) Lateral Velocity	20) On Ground Flag

It is expected that most simulations will be executed using standard airline practices (i.e., manual landing roll performance, thrust reverser until a prescribed speed, etc.) as this will give the research team a good practical database to calibrate REDIM for the Boeing 727-

200. In some of the high speed exit runs (i.e., 35 m/s) it might be necessary to advise crewmembers to inhibit the aircraft thrust reversers slightly earlier (say at 70 knots) to reduce the crew workload while executing the turnoff maneuver.

FIGURE 7.8 **Diagram for Runway Turnoff Location Experiments.**

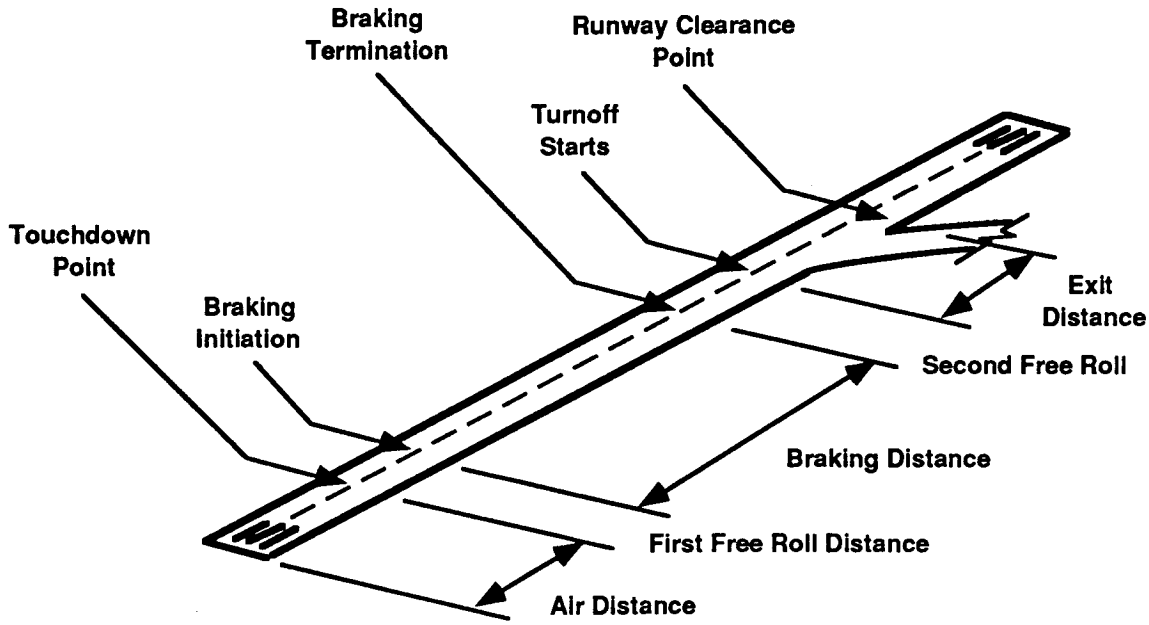

7.2.3 Runway Length Influence on Pilot Landing Roll Behavior

This part of the experiment will try to determine the influence of runway length on pilot landing deceleration technique. Currently REDIM uses an average deceleration schedule to estimate optimal rapid runway turnoff locations for every aircraft if the data base. It is however, known that pilots shape their aircraft deceleration pattern according to the runway length available, gate location, airline local motivational procedures, etc. Without any doubt the runway length is one of the most important parameters dictating the deceleration schedule used in most practical scenarios. For this reason the research team is interested in establishing a small database to validate a heuristic aircraft deceleration model within REDIM that accounts for the piloting behaviors under various runway lengths available.

The experiment will consists of simple approaches followed by full landing rolls under three different runway length scenarios to assess the influence of runway length on pilot's landing roll deceleration behavior. All these runs will be conducted on wet runways and no turnoffs available. This last measure will reduce biases in the deceleration schedule due to the existence of particular turnoff locations. Table 7.10 illustrates the three runway lengths considered typical for a medium-size transport type aircraft. Fig. 7.9 illustrates graphically this portion of the experiment. It should be noted that if the same crewmember

population is used (i.e., four crews) a total of 24 data points will be available for three runway scenarios. The reader should note that all data points obtained in this portion of the experiment will be invaluable to calibrate a heuristic method to account for pilot behavioral changes under variable runway length conditions.

TABLE 7.10 Runway Lengths Selected for Full Landing Roll Testing.

Runway Scenario Number	Runway Length meters/feet)	Runway Length Descriptor
I	1,800/5,900	Short
II	2,450/8,036	Medium
III	3,050/10,004	Long

FIGURE 7.9 Typical Aircraft Landing Roll Phases for Pilot Behavioral Studies for Various Runway Lengths.

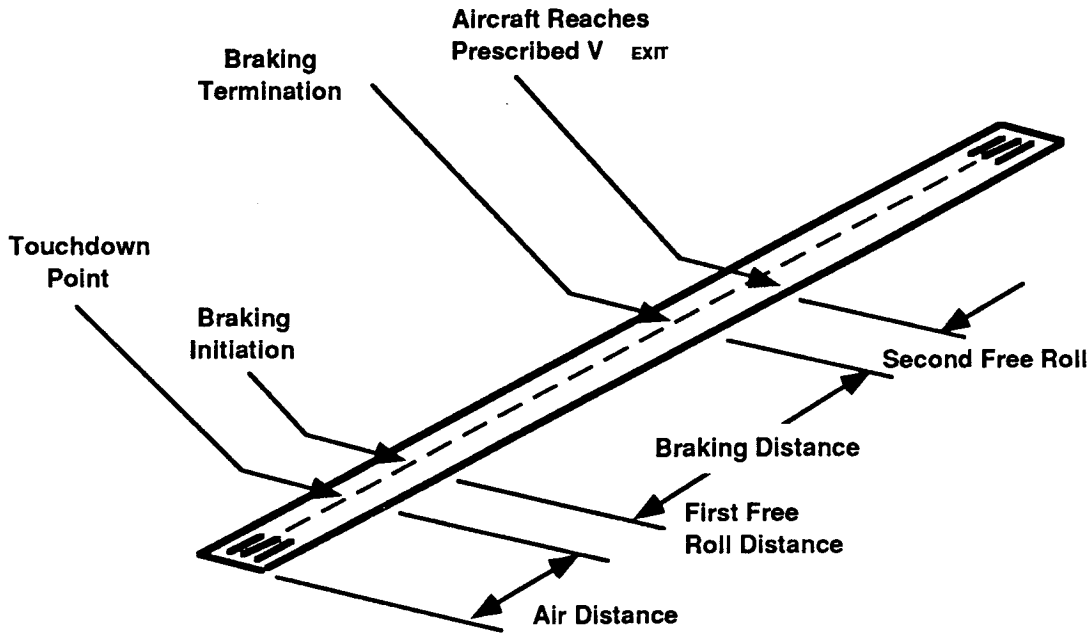

7.2.4 Experimental Design Procedures

In order to avoid biases during the experimentation it is suggested that a counter balancing assignment method be used for all crews. This method rotates the order of execution of every turnoff geometry scenario to avoid unwanted transfer of techniques for every subject. For the turnoff geometry experiments the following matrix can be constructed to exemplify the order of execution of each experiment. Table 7.11 illustrates the application of this

method for all runs to be made during the first set of experiments proposed dealing with turnoff geometries alone. Table 7.12 illustrates the sequence of runs needed to accomplish the second part of the experiment. Note once again that each scenario will be presented in a different fashion to each crew to avoid simulation transfers between experiments. Table 7.13 illustrates the rotation of trials for the third part of the experiments.

TABLE 7.11 Experimental Order of Execution for Turnoff Geometry Tests.

Crew	Base	I	II	III	IV	V	VI	VII	VIII
1a	1	2	3	4	5	6	7	8	9
2a	1	9	2	3	4	5	6	7	8
3a	1	8	9	2	3	4	5	6	7
4a	1	7	8	9	2	3	4	5	6
1b	1	6	7	8	9	2	3	4	5
2b	1	5	6	7	8	9	2	3	4
3b	1	4	5	6	7	8	9	2	3
4b	1	3	4	5	6	7	8	9	2

TABLE 7.12 Experimental Order of Execution for Turnoff Location Tests.

Crew	Base	I	II	III	IV	V	VI
1a[1]	1	2	3	4	5	6	7
2a	1	9	2	3	4	5	6
3a	1	8	9	2	3	4	5
4a	1	7	8	9	2	3	4
1b	1	6	7	8	9	2	3
2b	1	5	6	7	8	9	2
3b	1	4	5	6	7	8	9
4b	1	3	4	5	6	7	8

1. Implies a second run for this particular crew.

TABLE 7.13 Experimental Order of Execution for Turnoff Location Tests.

Crew	Runway Length Scenarios		
	Short	Medium	Long
1a[1]	1	2	3
2a	3	1	2
3a	2	3	1
4a	1	2	3

1. Implies a second run for this particular crew.

CHAPTER 8

Conclusions and Recommendations

8.1 Conclusions

The simulation/optimization approach adopted in this new version of REDIM provides airport planners and researchers alike with a better understanding of the complex issue of locating optimal runway exits and their associated geometries. Looking at existing data on runway occupancy times [Koenig, 1978; Weiss and Barrer, 1984, Weiss, 1985; and Ruhl, 1990] it is believed that the new REDIM model behaves in a realistic fashion for a multitude of scenarios tested. Comparison of previous empirical results obtained by previous researchers support the validity of this argument. Further empirical studies are being pursued in Phase III of this research project at six large and medium size airport hubs.

Following the approach adopted in the previous version of the REDIM model the description of fully variable turnoff geometries is approximated with two large radii of curvature. This simplifies the presentation of results within the model yet approximates very closely a turnoff geometry resembling a large transition spiral. The reader can compare results of high speed geometries defined with variable radii of curvature and the standardized spiral transitions used in association with the 30 deg. FAA standard geometry.

The characterization of the first order differential system used to describe the turnoff maneuver by various aircraft was investigated and verified with the use of a four-degree of freedom model which considered three force equations and one moment equation to describe the aircraft lateral, longitudinal, vertical and yawing motions. This model also suggested that tire forces for the geometries proposed are well within design limits.Chapter 4 presented selected results of this analysis.

The geometries generated by REDIM are dictated primarily by the jerk and normal acceleration in the first few seconds of the trajectory and by the aircraft rotational inertia limitations in the longer term (i.e., 3 or more seconds into the turn). In general, the geometries

obtained in REDIM differ from the FAA standard acute angle exit geometry in terms of their initial and steady state radii of curvature.Since this research is aimed at higher speeds than those adopted by the FAA standard criteria the results indicate longer and smoother trajectories which consume more of the runway longitudinal distance. This is an important detail as a runway length is a limited resource where only a few of these high speed exits can be located. Nonetheless as the results of Section 7.1 indicate the provision of even a limited number of high speed turnoffs might be easily justifiable from an operator's point of view if a reduction in ROT is needed. Another parameter equally important in this analysis is the reduction of the standard deviation of the ROT parameter (σ_{ROT}) since low values of σ_{ROT} are representative of better runway utilization across the entire aircraft population.

In order to provide guidance for implementation of high speed geometries a series of nomographs have been suggested in this report providing preliminary design guidelines for future use by airport planners. The graphs contained in Section 4.1 of the report document suggested lateral separations between runways and turnoffs for combinations of exit type, exit angle, and aircraft operational turnoff speeds (i.e., entry and final speeds). The lateral constraints dictated by operational aircraft criteria and runway exit geometric constraints were also programmed into the software package to allow further compliance with these proposed standards. Design nomographs have been derived for FAA standard high-speed exits (i.e., 30 deg. standard and 30 deg. modified geometry with 427 m. transition spiral) as well as for REDIM generated geometries. The results are presented in Chapter 4 of this report.

A desirable characteristic of the model addressed in this research phase has been the provision of variable exit angles for new geometries and the possibility of obtaining an absolute minimum WAROT value for a runway in question without lateral space constraints, with large number of exits and high exit speeds. This scenario, although fictitious in practice, has been provided to serve as a benchmark for comparing constrained and unconstrained optimization solutions.

Another aspect deserving attention are the calibration of some of the safety margins and assumptions made in the present modeling effort. In the overall conceptualization of REDIM safety margins were implemented in some of the dynamic module subroutines to account for the usual uncertainties associated with manual control tasks, such as the landing of an aircraft, the activation of braking devices, etc. However, the reduction of these uncertainties could significantly reduce the runway occupancy time (ROT) by reducing the margins of safety needed to cope with the original assumptions. This phenomena is similar to the anticipated reductions in the aircraft interarrival time (IAT) to the runway threshold through an improvement of the aircraft delivery accuracy (e.g., by reducing the final approach IAT separation buffers). The underlying assumptions made in this model have tried to establish a good balance between operational safety and the efficiency of the runway subsystem. This compromise was necessary because the model is expected to be applied in a variety of scenarios where the manual control uncertainties will be, in general, quite high. That is, the model could be either applied to small community airports where the proficiency and accuracy of the pilots might dictate slightly larger safety margins or to large transport-type airports where an increased number of automated landing rollout operations

could take place in the future.

8.2 Recommendations

It is expected that REDIM will be calibrated with the help of simulation and experimental results to be obtained through simulations at the FAA Aeronautical Center at Oklahoma City in order to gain more confidence in the output results of the model. This calibration is, in fact, one of the most important steps to follow in the development of REDIM. The calibration procedure has been outlined in Chapter 7 of this report and could be easily expanded to account for more aircraft/pilot variations since only a Boeing 727-200 flight simulator will be used in the current plan of calibration procedures.Data obtained from other flight simulators could prove to be very useful in this regard in order to have a more broad database.

It is suggested that further studies be undertaken to explore the complex aircraft interactions possible with the implementation of high speed geometries at the taxiway/runway system. The interactions resulting from the merging of high and low speed ground traffic on the runway/taxiway system could be either beneficial and detrimental to ground operations depending upon the airport configuration. Phase III is currently exploring the capacity and delay gains that could be derived from the use of high-speed turnoffs. Using a single runway discrete simulation model (RUNSIM) it was possible to quantify in a preliminary way the capacity and delay reductions expected with the implementation of high-speed turnoffs for single runway, mixed operation scenarios.Reductions in arrival delays are not possible alone with the use of high-speed geometries for current ATC separation criteria. However, if future separation standards are reduced to 2.0 and 1.5 nautical miles under IFR conditions the expected reductions in ROT will be necessary in order to balance runway service times and interarrival separations. For VFR conditions where closer interarrival times are possible reductions in ROT times are certainly welcome to increase the aircraft acceptance rate of a single runway with mixed aircraft operations.

Finally, under single runway mixed operation conditions a significant reduction in the departure delays were observed with the implementation of high-speed runways as more gaps between adjacent arrivals were created thus allowing more departures per unit of time. Results indicate that increases of 12-16 % in departure practical capacity are possible for a single runway under balanced mixed operations (50% arrivals and 50% departures) under a current ATC system. The reductions in departure delays could mean substantial fuel savings for airline operators over a twenty year life cycle which would be typical for runway turnoff economic assessment.

BIBLIOGRAPHY

1) Aviation Week and Space Technology, McGraw-Hill Publishing Company, various issues 1986-1990.

2) Barrer, J.N. and Dielh, J.M., *Toward a Goal-Oriented Plan for Identifying Technology to Increase Airfield Capacity*, The MITRE Corporation, McLean, Virginia, 1988.

3) Branstetter, J.R., J. A. Houck, and A. D. Guenther, "Flight Simulation of a Wide-Body Transport Aircraft to Evaluate MLS-RNAV Procedures", Journal of Aircraft, Volume 25, No. 6, June 1988.

4) Business and Commercial Aviation, McGraw-Hill Publishing Company, various issues 1989.

5) Carr, H., P. Reaveley, and L.B. Smith IV, "New Turnoffs for Optimal Runway Occupancy Times", Airport Forum, No. 3, 1980, pp. 21-26.

6) Colligan, W. E., *A Systems Dynamics Model of the Terminal Operations of the National Airspace System Plan*, Project and Report, Systems Engineering, Virginia Tech University, 1988.

7) Daellenbach, H.G., "Dynamic Programming Model for Optimal Location of Runway Exits", Transportation Research, Volume 8, Pergamon Press, 1974, pp. 225-232.

8) Denardo, E. V., *Dynamic Programming*, Models and Applications, Englewood Cliffs, New Jersey, 1982.

9) Desmond, J., "Improvements in Aircraft Safety and Operational Dependability from a Projected Flight Path Guidance Display", AIAA Paper 861732, August 1986.

10) Elmaghraby, S. E., *Manuscript on Dynamic Programming*, Department of Operational Research, North Carolina State University, 1989.

11) Federal Aviation Administration, *Airport Capacity Enhancement Plan*, DOT/FAA/CP 88-4, Washington, D.C., April 1988.

12) Federal Aviation Administration, *Air Traffic Activity and Delays Report for April 1988*, Air Traffic Operations Service, NAS Analysis Branch, May 1988.

13) Federal Aviation Administration, *Airport Design*, FAA/AC 150/5300-12, February 1983.

14) Federal Aviation Administration, *Airport Design*, FAA/AC 150/5300-13, September 1989.

15) Federal Aviation Administration, *General Aviation Pilot and Aircraft Survey*, Washington, D.C., 1989.

16) Federal Aviation Administration, *1990 Airport Activity Statistics of Certificated Route Air Carriers*, Washington, D.C., 1991.

17) Gosling, G.D., A. Kanafani, and S. Hockaday, *Measures to Increase Airfield Capacity by Changing Aircraft Runway Occupancy Characteristics*, Research Report UCB-ITS-RR-81-7, Institute of Transportation Studies, University of California, Berkeley, 1981.

18) Green, W., Swanborough, G. and Mowinski, J., *Modern Commercial Aircraft*, Crescent Books, New York, 1987.

19) Harrin, E.N., *Low Tire Friction and Cornering Forces on a Wet Surface*, NACA TN 4406, September, 1958.

20) Harris, R.M., *Models for Runway Capacity Analysis*, MITRE Technical Report No. 4102, The MITRE Corporation, McLean Virginia, December 1972.

21) Haury, R. L., "Fast Exit", Civil Engineering of ASCE, October 1987, pp. 75-77.

22) Hillier, S.H. and G. J. Lieberman, *Introduction to Operations Research*, Holden-Day, Inc., Oakland, Califonia, 1986.

23) Horne, W.B., Smiley, R.F., and Stephenson, B.H., *Low-Speed Yawed Rolling and Some Other Elastic Characteristics of Two 56-in Diameter, 24 Ply-Rating Tires*, NACA TN 3235, August 1954.

24) Horonjeff, R., Finch, D.M., Belmont, D.M., and Ahlborn, G.; *Exit Taxiway Location and Design*, Institute of Transportation and Traffic Engineering, University of California, Berkeley, August 1958.

25) Horonjeff, R., Grassi, R.C., Read, R.R., and Ahlborn, G.; *A Mathematical Model for Locating Exit Taxiways*, Institute of Transportation and Traffic Engineering, University of California, Berkeley, December 1959.

26) Horonjeff, R., Read, R.R., and Ahlborn, G.; *Exit Taxiway Locations*, Institute of Transportation and Traffic Engineering, University of California, Berkeley, September 1960.

27) Horonjeff, R. and McKelvey, F.X., *Planning and Design of Airports*, 3rd Edition, McGraw-Hill Book Company, New York, 1983.

28) Hosang, V.A., *Field Survey and Analysis of Aircraft Distribution on Airport Pavements*, Report DOT-FA71WAI-218, Washington, D.C., February, 1975.

29) *Jane's all the World's Aircraft 1987-1988*, Jane's Publishing Co. Ltd., England, 1988.

30) Joline, E.S., "Optimization of Runway Exit Configurations", Transportation Engineering Journal, American Society of Civil Engineers, Vol. 100, February 1974, pp. 85-102.

31) Koenig, S.E., *Analysis of Runway Occupancy Times at Major Airports*, MITRE Report MTR-7837, The MITRE Corporation, McLean, Virginia, 1978.

32) Lebron, J.E., *Estimates of Potential Increases in Airport Capacity Through ATC System Improvements in the Airport and Terminal Areas*, The MITRE Corporation, McLean, Virginia, FAA-DL5-87-1 (MTR-87W203), October 1987.

33) Miller and Thomas, "Takeoff and Landing Problems : Design for Runway Conditions", Journal of Aeronautical Society, Vol. 67, No. 633, September 1963, pp. 571-576.

34) Roskam, I. and E. Lan, *Airplane Aerodynamics and Performance* ., Roskam Aviation and Engineering Corporation, Ottawa, Kansas, 1981.

35) Roskam, J., *Airplane Design: Part I*, Roskam Aviation and Engineering Corporation, Ottawa, Kansas, 1985.

36) Rossow, V.J, and Tinlin, B.E., "Research on Aircraft/Vortex-Wake Interactions to Determine Acceptable Level of Wake Intensity", Journal of Aircraft, Volume 25, No. 6, June 1988.

37) Ruhl, T.A., "Empirical Analysis of Runway Occupancy with Applications to Exit Taxiway Location and Automated Exit Guidance", Transportation Research Board Meeting, January 7-11, Washington, 1990.

38) Schoen, M.L. et al., *Probabilistic Computer Model of Optimal Runway Turnoffs*, NASA Contractor Report 172549, April 1985.

39) Simpson, R.W., Odoni, A.R. and Salas-Roche, F., *Potential Impacts of Advanced Technologies on the ATC Capacity of High-Density Terminal Areas*, NASA Contractor Report 4024, October 1986.

40) Swedish, W.J., *Evaluation of the Potential for Reduced Longitudinal Spacing on Final Approach*, MITRE Report MTR-79-000280, August, 1979.

41) Smith, J.M., *Mathematical Modeling and Digital Simulation for Engineers and Scientists*, John Wiley and Sons Inc., New York, 1987.

42) Tansel. B. C., R. L. Francis, and T. J. Lowe," Location on Networks : A survey, Part I, The p-centered and p-median Problems", Management Science, Vol. 29, No. 4, April 1983, pp. 482-497.

43) Trani, A.A., Hobeika, A.G., Sherali, H.D., Kim, B.J., and Saddam, C.K., *Runway Exit Designs for Capacity Improvement Demonstrations. Phase I : Algorithmic Development*, FAA/DOT Report RD 90-32,I, Washington, D.C., June 1990.

44) Tosic', V., D. Teodorovic', and O. Babic', "Optimum Runway Exit Location", Transportation Planning and Technology, Vol 10, 1985, pp. 135-145.

45) Torenbeek, E., *Synyhesis of Subsonic Airplane Design*, Van Niehoff, Netherlands, 1981.

46) Transportation Research Board, National Research Council, *Future Development of the U. S. Airport Network*, TRB, NRC, Washington, D. C., 1988.

47) United States Department of Transportation, Transportation Systems Center, "Symposium on Aviation System Concepts for the 21st Century", September 28 and 29, 1988.

48) Walpole. R.E, and Myers, R.H., *Statistics for Engineers and Scientists*, 2nd Edition, McMillan Company, New York, 1978.

49) Williams, J., *Aircraft Performance Prediction Methods and Optimization*, AGARD Lecture Series No. 56, NATO, 1972.

50) Witteveen, N. D., "Modified Rapid Runway Exit Taxiways To Reduce Runway Occupancy Time", Presented at :f. 21 sup st :ef. International Air Transport Association Conference on System Demand and System Capacity, Montreal, Canada, September 1987.

51) Wong, J. Y., *Theory of Ground Vehicles*, John Wiley and Sons, New York, 1958.

52) Weiss, W. E., and Barrer, J.N.., *Analysis of Runway Occupancy Time and Separation Data Collected at La Guardia, Boston, and Newark Airports*, MITRE Report MTR-84W228, McLean, VA, 1984.

53) Weiss, W. E., *Analysis of Runway Occupancy Time and Separation Data Collected at Los Angeles, San Francisco, Atlanta and Dallas-Forth Worth Airports*, MITRE Report MTR-85W179, McLean, VA, 1985.

54) Yager, T.J., and White, E.J., *Recent Progress Towards Predicting Aircraft Ground Handling Performace*, NASA Technical Memorandum 81952, Hampton, VA, 1981.

Intentionally Left Blank

APPENDIX A

Comparison of Turnoff Geometries

This appendix contains pertinent turnoff information to compare the existing standard turnoff geometries with those proposed in this research. Figure A.1 illustrates the characteristics of two standard FAA, 30 degree angle turnoff geometries compared with a REDIM generated turnoff (using a Boeing 727-200 as critical vehicle) designed for an entry speed of 35 m/s and an exit angle of 20 degrees. The practical design speed for the FAA standard turnoff geometries is on the order of 26.7 m/s (60 m.p.h.) according to empirical data obtained by Horonjeff [Horonjeff et al., 1960].

Figure A.2 compares the same standard FAA 30 deg. angle geometries (top figure is the modified geometry with a 427 m. spiral) with a 35 m./s. exit speed REDIM geometry sized for a Boeing 747-200. Note that the exit angle for the REDIM geometries has been reduced from thirty to twenty degrees to comply with a 183 m. (600 ft.) lateral separation from runway to taxiway.

Figure A.3 illustrates a comparison of a standard wide throat geometry with a 35 m./s. REDIM geometry sized for a medium transport-type aircraft (i.e., Boeing 727-200). Note the differences in longitudinal distance requirements for both geometries. The useful wide throat exit speed is around 15-17 m/s. The appeal of the wide throat geometry would be its use under heavily constrained runway environments where longitudinal spaces available to place a new geometry are relatively small. The wide throat geometry, however, has relatively low exit speeds and thus willl not resut in substantial reductions in ROT. The bottom figure illustrates a comparison between a 30 m./s. REDIM geometry (Boeing 747-200 as critical aircraft) and a standard FAA 30 deg. modified geometry. Notice that the entrance fillet in REDIM generates geometries is significantly changed providing pilots with better visibility of the turnoff.

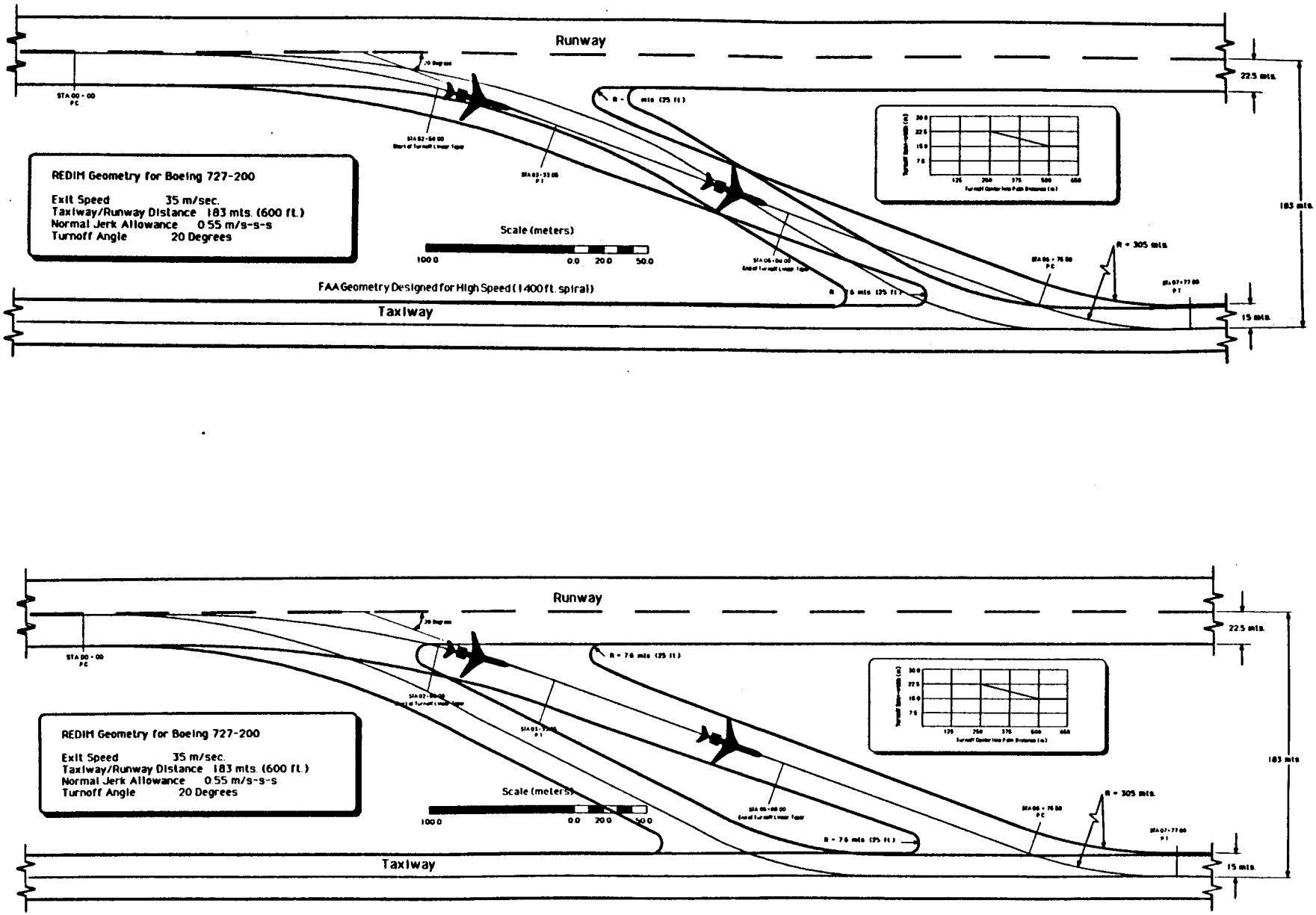

FIGURE A.1 **Comparison of FAA Standard Geometries and REDIM 3520 Geometry (Boeing 727-200 used as critical aircraft).**

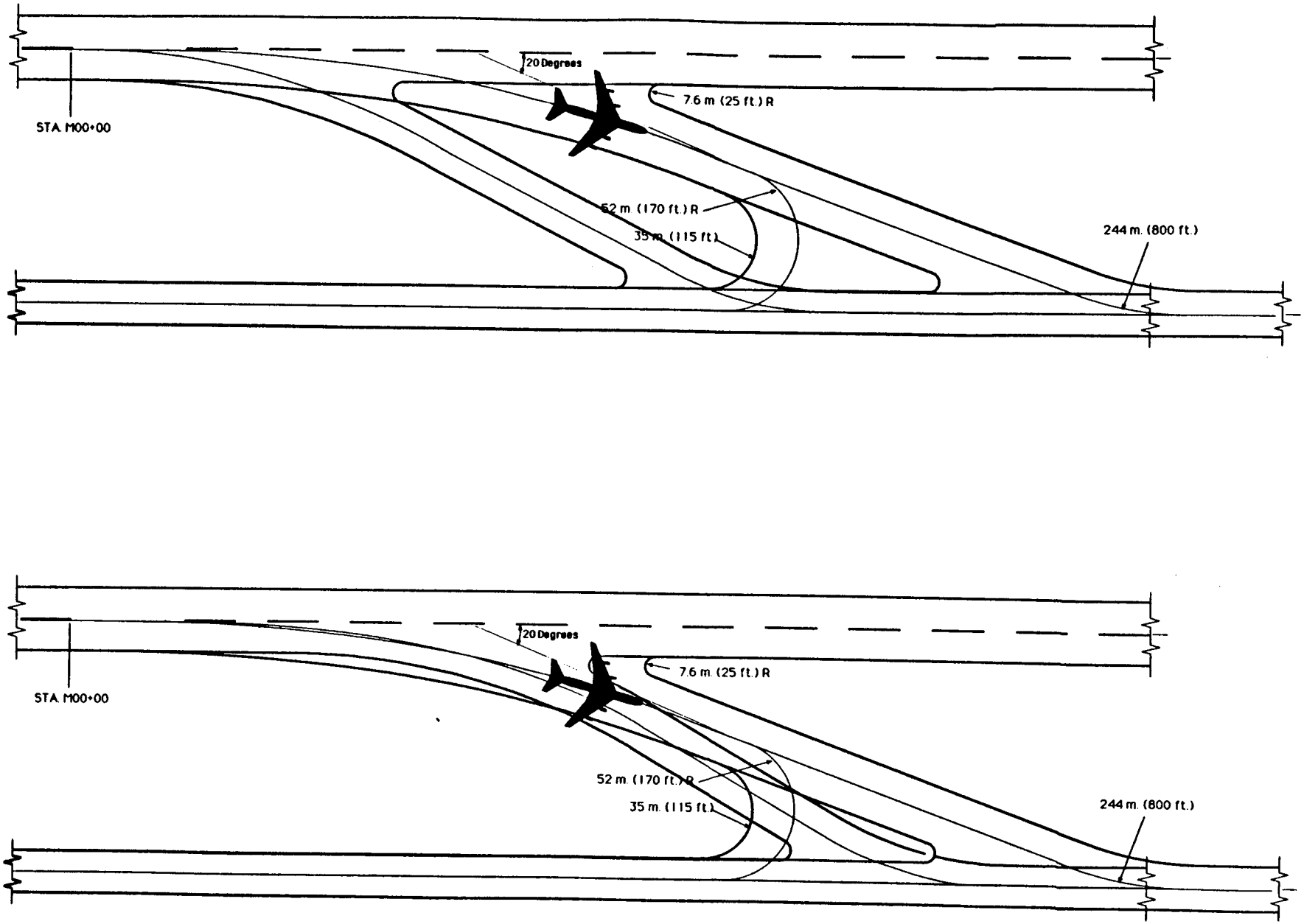

FIGURE A.2 **Comparison of FAA Standard Geometries and REDIM 3520 Geometry (Boeing 747-200 used as critical aircraft).**

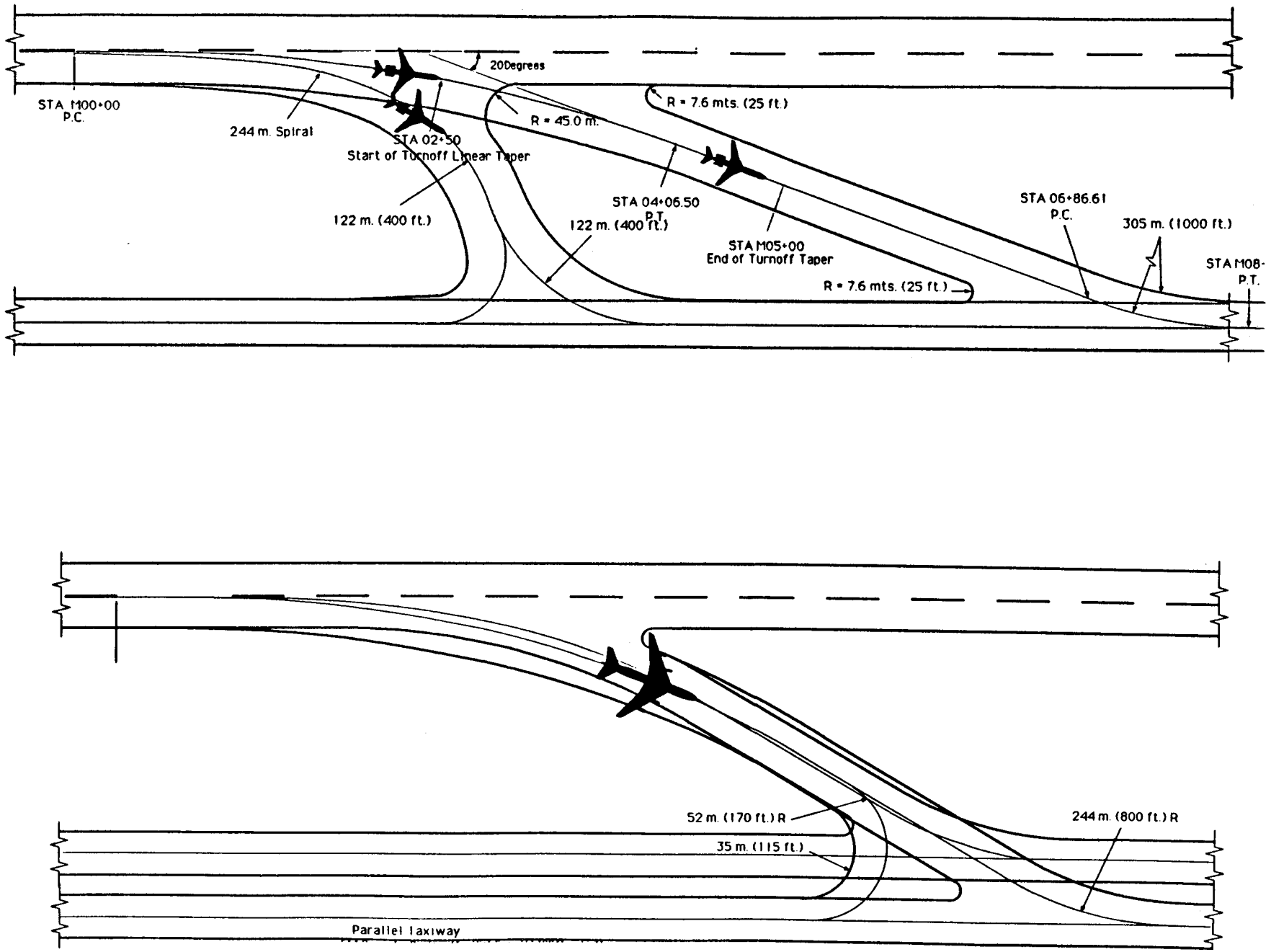

FIGURE A.3 **Wide Throat Geometry Comparison with REDIM 3520 Geometry (Boeing 727-200 used as critical aircraft).**

APPENDIX B Aircraft Data

This appendix contains pertinent aircraft data spanning four TERP classification groups. The data has been gathered from reliable sources such as aircraft manufacturer data, Jane's All the World's Aircraft, Aviation Week and Space Technology, Business and Commercial Aviation Planning Handbook and Various other respected magazines covering the world of aviation.

The appendix lists pertinent aircraft data characteristics used in REDIM 2.0 to execute both the optimization and dynamic aircraft simulation procedures. Table B.1 illustrates the characteristics of transport-type aircraft corresponding to TERP categories C and D.

TABLE B.1 Aircraft Data for TERP Categoryies C and D.

Aircraft Name	REDIM Code	Max. Landing Mass (Kg)	Oper. Empty Mass (Kg.)	Aircraft Wingspan (m.)	Aircraft Wheel-Base (m.)	% Load on Main Gears
Airbus A-300-600	A-300	140,000	92,160	44.80	18.60	92.50
Airbus A-310-300	A-310	124,000	80,050	43.90	15.21	91.60
Airbus A-320-200	A-320	64,500	39,750	33.91	12.63	90.50
Fokker 100	F100	39,915	24,375	28.08	14.00	89.50

TABLE B.1 Aircraft Data for TERP Categoryies C and D.

Aircraft Name	REDIM Code	Max. Landing Mass (Kg)	Oper. Empty Mass (Kg.)	Aircraft Wingspan (m.)	Aircraft Wheel-Base (m.)	% Load on Main Gears
BAe 146-200	BAe-146	36,741	23,882	26.34	11.20	92.30
Boeing 727-200	B-727-200	73,028	46,164	36.75	16.75	92.50
Boeing 737-300	B-737-300	51,710	31,561	28.88	12.35	93.50
Boeing 747-200	B-747-200	255,825	170,180	28.88	12.50	92.50
Boeing 747-400	B-747-400	285,765	177,374	59.64	25.60	94.60
Boeing 757-200	B-757-200	89,813	57,267	63.30	25.60	94.00
Boeing 767-200	B-767-200	116,573	79,923	38.05	18.29	93.50
McDonnell MD-83	MD-83	63,276	36,546	47.57	19.69	92.20
McDonnell MD-87	MD-87	58,967	33,183	32.87	22.07	90.30
Mc. Donnell DC-10-30	DC-10-30	182,766	121,198	32.87	19.18	91.20
Douglas DC-8-73	DC-8-73	117,000	75,500	50.40	22.05	94.00
McDonnell MD-11	MD-11	195,047	125,646	53.00	28.27	93.80
Lockheed L-1011	L-1011	166,920	111,312			

Table B.2 illustrates the aircraft data representative of TERP category A aircraft. Note that the sequence of this table is the same as that used in the REDIM 2.0 master file definition. The number of aircraft in every TERP database can be increased to 20 aircraft.

TABLE B.2 Data for Single Engine Aircraft (TERP Category A).

Aircraft Name	REDIM Code	Max. Landing Mass (Kg)	Oper. Empty Mass (Kg.)	Aircraft Wingspan (m.)	Aircraft Wheel-Base (m.)	% Load on Main Gears
Piper PA-38-112	PA-38-112	757	502	10.36	1.45	77.45
Piper PA-28-161	PA-28-161	1,109	596	10.67	2.03	82.18

TABLE B.2 **Data for Single Engine Aircraft (TERP Category A).**

Aircraft Name	REDIM Code	Max. Landing Mass (Kg)	Oper. Empty Mass (Kg.)	Aircraft Wingspan (m.)	Aircraft Wheel-Base (m.)	% Load on Main Gears
Piper PA-28-235	PA-28-235	1,363	705	10.92	1.98	81.73
Piper PA-32-301	PA-32-301	1,636	878	11.02	2.36	85.92
Piper PA-46-310P	PA-46-310P	1,772	1,118	13.66	2.44	83.31
Beechcraft F33A	BE F33F	1,545	964	10.21	2.13	81.51
Cessna 172	CE 172	1,090	676	10.92	1.70	77.93
Cessna 208	CE 208	3,615	2,230	15.88	2.11	81.20
Cessna 182	CE 182	1,338	790	10.92	1.69	78.85
Cessna 210	CE 210	1,772	1,007	11.20	1.81	77.60

TABLE B.3 **Data for Twin-Engine Business Aircraft (TERP Category B).**

Aircraft Name	REDIM Code	Max. Landing Mass (Kg)	Oper. Empty Mass (Kg.)	Aircraft Wingspan (m.)	Aircraft Wheel-Base (m.)	% Load on Main Gears
Beechcraft BE-58	BE-58	2,500	1,579	11.53	2.72	84.73
Beechcraft 300	BE 300	6,363	3,851	16.81	4.56	89.13
Cessna 402C	CE 402C	3,107	1,863	13.45	3.18	88.12
Cessna 421	CE 421	3,266	2,298	12.53	3.20	87.19
Beechcraft 2000	BE 2000	6,366	4,323	16.46	6.86	92.27
Cessna 406	CE 406	4,250	2,287	15.04	3.81	85.37
Piper PA-34-220T	PA-34-220T	2,160	1,296	11.85	2.13	82.13
Piper PA-42-1000	PA-42-1000	5,477	3,493	14.53	3.23	87.22
Piaggio P180	PD 180	4,777	3,27245	13.84	5.80	91.41

TABLE B.4 **Data for Business, Turbofan-Powered Aircraft (TERP Categories B and C).**

Aircraft Name	REDIM Code	Max. Landing Mass (Kg)	Oper. Empty Mass (Kg.)	Aircraft Wingspan (m.)	Aircraft Wheel-Base (m.)	% Load on Main Gears
Cessna CE-550	CE-550	5,773	3,351	15.90	5.55	92.61
Cessna CE-650	CE-650	9,090	5,306	16.31	6.50	92.95
Learjet 31	LEAR-31	6,940	4,514	13.34	6.15	93.42
Learjet 55	LEAR-55	8,165	5,737	13.34	7.01	93.27
Grumman G-IV	G1159	26,535	18,098	23.72	11.62	93.70
British Aeros. 125-800	BAE125	10,590	7,858	15.66	6.41	93.10
IAI 1124 (Westwind II)	IAI-1124	8,636	6,022	13.65	7.79	94.77
Beechcraft 400	BE-400	6,454	4,500	13.25	5.86	92.68
IAI 1125 (Astra)	IAI-1125	9,409	5,759	16.05	7.34	94.38
Dassault Falcon 100	DA-100	8,020	4,909	13.08	5.30	92.77
Dassault Falcon 200	DA-200	13,090	8,545	16.30	5.74	90.94
Dassault Falcon 50	DA-50	17,857	9,590	18.86	7.24	92.19
Canadair CL-601-3A	CL-601	16,363	11,220	19.61	7.99	92.86

TABLE B.5 Aircraft Data for Commuter Aircaft TERP (Category B).

Aircraft Name	REDIM Code	Max. Landing Mass (Kg)	Oper. Empty Mass (Kg.)	Aircraft Wingspan (m.)	Aircraft Wheel-Base (m.)	% Load on Main Gears
Saab 340-2	SAAB-340	12,020	7194	21.44	7.14	90.88
British Aeros. 31	BAE-31	6,600	4,131	15.05	4.60	87.18
Embraer 120	EMB-120	11,250	6,878	19.78	6.97	90.77
Boeing DeHavilland 6	DCH-6	5,579	3,363	19.81	4.53	87.16
Boeing DeHavilland 7	DHC-7	19,958	12,560	28.35	8.38	90.89
Boeing DeHavilland 8	DHC-8-200	15,375	9,793	25.91	9.60	91.63
Beechcraft 1900C	BE-1900	7,302	3,946	16.61	7.25	93.72
Fairchild Metro III	SA-227	6,590	3,963	16.60	5.38	88.74
Embraer 110-P1	EMB-110	5,712	3,855	15.33	5.10	90.70
CASA 212-200	CASA-212	7,465	3,780	19.00	5.55	88.07
NRT 235-200	NRT-235	14,229	9,892	25.81	6.92	89.70
Aeros./Alenia ATR-72	ATR-72	21,385	13,460	27.05	10.70	93.26
Aeros./Alenia ATR-42	ATR-42	15,500	9,973	25.57	8.78	92.71
Fokker 50	F-50	18,890	12,520	29.00	9.70	92.13
British Aeros. ATP	BAE-ATP	21,773	13,594	30.63	9.70	92.62
Dornier 228-100	DO-228	6,213	3,547	16.97	6.29	91.05
Shorts 360	S-360	10,251	7,689	22.76	6.15	87.93

Intentionally Left Blank

APPENDIX C

ROT Results for Selected Aircraft Populations

This appendix contains the simulation results for a single runway an selected aircraft mixes designated by the Federal Aviation Administration using REDIM 2.0. The idea behind these simulations was to determine possible combinations of exits and exit speeds to comply with specific ROT values using selected aircraft populations representative of many current airport facilities.

Aircraft selected by the contractor encompassed two TERP categories: C and D with most of them being medium-range transport aircraft typical of today's airline fleets. Table C.1 presents results obtained for a population of McDonnell Douglas MD-80, Boeing 727-200, B 737-300 and B 757-200 aircraft (equal percentages for each one).

TABLE C.1 **Optimal Turnoff Locations for MD-80, B727, B737 and B757 Population and 40 and 50 second ROT Limits.**

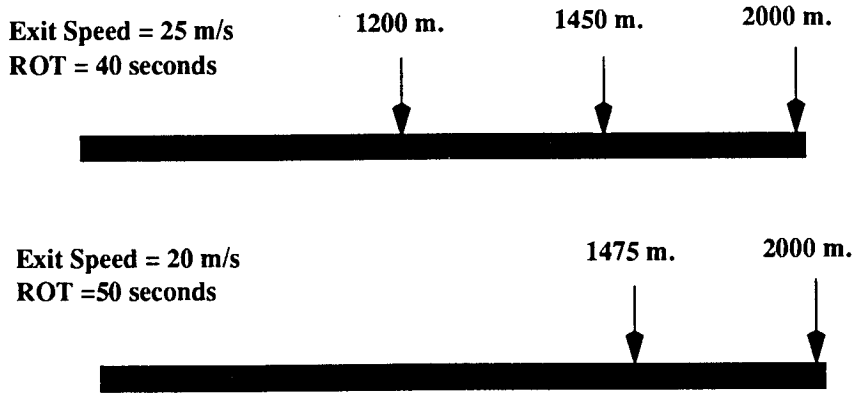

Table C.2 presents results obtained for a population of McDonnell Douglas DC-10-32, Boeing 747-200, B 767-300 and Lockhedd L 1011-500 aircraft (equal percentages for each one).

TABLE C.2 **Optimal Turnoff Locations for DC-10, B747, B767 and L 1011 Population and 40 and 50 second ROT Limits.**

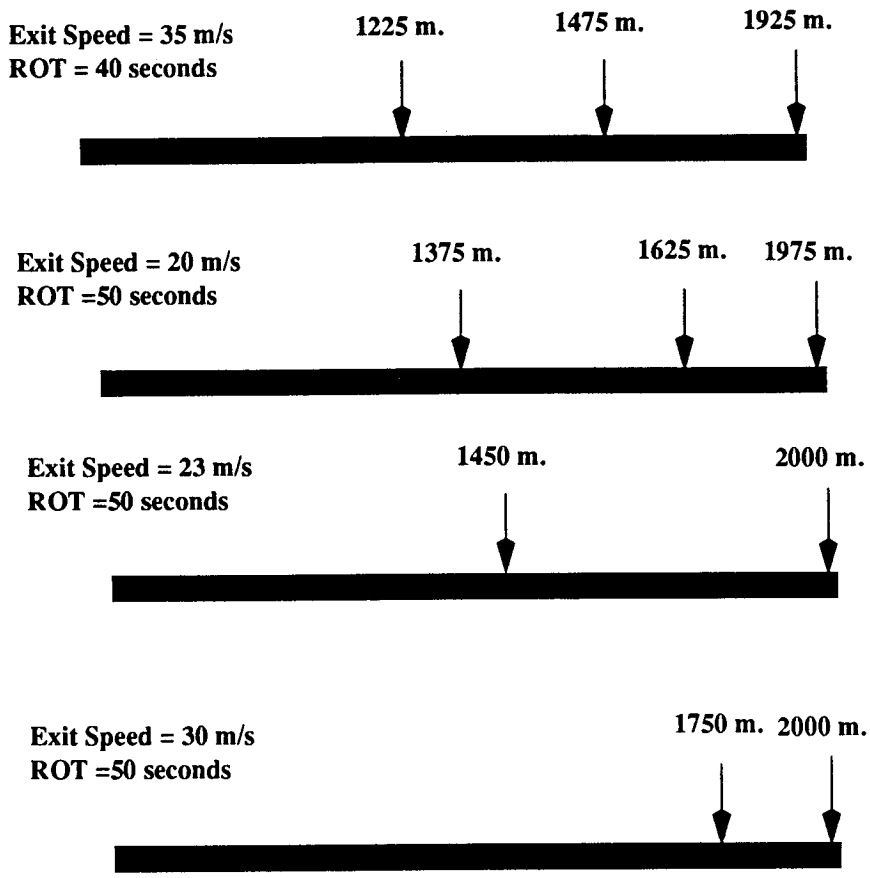

Table C.3 presents results obtained for a Boeing 727-200 using REDIM 2.0 and complying with various ROT limits.

TABLE C.3 Boeing 727-200 Optimal Location Results for Various Exit Speeds and ROT Limits (95% Reliability).

Condition	Exit Speed (m/s)	Location (m.)	ROT (sec.)
Dry	30	1190	35
Dry	25	1296	40
Dry	8	1400	50
Wet	35	1225	35
Wet	27	1347	40
Wet	15	1500	50
Wet	8	1570	55